

# Induced pseudoscalar coupling of the proton weak interaction.

Tim Gorringer \*

*Dept. of Physics and Astronomy, Univ. of Kentucky, Lexington, KY, 40506, U. S. A.*

Harold W. Fearing †

*TRIUMF, Vancouver, British Columbia, V6T 2A3, Canada*

The induced pseudoscalar coupling  $g_p$  is the least well known of the weak coupling constants of the proton's charged-current interaction. Its size is dictated by chiral symmetry arguments, and its measurement represents an important test of quantum chromodynamics at low energies. During the past decade a large body of new data relevant to the coupling  $g_p$  has been accumulated. This data includes measurements of radiative and non radiative muon capture on targets ranging from hydrogen and few-nucleon systems to complex nuclei. Herein the authors review the theoretical underpinnings of  $g_p$ , the experimental studies of  $g_p$ , and the procedures and uncertainties in extracting the coupling from data. Current puzzles are highlighted and future opportunities are discussed.

PACS numbers: 23.40.-s, 11.40.Ha, 13.10.+q, 11.30.Rd, 25.30.-c, 11.40.-q

## Contents

	5. Large $\Delta$ resonance effects	18
	6. Other possibilities	18
	F. Summary and outlook for hydrogen	19
<b>I. Introduction</b>	2	
<b>II. Theoretical predictions for <math>g_p</math></b>	3	
A. PCAC, $g_p$ , and the Goldberger-Treiman relation	3	
B. ChPT derivations of $g_p$	4	
<b>III. Sources of information on <math>g_p</math></b>	4	
<b>IV. Muon chemistry and the initial spin state</b>	5	
A. Muons in pure hydrogen	5	
B. Muons in pure deuterium	7	
C. Muons in hydrogen-deuterium mixtures	7	
<b>V. Muon capture in hydrogen</b>	8	
A. Theory of ordinary muon capture	8	
1. Standard diagram calculations	8	
2. ChPT calculations	8	
3. Spin effects	9	
B. Theory of radiative muon capture	9	
1. Standard diagram calculations	9	
2. ChPT calculations	10	
3. Model calculations	11	
4. Spin effects	11	
C. Experimental methods for hydrogen and deuterium	12	
1. Bubble chamber studies	12	
2. Lifetime method	12	
3. Neutron method	13	
4. Radiative capture	13	
D. Comparison of experiment and theory	14	
E. Attempts to resolve the discrepancy	16	
1. General comments	16	
2. Value of the ortho-para transition rate $\Lambda_{op}$	16	
3. Admixtures of a $J = 3/2$ ortho-molecular state	17	
4. Direct singlet - para transitions	17	
	<b>VI. Muon capture in deuterium</b>	20
	A. Theory of muon capture in deuterium	20
	B. Experiments on muon capture in deuterium	21
	<b>VII. Muon capture in <math>^3\text{He}</math></b>	22
	A. Theory of ordinary muon capture in $^3\text{He}$	22
	B. Experiments on OMC in $^3\text{He}$	23
	1. $^3\text{He}$ capture rate experiments	23
	2. $^3\text{He}$ recoil asymmetry experiments	24
	C. Radiative muon capture in $^3\text{He}$	25
	1. Theoretical calculations	25
	2. Experimental results	25
	<b>VIII. Other few body processes</b>	26
	<b>IX. Exclusive OMC on complex nuclei</b>	26
	A. Free couplings versus effective couplings	26
	B. Physical observables	27
	1. Capture rates	27
	2. Recoil asymmetries	27
	3. Recoil orientations	28
	4. Gamma-ray correlations	28
	C. Helicity representation	29
	1. Capture on zero-spin targets	29
	2. Capture on nonzero-spin targets	29
	D. Induced currents	30
	1. Asymmetries, orientations and correlations	30
	2. Hyperfine dependences	30
	3. Capture rates	31
	E. Experimental studies of partial transitions	31
	1. $^{12}\text{C}(0^+, 0) \rightarrow ^{12}\text{B}(1^+, 0)$	32
	2. $^{11}\text{B} \rightarrow ^{11}\text{Be}$ and $^{23}\text{Na} \rightarrow ^{23}\text{Ne}$	33
	3. $^{16}\text{O}(0^+, 0) \rightarrow ^{16}\text{N}(0^-, 120)$	35
	4. $^{28}\text{Si}(0^+, 0) \rightarrow ^{28}\text{Al}(1^+, 2201)$	35
	F. Theoretical framework for exclusive OMC	37
	1. Multipole operators	37
	2. Impulse approximation	37
	3. Exchange currents	38

\*Electronic address: gorringer@pa.uky.edu

†Electronic address: fearing@triumf.ca

G. Nuclear models for partial transitions	38
1. $^{11}\text{B}(3/2^-, 0) \rightarrow ^{11}\text{Be}(1/2^-, 320)$	38
2. $^{12}\text{C}(0^+, 0) \rightarrow ^{12}\text{B}(1^+, 0)$	39
3. $^{23}\text{Na}(3/2^+, 0) \rightarrow ^{23}\text{Ne}(1/2^+, 3458)$	39
4. $^{28}\text{Si}(0^+, 0) \rightarrow ^{28}\text{Al}(1^+, 2201)$	40
5. $^{16}\text{O}(0^+, 0) \rightarrow ^{16}\text{N}(0^-, 120)$	40
H. Coupling $g_p$ from partial transitions	40
1. Recommended values of $g_p/g_a$	40
2. Model sensitivities of $g_p/g_a$	41
3. Conclusions and outlook for $g_p/g_a$	43
X. Inclusive RMC on complex nuclei	43
A. Theory of nuclear RMC	43
B. Measurement of nuclear RMC	45
C. Interpretation of nuclear RMC	45
D. Comments on photon asymmetries in nuclear RMC	48
XI. Summary	48
Acknowledgments	50
References	50

## I. INTRODUCTION

It is well known that the weak interactions of leptons are governed by a current-current interaction, where the currents are given by a simple  $V - A$  form,  $\gamma_\mu(1 - \gamma_5)$ . When hadrons are involved, the interaction is still current-current and still  $V - A$  but the individual vector and axial vector currents become more complicated, picking up both form factors and new structures involving the momentum transfer  $q$ . The couplings associated with these new structures are the so called ‘induced’ couplings which have been a topic of investigation, both theoretical and experimental, for a long time. We are concerned in this review with one of these, the induced pseudoscalar coupling,  $g_p$ .

The most general weak current, actually the matrix element of that current, for say a neutron and proton can be written as

$$\bar{u}_n \left( + g_v \gamma^\mu + \frac{ig_m}{2m_N} \sigma^{\mu\nu} q_\nu + \frac{g_s}{m_\mu} q^\mu - g_a \gamma^\mu \gamma_5 - \frac{g_p}{m_\mu} q^\mu \gamma_5 - \frac{ig_t}{2m_N} \sigma^{\mu\nu} q_\nu \gamma_5 \right) u_p \quad (1)$$

where the notation for gamma matrices, spinors, etc. is that of Bjorken and Drell (1964) and  $m_\mu$  and  $m_N$  are respectively the muon and nucleon masses. The momentum transfer  $q = p_n - p_p$ , with  $p_p$ ,  $p_n$  respectively the proton and neutron momenta. This most general form for the current contains six coupling ‘constants’, which are actually functions of  $q^2$ , namely  $g_v$  and  $g_a$ , the vector and axial vector couplings,  $g_m$ , the weak magnetism coupling,  $g_p$ , the induced pseudoscalar coupling, and  $g_s$  and  $g_t$ , the second class induced scalar and induced tensor couplings.<sup>1</sup>

Of these six, the second class terms  $g_s$  and  $g_t$  transform differently than the others under G-parity, which is a combination of charge conjugation and a rotation in isospin space. In the standard model they are generated only via quark mass differences or electromagnetic effects and are thus predicted to be small (Grenacs , 1985; Shiomi , 1996). Thus although the experimental evidence is not unequivocal (Minamisono *et al.*, 2001; Wilkinson , 2000a,b), they are normally assumed to be zero and will be ignored in this review. The vector terms

---

<sup>1</sup> There is an unfortunate confusion about the signs of the axial couplings which has arisen as conventions have changed over the years. In very early calculations in a different metric, the signs were such that  $g_a$  was positive. With the widespread use of the metric of Bjorken and Drell (1964) it became conventional to write the weak current like Eq. (1) only with all signs positive. This was the convention used in Beder and Fearing (1987, 1989); Fearing (1980) and most other modern papers, and implies that  $g_a$  and  $g_p$  are negative. With the advent of chiral perturbation theory, for which  $g_a$  is normally taken to be positive, the convention changed again. We have adopted this latter convention. This means that the axial current of Eq. (1) has an explicit overall minus sign and that  $g_a$  and  $g_p$  are positive numbers.

$g_v$  and  $g_m$  are related by the Conserved Vector Current (CVC) theory to the isovector electromagnetic current. Thus their static values are related to the charge and anomalous magnetic moments of the nucleons and their  $q^2$  dependence is given by measurements of the isovector electromagnetic form factors of the proton and neutron. The axial vector coupling  $g_a$  can be determined precisely from neutron beta decay and its  $q^2$  dependence from neutrino scattering (Ahrens *et al.*, 1988) or from pion electroproduction (Bernard *et al.*, 1992; Choi *et al.*, 1993; Del Guerra *et al.*, 1976; Esaulov *et al.*, 1978).

This leaves the induced pseudoscalar coupling,  $g_p$ , which is by far the least well known. In principle it can be predicted using the Partially Conserved Axial Current (PCAC) theory via a relation known as the Goldberger-Treiman relation (Goldberger and Treiman, 1958). The details of this derivation will be discussed in the next section. Physically the dominant diagram is one in which the nucleon emits a pion which propagates and then couples to the  $\mu - \nu$  or  $e - \nu$  vertex. The coupling  $g_p$  thus contains a pion pole. In practice however it has been difficult to verify this relation and there are some situations, notably radiative muon capture in liquid hydrogen, where experiment and theory do not agree.

Thus the main purpose of this review is to discuss in detail the information available, both theoretical and experimental, regarding the value of  $g_p$ . In Sec. II we discuss the theoretical prediction for  $g_p$  arising from PCAC and from the more modern approaches using chiral perturbation theory. Sections III and IV describe in general some of the sources of experimental information and some of the atomic and molecular physics required to understand muon processes in hydrogen or deuterium. The remainder of the review is divided into three main parts which discuss the three main areas which have led to information on  $g_p$ . The first of these, Secs. V-VIII, deals with ordinary, non radiative, muon capture (OMC) and radiative muon capture (RMC) on the proton, deuteron, and  $^3\text{He}$ . Here the experiments are difficult, but the results presumably are not obscured by unknown details of nuclear structure. In the next major part, Sec. IX, exclusive OMC on complex nuclei is discussed, with particular emphasis on spin observables in partial transitions. Here the sensitivity to  $g_p$  is high, but the experiments are often difficult and their interpretation is model dependent. Then in the final part, Sec. X, inclusive RMC on complex nuclei is examined. RMC is quite sensitive to  $g_p$  and nowadays measurements of inclusive RMC on  $Z > 2$  nuclei are relatively straightforward. However model dependence in the theory makes the extraction of a unique value of  $g_p$  very difficult. Finally in Sec. XI we will summarize the current situation with regard to  $g_p$  and make some suggestions for further work.

Related review articles include those of Mukhopadhyay (1977), Grenacs (1985), Gmitro and Truöl (1987), Measday (2001), and Bernard *et al.* (2001a).

## II. THEORETICAL PREDICTIONS FOR $g_p$

### A. PCAC, $g_p$ , and the Goldberger-Treiman relation

Historically the measurement of  $g_p$  has been considered interesting and important because there is a very definite prediction for its value derived many years ago (Goldberger and Treiman, 1958) based on the very fundamental notion of the Partially Conserved Axial Current (PCAC). Detailed derivations are given in textbooks, e.g. Bjorken and Drell (1964), so we simply outline the basic ideas here. The underlying assumption is that the divergence of the axial current is proportional to the pion field. Applying this idea to the divergence of the axial current of Eq. (1), taking matrix elements, and evaluating at four-momentum transfer  $q^2 = 0$ , gives the relation known as the Goldberger-Treiman relation:

$$g_{\pi NN}(0)F_\pi = m_N g_a(0) \quad (2)$$

where  $g_{\pi NN}$  is the pion nucleon coupling constant,  $F_\pi = 92.4 \pm 0.3$  MeV is the pion decay constant, and  $m_N$  is the nucleon mass. This equation is rather well satisfied when one uses modern values of  $g_{\pi NN}$ . A measure of the difference, which is known as the Goldberger-Treiman discrepancy, is given by the equation

$$\Delta_{GT} = 1 - \frac{m_N g_a(0)}{g_{\pi NN}(m_\pi^2) F_\pi}. \quad (3)$$

The value of  $\Delta_{GT}$  was about 6% using the older (larger) value of  $g_{\pi NN} = 13.4$ , and there were a number of papers discussing possible sources of this discrepancy. See e.g. Coon and Scadron (1981, 1990); Jones and Scadron (1975) and references cited therein. With the newer and somewhat smaller value of  $g_{\pi NN}(m_\pi^2) = 13.05 \pm 0.08$  (Arndt *et al.*, 1995; de Swart *et al.*, 1997; Stoks *et al.*, 1993), and updated values of  $g_a$  and  $F_\pi$  the discrepancy is now 2% or less. See e.g. Goity *et al.* (1999); Nasrallah (2000) and references cited therein. Thus at  $q^2 = 0$  the Goldberger-Treiman relation is quite well satisfied.

Now consider the matrix element of the divergence of the axial current for non-zero  $q^2$ . This leads, using Eq. (2), to an expression for  $g_p$  given by

$$g_p(q^2) = \frac{2m_\mu m_N}{m_\pi^2 - q^2} g_a(0) \quad (4)$$

with  $m_\pi$  the charged pion mass. This is known as the Goldberger-Treiman expression for  $g_p$ . Observe the explicit presence of a pion pole. At  $q^2 = -0.88m_\mu^2$ , which is the relevant momentum transfer for muon capture on the proton, this formula gives  $g_p(-0.88m_\mu^2) = 6.77g_a = 8.58$ , where we have used the latest value of  $g_a(0) = 1.2670 \pm 0.0035$  from the Particle Data Group (2000) and taken for  $m_N$  the average of neutron and proton masses. This is what we shall refer to in subsequent sections as the lowest order PCAC value  $g_p^{PCAC}$ . At  $q^2 = -m_\mu^2$  the result is  $g_p(-m_\mu^2) = 6.47g_a = 8.20$ .

Somewhat later the first order correction to this, proportional to the derivative of  $g_a$ , was derived using current algebra techniques (Adler and Dothan, 1966). Numerically however the correction is rather small, as described in the next section.

## B. ChPT derivations of $g_p$

In the years since the original derivations of the Goldberger-Treiman relation there have been major advances in our understanding of the way to include chiral symmetry in such analyses, particularly in the framework of what is known as chiral perturbation theory (ChPT), or, when nucleons are involved, heavy baryon chiral perturbation theory (HBChPT). This approach provides a way of incorporating the symmetries of QCD into a systematic low energy expansion, where the expansion parameter is something of the order  $m_\pi/m_N$ . Thus one can reproduce all the old current algebra results, but more importantly calculate in a systematic way the corrections to these results.

This approach was applied (Bernard *et al.*, 1994) to obtain for  $g_p$  the result

$$g_p(q^2) = \frac{2m_\mu g_{\pi NN}(q^2) F_\pi}{m_\pi^2 - q^2} - \frac{1}{3} g_a(0) m_\mu m_N r_A^2, \quad (5)$$

where  $r_A^2$  is the axial radius of the nucleon, defined in the usual way via  $g_a(q^2) = g_a(0)(1 + q^2 r_A^2/6 + \mathcal{O}(q^4))$ . This is essentially the result obtained much earlier by Adler and Dothan (1966) and by Wolfenstein (1970), but the systematic approach allows us to be confident that the corrections are of higher order.

Using the value of the axial radius  $r_A^2 = 0.42 \pm 0.04$  fm obtained from anti neutrino-nucleon scattering (Ahrens *et al.*, 1988), this formula leads to  $g_p(-0.88m_\mu^2) = 8.70 - 0.45 = 8.25$ , so the correction term is indeed rather small.

An alternative approach, still within HBChPT, is simply to calculate the amplitude for muon capture, as was done by Fearing *et al.* (1997), and identify  $g_p$  by comparing with Eq. (1). This gives, up to corrections of  $\mathcal{O}(p^4)$ ,

$$g_p(q^2) = \frac{2m_\mu m_N}{(m_\pi^2 - q^2)} \left[ g_a(q^2) - \frac{m_\pi^2}{(4\pi F_\pi)^2} (2b_{19} - b_{23}) \right] \quad (6)$$

where  $b_{19}$  and  $b_{23}$  are low energy constants (LEC's) of the basic Lagrangian. At first glance this appears to be different than the result above, but can be put in the form of Eq. (5) by noting that in the same approach  $g_{\pi NN}$  and the axial radius squared  $r_A^2$  are given by

$$g_{\pi NN}(q^2) = \frac{m_N}{F_\pi} \left( g_a(0) - \frac{m_\pi^2 b_{19}}{8\pi^2 F_\pi^2} \right). \quad (7)$$

and

$$r_A^2 = -6 \frac{b_{23}}{g_a(0)(4\pi F_\pi)^2} \quad (8)$$

If one wants to express  $g_p$  in terms of  $g_a$ , as is conventional, rather than  $f_\pi g_{\pi NN}$ , some simple manipulation of Eq. (5) using Eq. (2) gives

$$g_p(q^2) = \frac{2m_\mu m_N}{(m_\pi^2 - q^2)} g_a(0)(1 + \tilde{\epsilon}) - \frac{m_\mu m_N g_a(0) r_A^2}{3} \quad (9)$$

where  $(1 + \tilde{\epsilon}) = [g_{\pi NN}(q^2)/g_{\pi NN}(0)]$ . Note that  $(1 + \tilde{\epsilon}) = 1$  if one neglects the  $q^2$  dependence of  $g_{\pi NN}$ , which we will do in this review. This gives  $g_p(-0.88m_\mu^2) = 8.58 - 0.45 = 8.13$  where the slight difference from the result of Eq. (5) originates in the difference between left and right hand sides of Eq. (2) when experimental values are used. It is this latter value, 8.13, which we will take as  $g_p^{PCAC}$  when the constant term is included.

It is important to note that the specific results in terms of the LEC's of ChPT depend on the specific choice of starting Lagrangian and the details of the calculation. The expressions of Eqs. (6), (7), and (8) come from Fearing *et al.* (1997), but similar results were subsequently obtained by Bernard *et al.* (1998) and Ando *et al.* (2000). However the expressions in terms of the physically measurable quantities, as given in Eqs. (5) or (9) are independent of the detailed conventions of the approach.

Finally we can summarize this section by observing that theoretical prediction for  $g_p$  as given in Eqs. (5) or (9) and based on chiral symmetry seems to be quite robust. The original Goldberger-Treiman relation is understood as the first term in an expansion and correction terms have been evaluated and are understood via a ChPT calculation carried out through the first three orders. Thus a test of this prediction should be an important test of our understanding of chiral symmetry and of low energy QCD.

## III. SOURCES OF INFORMATION ON $g_p$

At the simplest level  $g_p$  appears as a phenomenological parameter in the fundamental definition of the weak nucleon current, Eq. (1), so it should be obtainable from any process which directly involves this current. This would include beta decay, muon capture, radiative muon capture, and in principle any of the crossed versions of these reactions, as for example processes initiated by neutrinos. The  $g_p$  term is proportional to the momentum transfer however, so in practice beta decay is not a useful source of information since the momentum transfer is so small. Neutrino processes are of course extremely difficult to measure. This leaves ordinary muon capture and radiative muon capture as the two main sources of information on  $g_p$ .

Thus for ordinary, i. e., non radiative, muon capture,  $g_p$  is purely a phenomenological parameter which appears in the most general weak current. PCAC is not needed and it is quite reasonable to simply fit to data, treating  $g_p$  as a free parameter. This is what has typically been done, with the result looked upon as a test of the PCAC prediction.

At a somewhat deeper level the  $g_p$  coupling is understood to arise from the diagram in which a pion, emitted from a nucleon, couples to the weak leptonic current. Since this pion-nucleon coupling is a component of the axial current, other processes involving this current such as pion electroproduction for example, also in principle allow one to obtain information on  $g_p$ . The interpretation of information from such processes must be somewhat different, however, than that obtained from processes like muon capture which contain the phenomenological weak current explicitly. For processes like electroproduction the direct information available is really information about the  $\pi NN$  vertex. Thus the connection to  $g_p$  is only via the theoretical infrastructure of chiral symmetry and of PCAC and the interpretation that  $g_p$  originates in a pion exchange diagram. If PCAC were in fact wrong, the whole connection would break down and there would be no convincing physical reason why fitting data using for  $g_p$  a multiple of the PCAC expression containing the pion pole should work.

It is interesting to note that RMC is somewhere in between the situations corresponding to OMC and pion electroproduction. The dominant diagrams contain the phenomenological weak current directly, albeit with one leg off shell, but there is also a diagram which explicitly contains pion exchange.

Finally there is a third level where the weak current and one pion exchange do not appear directly but where, in the context of HBChPT, some of the LEC's needed for  $g_p$  do appear. For such processes it is, at least in principle, possible to determine those LEC's, and thus determine  $g_p$ , at least indirectly, via an equation analogous to Eq. (6). Again such information must be interpreted in a context which accepts the validity of PCAC.

For all of these processes it may be that measurable quantities such as correlations relative to some of the particle spins, or capture from hyperfine states, or capture to or from a specific nuclear state, or some such more detailed observable may provide more information than just the overall rate, so these should be considered.

We will begin by looking at these various processes, starting with the simplest, muon capture on the proton, and working up through reactions on nuclei to see what has been learned and what potentially could be learned with regard to  $g_p$ .

#### IV. MUON CHEMISTRY AND THE INITIAL SPIN STATE

When a negative muon is stopped in matter a muonic atom is formed. Unfortunately in hydrogen and deuterium such atoms undergo a complicated sequence of chemical processes, changing the spin-state populations with time, as the muons eventually reach the level from which they are captured. As discussed elsewhere, the capture rates for muonic hydrogen and muonic deuterium are strongly dependent on the spin state of the  $\mu$ -nucleus

system. Thus a detailed knowledge of this muon chemistry is required in order to determine  $g_p$  from  $H_2/D_2$  experiments and it is appropriate to discuss this chemistry before considering the capture process. Below we denote the two hyperfine states of the muonic atom by  $F_{\pm} = I \pm 1/2$  where  $I = 1/2$  for the proton and  $I = 1$  for the deuteron, so that  $F$  is the total spin of the atom.

Before we discuss the details we make a few general comments. One important aspect of muon chemistry is  $\mu$ -atom scattering from surrounding molecules which results in the hyperfine depopulation of the upper F-state into the lower F-state. Another important aspect is collisional formation of muonic molecules which results in additional arrangements of  $\mu$ -nucleus spin states. Also muon recycling from molecular states to atomic states via  $\mu$ -catalyzed fusion occurs for  $d\mu d$  molecules and  $p\mu d$  molecules. How these effects unfold for muons in hydrogen and deuterium, as a function of the density, is the focus of our discussion in this section.

In Secs. IV.A and IV.B, respectively, we discuss the chemistry of  $\mu p$  atoms in pure  $H_2$  and  $\mu d$  atoms in pure  $D_2$ . In Sec. IV.C we describe the chemistry of muons in  $H_2/D_2$  mixtures. Related review articles are those of Bracci and Fiorentini (1982); Breunlich *et al.* (1989); Froelich (1992); Ponomarev (1973).

##### A. Muons in pure hydrogen

To assist the reader a simplified diagram of muon chemistry in pure  $H_2$  is given in Fig. 1. The figure shows the  $F_+$  and  $F_-$  states of the  $\mu p$  atom, the ortho ( $I=1$ ) and para ( $I=0$ ) states of the  $p\mu p$  molecule, and relevant atomic and molecular transitions.

The  $\mu p$  atom is initially formed in a highly excited state with a principal quantum number  $n \sim 14$  and a kinetic energy  $\sim 1$  eV. The excited atom then rapidly de-excites via combinations of Auger emission

$$(\mu p)_n + e \rightarrow (\mu p)_{n'} + e, \quad (10)$$

radiative decay

$$(\mu p)_n \rightarrow (\mu p)_{n'} + \gamma, \quad (11)$$

and Coulomb de-excitation

$$(\mu p)_n + p \rightarrow (\mu p)_{n'} + p. \quad (12)$$

Note that in Auger emission and radiative decay the  $\mu p$  recoil has a relatively small kinetic energy, since the  $e$  or  $\gamma$  carry the released energy, while in Coulomb de-excitation the  $\mu p$  recoil has a relatively large kinetic energy, since the  $\mu p$  and  $p$  share the released energy. Consequently when formed the ground state atom has kinetic energies of typically about 1 eV but occasionally up to 100 eV. For recent experiments on energy distributions of ground state  $\mu p/\pi p$  atoms see Sigg *et al.* (1996) and Schottmüller *et al.* (1999). Note that at formation of the ground state

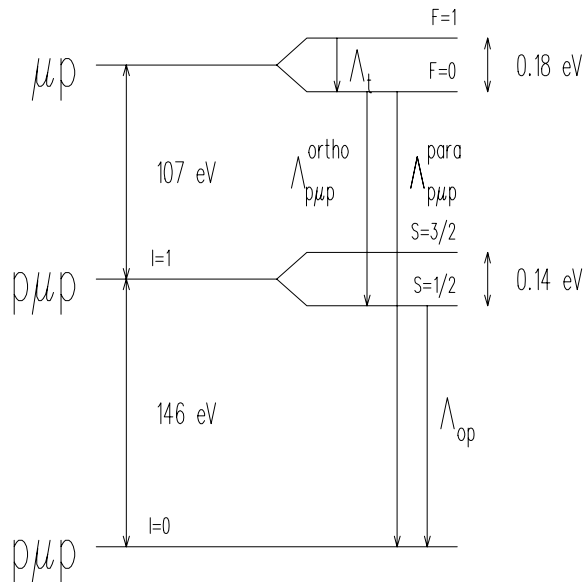
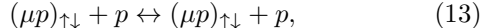


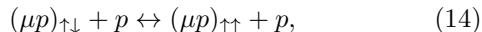
FIG. 1 A simplified diagram of the various atomic and molecular states and transitions relevant to muon capture in pure  $H_2$ .

atom the hyperfine states are statistically populated, *i.e.* 3:1 for  $F_+ : F_-$ .

This ‘hot’ ground state atom is rapidly thermalized by elastic scattering,



and spin-flip collisions,

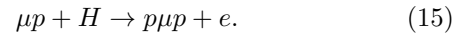


from the atomic nuclei of the neighboring molecules. Here  $\uparrow\uparrow$  denotes the triplet state and  $\uparrow\downarrow$  denotes the singlet state. Once the  $\mu p$  kinetic energy falls below the 0.18 eV  $\mu p$  hyperfine splitting the singlet-to-triplet transitions are energetically forbidden and triplet-to-singlet transitions depopulate the upper  $F_+$  state. The resulting  $F_+$  state lifetime is about 0.1 ns in liquid  $H_2$  and about 10 ns in 10 bar  $H_2$  gas. The short lifetime arises from the large  $\mu p$  scattering cross sections due to a near-threshold  $\mu p + p$  virtual state. For further details of experimental studies of  $\mu p$  scattering in  $H_2$  environments see Abbott *et al.* (1997) and references therein.

At sufficient densities, *i.e.* at pressures exceeding 10 bar, the formation of  $p\mu p$  molecules is important. The molecule (see Fig. 1) comprises a para-molecular ground state, with total orbital angular momentum  $\ell = 0$  and nuclear spin  $I = 0$ , and an ortho-molecular excited state, with total orbital angular momentum  $\ell = 1$  and nuclear spin  $I = 1$ . Note spin-spin and spin-orbit interactions produce a five-fold splitting of the ortho-molecular state with two  $S = 1/2$  sub-states and three  $S = 3/2$  sub-states, where  $S$  is the total spin angular momentum of the  $p\mu p$  complex. Importantly the different states have

different make-ups in terms of  $\mu p$  components with parallel spins (*i.e.*  $F_+$ ) and anti-parallel spins (*i.e.*  $F_-$ ). Specifically the para-state is 3:1 triplet-to-singlet, the  $S = 1/2$  ortho-states are 1:3 triplet-to-singlet, and the  $S = 3/2$  ortho-states are pure triplet. For further details see Bakalov *et al.* (1982).

The  $p\mu p$  molecules are formed by Auger emission



Calculations of the rates for the process have been performed by Faifman and Men’shikov (1999), Faifman (1989), Ponomarev and Faifman (1976), and Zel’dovich and Gershtein (1959). Formation of the ortho-state involves an E1 transition with a predicted rate  $\Lambda_{p\mu p}^{ortho} \simeq n/n_o \times 1.8 \times 10^6 s^{-1}$  and formation of the para-state involves an E0 transition with a predicted rate  $\Lambda_{p\mu p}^{para} \simeq n/n_o \times 0.75 \times 10^4 s^{-1}$ , where  $n/n_o$  is the  $H_2$  target number density normalized to the liquid  $H_2$  number density. Recent measurements of the summed, *i.e.* ortho and para, rate are typically 30% greater than the calculated rate. See Mulhauser *et al.* (1996) for further details.

Note that the E1 transition feeding the ortho-molecular state populates only the  $S = 1/2$  sub-states (*i.e.* yielding a 1:3 ratio of  $F_+ : F_-$  spin-states). Weinberg (1960) and Ando *et al.* (2000) have discussed the possible mixing of the  $S = 1/2, 3/2$  levels which would lead to changes in the 1:3 triplet-to-singlet ratio for the ortho-molecule. However the available calculations of Halpern (1964a,b); Wessel and Phillipson (1964) and Bakalov *et al.* (1982) have suggested such effects are negligible.<sup>2</sup>

At first glance the  $\Delta I = 0$  selection rule for E1 transitions forbids decay of the ortho excited state to the para ground state. However as discussed by Bakalov *et al.* (1982), via the small components of the relativistic wave functions, the ortho state contains  $I = 0$  admixtures and the para state contains  $I = 1$  admixtures. Therefore ortho-to-para E1 transitions occur via cross-combinations of the small components and the large components of the molecular wave functions. Note the rate  $\Lambda_{op}$  for this Auger process is a function of the electron environment of the  $p\mu p$  molecule. Bakalov *et al.* (1982) obtained  $\Lambda_{op} = 7.1 \pm 1.2 \times 10^4 s^{-1}$  assuming an environment consisting of 75%  $[(p\mu p)^+ 2p2e]^+$  and 25%  $[(p\mu p)^+ e]$ . These proportions are a consequence of the Hirshfelder reaction (Hirshfelder *et al.*, 1936) involving  $p\mu p$  complexes and  $H_2$  molecules as discussed by Faifman (1989); Faifman and Men’shikov (1999). Note that the only published experimental value of  $\Lambda_{op} = (4.1 \pm 1.4) \times 10^4 s^{-1}$  from Bardin (1982); Bardin *et al.* (1981b) is in marginal disagreement with the calculation at the  $2\sigma$  level.

<sup>2</sup> In addition the relative rates for  $\mu$  capture in  $H_2$  gas (mostly singlet-atom capture) and  $H_2$  liquid (mostly ortho-molecule capture) are consistent with a 1:3 triplet:singlet make-up of the ortho-molecule. For details see Sec. V.D.

In summary, in  $H_2$  gas at pressures  $0.1 < P < 10$  bar, where the  $F = 1$  atoms disappear very quickly and the  $p\mu p$  molecules form very slowly, the capture process is essentially dominated by singlet atoms. However in liquid  $H_2$  the molecular formation rate  $\Lambda_{p\mu p}$  and ortho-to-para transition rate  $\Lambda_{op}$  are important. Here the rate is a superposition of singlet atomic capture, ortho-molecule capture and para-molecule capture and depends on  $\Lambda_{p\mu p}$ ,  $\Lambda_{op}$ , and the measurement time window.

## B. Muons in pure deuterium

The atomic capture and cascade processes for muons in pure  $D_2$  and pure  $H_2$  are very similar. Most importantly for muons in  $D_2$  the ground state  $\mu d$  atoms are rapidly formed in a statistical mixture of the hyperfine states, *i.e.* 2:1 for  $F_+ : F_-$ .

The  $\mu d$  atoms are then thermalized by elastic scattering

$$(\mu d)_{\uparrow\downarrow} + d \leftrightarrow (\mu d)_{\uparrow\uparrow} + d \quad (16)$$

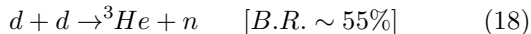
and spin-flip collisions

$$(\mu d)_{\uparrow\downarrow} + d \leftrightarrow (\mu d)_{\uparrow\uparrow} + d \quad (17)$$

on surrounding nuclei. When the  $\mu d$  kinetic energy falls below the 0.043 eV hyperfine splitting the spin-flip collisions then depopulate the higher lying  $F_+$  state. However the cross sections are considerably smaller for  $\mu d + d$  than  $\mu p + p$  and consequently the  $F_+$  lifetime is considerably longer in deuterium than hydrogen. For example in liquid  $D_2$  at 34 K, the hyperfine depopulation rate is  $\Lambda = 42.6 \times 10^6 s^{-1}$ . For further details see Kammel *et al.* (1982, 1983).

An interesting feature of  $\mu d$  chemistry is resonant formation of  $d\mu d$  molecules. For example in liquid  $D_2$ , while  $d\mu d$  formation from  $F = 1/2$   $\mu d$  atoms involves a non-resonant Auger process, the  $d\mu d$  formation from  $F = 3/2$   $\mu d$  atoms involves a resonant excitation process, *i.e.* one where the  $d\mu d$  binding energy is absorbed by  $D_2$  vibro-rotational modes. In liquid  $D_2$  at 34 K the effective rates are  $\Lambda_{d\mu d}^{1/2} \sim 5 \times 10^4 s^{-1}$  for non-resonant, *i.e.* doublet, formation and  $\Lambda_{d\mu d}^{3/2} \sim 4 \times 10^6 s^{-1}$  for resonant, *i.e.* quartet, formation. Note that the resonant formation is temperature dependent. For further details see Breunlich *et al.* (1989).

When  $d\mu d$  molecules are formed, the two deuterons immediately fuse via  $\mu$ -catalyzed fusion



which quickly recycles the muon from the molecular states to the atomic states. Consequently for muons in pure  $D_2$  the deuterium capture is from  $\mu d$  atoms and not

$d\mu d$  molecules, independent of density and temperature. However the  $\mu$  sticking probability in  $\mu$  catalyzed fusion, 13% in Eq. (18) and 1% in Eq. (19), is non-negligible. Consequently with increasing  $D_2$  target density an increasing  $\mu^3He$  capture background is unavoidable.

In summary, for muons in pure  $D_2$  the capture is a superposition of the rates from the doublet atom and the quartet atom and  $\mu$  capture from  $d\mu d$  molecules is completely negligible. Actually for the particular conditions of the  $\mu d$  experiments by Bardin *et al.* (1986) and Cargnelli *et al.* (1989) the deuterium capture is almost entirely from doublet atoms. See Sec. VI.B for details. However due to muon sticking in the  $d\mu d$  fusion process, a correction for backgrounds from  $\mu^3He$  capture is necessary in liquid  $D_2$ .

## C. Muons in hydrogen-deuterium mixtures

Our interest in hydrogen-deuterium mixtures is two-fold. First ‘pure- $H_2$ ’ experiments and ‘pure- $D_2$ ’ experiments must inevitably be concerned with contamination from other isotopes. Second some early experiments on deuterium capture used hydrogen-deuterium mixtures, *e.g.* Wang *et al.* (1965) used 0.3%  $D_2$  in  $H_2$  liquid and Bertin *et al.* (1973) used 5%  $D_2$  in  $H_2$  gas.

Muon transfer from  $\mu p$  atoms to  $\mu d$  atoms



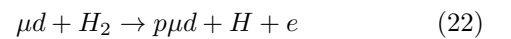
occurs with an energy release of 135 eV and a transfer rate of  $n/n_o \times c_d \times 1.7 \times 10^{10} s^{-1}$ , where  $c_d$  is the  $D_2$  concentration in the  $H_2$  target and  $n/n_o$  the target number density relative to liquid  $H_2$  (Adamczak *et al.*, 1992). Consequently, in  $H_2$  liquid a  $10^{-3}$   $D_2$  concentration and in  $P > 10$  bar  $H_2$  gas a  $10^{-2}$   $D_2$  concentration, is sufficient to engineer the transfer in roughly 100 ns.

Following transfer, the  $\mu d$  atom is thermalized via collisions with  $H_2$  molecules. An interesting feature of  $\mu d + p$  scattering is the Ramsauer-Townsend minimum at a kinetic energy 1.6 eV. The tiny  $\mu d + p$  cross section means slow thermalization and large diffusion of  $\mu d$  atoms in  $H_2$  gas. In addition the slow thermalization and small deuterium concentration makes hyperfine depopulation via spin-flip collisions

$$(\mu d)_{\uparrow\downarrow} + d \leftrightarrow (\mu d)_{\uparrow\uparrow} + d \quad (21)$$

very slow by comparison to  $\mu p$  atoms in pure  $H_2$  and  $\mu d$  atoms in pure  $D_2$ .

At sufficient densities the formation of  $p\mu d$  molecules occurs by Auger emission



with a rate in liquid  $H_2$  of  $\Lambda_{p\mu d} = 5.6 \times 10^6 s^{-1}$  (Petitjean *et al.*, 1990/91). The formation of molecules is important as (i) capture is consequently a superposition of  $\mu d$  reactions and  $\mu p$  reactions, and (ii) the various  $p\mu d$  states have different decompositions into  $\mu d$   $F$ -states. Further

the parent distribution of  $\mu d$  atom  $F^-$ -states effects the resulting distribution of  $p\mu d$  molecule states, making the relative population of  $p\mu d$  states a complicated function of target density and deuterium concentration.

Muon catalyzed fusion from  $p\mu d$  molecules occurs via both radiative reactions



and non-radiative reactions



The radiative rates (Petitjean *et al.*, 1990/91) are  $\Lambda_{1/2} = 0.35 \times 10^6 s^{-1}$  and  $\Lambda_{3/2} = 0.11 \times 10^6 s^{-1}$  and the non-radiative rates are  $\Lambda_{1/2} = 0.056 \times 10^6 s^{-1}$  and  $\Lambda_{3/2} = 0$ , where the subscripts 1/2, 3/2 denote the p-d spin states. The slow rates make  $\mu$  capture from  $p\mu d$  molecules an important contribution at high target densities. Further the 100% sticking probability for the radiative reaction makes  $\mu$  capture in muonic  $^3\text{He}$  a troublesome background.

In summary, both  $\sim 10^{-3}$  D<sub>2</sub> admixtures in H<sub>2</sub> liquid and  $\sim 10^{-2}$  D<sub>2</sub> admixtures in H<sub>2</sub> gas have been used in the study of  $\mu d$  capture. Unfortunately the hyperfine depopulation of  $\mu d$  atoms in H<sub>2</sub>/D<sub>2</sub> mixtures is slow and therefore the doublet-quartet make-up in H<sub>2</sub>/D<sub>2</sub> experiments is dependent on target density and deuterium concentration. Further at densities where  $p\mu d$  molecules are formed, the observed rate of muon capture is a complicated superposition of the  $\mu p$ ,  $\mu d$  and  $\mu^3\text{He}$  rates and thus disentangling the outcome is difficult.

## V. MUON CAPTURE IN HYDROGEN

### A. Theory of ordinary muon capture

#### 1. Standard diagram calculations

The simplest of the muon capture reactions is OMC on the proton,  $\mu + p \rightarrow n + \nu$ , which has been studied theoretically for many years. Some of the early work included that of Primakoff (1959) and Fujii and Primakoff (1959). Opat (1964) evaluated amplitudes for both OMC and RMC in an expansion in powers of  $1/m_N$ . Many other authors have performed similar evaluations of the OMC rate.

The basic physics is completely determined by the weak nucleon current given in Eq. (1), which is the most general possible form consistent with the known current-current form of the weak interaction. Given this current, the OMC amplitude is determined by its product with the leptonic weak current. One then uses standard diagrammatic techniques to square the amplitude, put in phase space and thus obtain an expression for the rate in terms of the coupling parameters  $g_v, g_m, g_a$ , and  $g_p$ . This expression is the same whether the couplings are obtained from purely phenomenological sources or from some detailed fundamental model.

Fortunately a lot is known about the couplings. The weak vector current is completely determined by the well established Conserved Vector Current theory which tells us that the weak vector current is simply an isospin rotation of the isovector electromagnetic current. In practice this means that  $g_v(q^2) = F_1^p(q^2) - F_1^n(q^2)$  and  $g_m(q^2) = \kappa_p F_2^p(q^2) - \kappa_n F_2^n(q^2)$  where  $\kappa_p = 1.79285, \kappa_n = -1.91304$  are the proton and neutron anomalous magnetic moments and where  $F_1^p(q^2), F_1^n(q^2), F_2^p(q^2)$ , and  $F_2^n(q^2)$  are the usual proton and neutron isovector electromagnetic form factors. The coupling  $g_a$  is well determined from neutron beta decay,  $g_a(0) = 1.2670 \pm 0.0035$  (Particle Data Group, 2000). The momentum dependence is known, at least at low momentum transfers, from neutrino scattering (Ahrens *et al.*, 1988) or from pion electroproduction (Choi *et al.*, 1993; Del Guerra *et al.*, 1976; Esaulov *et al.*, 1978). For a long time there was some disagreement between these two sources, but that has now been resolved by a more careful analysis of the corrections necessary in pion electroproduction (Bernard *et al.*, 1992). Thus all of the ingredients for a theoretical calculation of the OMC rate on the proton are well determined by general principles which have been verified in many other situations, except for the value of  $g_p$ , which is given primarily by the theoretical predictions discussed in Section II above.

#### 2. ChPT calculations

The amplitude for OMC on the proton has also been evaluated in the context of HBChPT by Fearing *et al.* (1997). Such calculations start with the general ChPT Lagrangian, in this case through  $O(p^3)$ , and evaluate the amplitude consisting of tree and one loop diagrams. The outcome of such calculations are expressions for couplings appearing in the most general amplitude of Eq. (1) in terms of the LEC's appearing in the Lagrangian. This approach thus provides a systematic way of calculating couplings and their corrections, as was described for  $g_p$  in Section II.B above. However the vector part of the amplitude must still satisfy CVC,  $g_a$  must still reproduce neutron beta decay, etc., so in actual fact the couplings to be used are exactly the same as those which have always been used in the phenomenological approach and there is no new information arising from a ChPT calculation, except perhaps for the (small) correction term appearing in  $g_p$ , Eq. (5). What is accomplished by such a calculation however is to evaluate some of the LEC's which are needed for other calculations, such as RMC.

Similar ChPT evaluations of OMC were subsequently carried out by Ando *et al.* (2000) and Bernard *et al.* (1998). In the latter case the so called small scale expansion was used, which is a way of including the  $\Delta$  as an explicit degree of freedom in the ChPT formalism, rather than absorbing its effects in the LEC's.



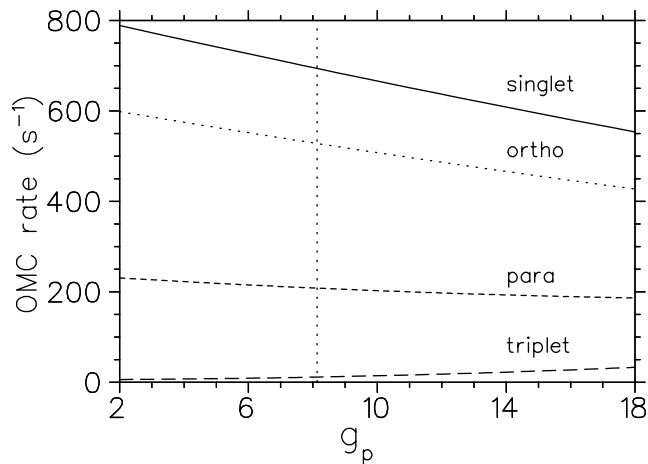


FIG. 2 Capture rates for OMC on a proton plotted versus  $g_p(-0.88m_\mu^2)$  for the muon initially in the singlet or triplet state of the  $\mu p$  atom or in the ortho or para state of the  $p\mu p$  molecule. The vertical line corresponds to the PCAC value of  $g_p = 8.13$ , as defined in Eq. (9), which includes the constant term. Details of the model used are described in Sec. V.D

### 3. Spin effects

When a muon is stopped in hydrogen it proceeds via a rather complicated series of atomic and molecular processes, as was described above, to a low level state in either a  $\mu p$  atom or a  $p\mu p$  molecule from which the muon is captured. The details of this cascade process and relative probabilities for population of the various states depend on the density of the target and the time at which one starts detecting the captures. For now it suffices to note that the capture from any initial state will be a linear combination of captures from the singlet and triplet  $\mu p$  states. Thus it is important to calculate separately the rates from these two spin states.

Figure 2 shows the individual singlet and triplet captures rates for OMC, using a standard diagram calculation<sup>3</sup> (Fearing, 1980), plotted versus the value of  $g_p$ . Clearly the capture rate from singlet state is much larger than that from the triplet state. However it is also much less sensitive to the value of  $g_p$ . Unfortunately, although one can increase the sensitivity to  $g_p$  to some extent by choosing conditions that enhance the triplet contribution, the singlet rate is so much larger that it dominates in essentially all circumstances.

## B. Theory of radiative muon capture

We now want to consider the radiative muon capture process  $\mu + p \rightarrow n + \nu + \gamma$ . The basic ingredients are the same as for OMC and the additional coupling of the photon is known. However the presence of the photon changes the range of momentum transfers available and leads to contributions coming from regions much closer to the pion pole than for OMC. More specifically, for OMC on the proton the momentum transfer is fixed at  $q^2 = -0.88m_\mu^2$ . For RMC however the momentum transfer for some of the diagrams can approach  $+m_\mu^2$ . These diagrams, all of which involve radiation from hadronic legs, are not the dominant ones. The muon radiating diagram dominates, at least in the usual gauge, and it involves similar momentum transfer as for OMC. However the other diagrams contribute enough in the measurable photon energy region  $k > 60$  MeV that the overall sensitivity of RMC to  $g_p$  is significantly increased as compared to OMC.

### 1. Standard diagram calculations

The standard approach to RMC on the proton has been a Feynman diagram approach, Fig. 3(a)-(e), which includes the diagrams involving radiation from the muon, the proton, the neutron via its magnetic moment, and from the exchanged pion which generates the induced pseudoscalar term. The fifth diagram makes the result gauge invariant using a minimal substitution. Opat (1964) performed one of the earliest such calculations, using however a  $1/m_N$  expansion of the amplitude. The completely relativistic calculation of Fearing (1980) is an example of a more modern calculation using this approach.<sup>4</sup>

There are some possible enhancements to this basic approach. For example the intermediate nucleon, between weak and electromagnetic vertices, can in principle be a  $\Delta$ . Such effects, Fig. 3(f)-(g), were considered by Beder and Fearing (1987, 1989). They increase the photon spectrum by amounts ranging from 2-3% at 60 MeV to 7-8% at the upper endpoint. Truhlik and Khanna (2001) found a similar sized effect.

Some additional terms, higher order in an expansion of the RMC amplitude in powers of the photon momentum  $k$  or the momentum transfer  $q$ , were obtained originally by Adler and Dothan (1966). These arise via the requirements of gauge invariance and PCAC for the full amplitude. Similar terms were obtained by Christillin and Servadio (1977) and by Klieb (1985). They however seem to be fairly small.

<sup>3</sup> The calculation has been updated to include form factors and modern values of the couplings, particularly  $g_a$ . The general table of numerical values, Table I, gives the values of parameters and constants used.

<sup>4</sup> Hwang and Primakoff (1978) also evaluated RMC in hydrogen using what they called a linearity hypothesis. This was shown to be incorrect however by Wullschlegel and Scheck (1979), Fearing (1980), and Gmitro and Ovchinnikova (1981).

TABLE I Numerical values of the parameters and derived quantities used in the text and in our evaluations of rates for comparison with experiment.

Symbol	Description	Value	Reference
$F_\pi$	pion decay constant	$92.4 \pm 0.3$ MeV	Particle Data Group (2000)
$g_{\pi NN}(m_\pi^2)$	pion nucleon coupling	$13.05 \pm 0.08$	de Swart <i>et al.</i> (1997)
$G_F V_{ud}$	Fermi constant for $\beta$ decay	$1.13548 \times 10^{-5} \text{GeV}^{-2}$	Particle Data Group (2000)
$g_a(0)$	axial coupling from $\beta$ -decay	$1.2670 \pm 0.0035$	Particle Data Group (2000)
$r_A^2$	rms radius squared for $g_a$	$0.42 \pm 0.04 \text{fm}^2$	Ahrens <i>et al.</i> (1988)
$g_p^{PCAC}$	PCAC value, $g_p(-0.88m_\mu^2)$	$6.77 g_a(0) = 8.58$	Eq. (4)
	PCAC value, including constant term	$6.42 g_a(0) = 8.13$	Eq. (9)
$\Lambda_{p\mu p}$	$p\mu p$ molecular formation rate	$2.5 \times 10^6 \text{s}^{-1}$	average, Wright <i>et al.</i> (1998)
$\Lambda_{p\mu p}^{ortho} / \Lambda_{p\mu p}^{para}$	ratio of ortho to para molecular formation	240 : 1	Faifman and Men'shikov (1999)
$\Lambda_{op}$	ortho to para transition rate	$4.1 \pm 1.4 \times 10^4 \text{s}^{-1}$	Bardin <i>et al.</i> (1981a)
$2\gamma^{ortho}$	ortho-molecular overlap factor	$1.009 \pm 0.001$	Bakalov <i>et al.</i> (1982)
$2\gamma^{para}$	para-molecular overlap factor	$1.143 \pm 0.001$	Bakalov <i>et al.</i> (1982)
$g_m(0)$	weak magnetism coupling, $\kappa_p - \kappa_n$	3.70589	Particle Data Group (2000)
$r_m^2$	rms radius squared for $g_m$	$0.80 \text{fm}^2$	Mergell <i>et al.</i> (1996)
$r_v^2$	rms radius squared for $g_v$	$0.59 \text{fm}^2$	Mergell <i>et al.</i> (1996)

This basic diagrammatic approach clearly contains most of the important physics. However there are some things it does not contain. In particular in the simplest approach gauge invariance is imposed only via a minimal substitution  $p \rightarrow p - eA$  on the explicit momentum dependence of the operators in the weak vertex, Eq. (1). Thus one picks up only two terms, one from the explicit  $q$  in the  $g_m$  term and one from the  $q$  in the  $g_p$  term. In principle there may be many other terms, gauge invariant by themselves, for example coming from situations where the photon couples to some internal loop structure of the  $\pi NN$  vertex.

Also for RMC it is difficult to put form factors in at the various vertices in a general way, though lowest order form factor effects can be included via a low energy expansion as done by Adler and Dothan (1966). This is because the momentum transfer at the various vertices in different diagrams is different and so putting in form factors evaluated at these different momenta would destroy the delicate cancellation needed for gauge invariance. This is not a problem unique to RMC. It appears in any electromagnetic process described by more than one diagram if the momentum transfers are different. Various prescriptions have been proposed to address this problem, but all are pretty much ad hoc. In OMC introducing form factors reduces the rate, but only by a few percent. This is because the relevant momentum transfer is small compared to the scale relevant for the form factor. In RMC all momentum transfers are comparable or smaller than that for OMC, so hopefully the form factors

introduce only a small correction in RMC as well. This turns out to be the case in the simple approach described below.

## 2. ChPT calculations

Just as for OMC, it is possible to calculate the amplitude for RMC using HBCChPT. Unlike OMC however such a calculation introduces some new physics. The ChPT Lagrangian is constructed to satisfy gauge invariance and also CVC and PCAC. Thus the calculated amplitude will satisfy all of these general principles. This means for example that such a calculation may contain explicitly gauge terms beyond the simple minimal substitution used in the standard diagrammatic approach. Figure 4 shows some examples of such terms present in a ChPT calculation which are not present in the diagrammatic calculation. A second advantage of such a calculation is that it automatically incorporates form factors, at least to the order of the calculation. One can calculate weak and electromagnetic form factors explicitly as was done by Fearing *et al.* (1997) or Bernard *et al.* (1998) within ChPT. The same sub-diagrams responsible for these form factors will appear in the RMC calculation, so the form factors will be present in such a calculation, and in a gauge invariant way.

The ChPT approach has one disadvantage however, not shared by the diagrammatic approach. It is an expansion in a small parameter. Thus the calculations are done at best to  $\mathcal{O}(p^3)$  which is sufficient to include tree

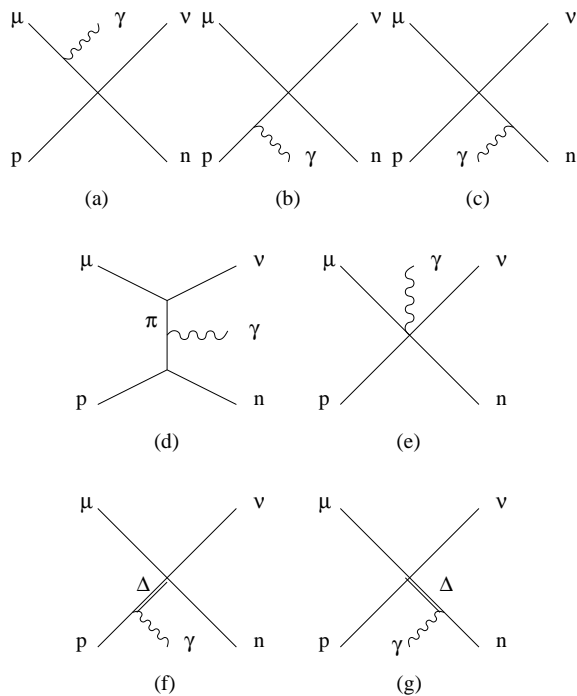


FIG. 3 Diagrams contributing to the standard diagrammatic approach to RMC: (a)-(e) are the standard diagrams, (f) and (g) are those involving  $\Delta$  contributions

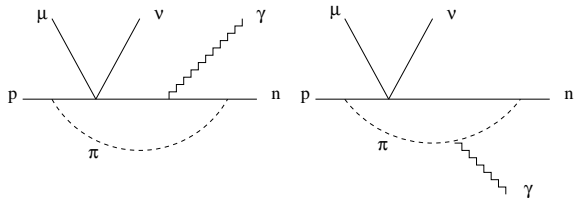


FIG. 4 Several examples of diagrams which appear in a HBChPT calculation but which are not included in the usual minimal substitution gauge contribution of the diagrammatic approach.

level and the lowest contribution to one loop diagrams. In principle a diagrammatic calculation keeps all orders of whatever diagrams are included. In practice however diagrammatic calculations are limited to tree level graphs, so do not include the loop contributions of ChPT and probably at most have only a few higher order terms coming from relativistic corrections which would not be included in the ChPT approach.

The most complete of the HBChPT calculations of RMC has been done by Ando and Min (1998), who worked to third order, *i.e.*  $\mathcal{O}(p^3)$ , or in their terminology NNLO (next to next to leading order). They found that the loop contributions contributed less than 5% correction to the tree level amplitude and that the result was in reasonable agreement with the standard diagrammatic approach.

A similar calculation, but just involving tree level diagrams, and working only to  $\mathcal{O}(p^2)$  was performed by Meissner *et al.* (1998). They initially found a photon spectrum harder by 10% or so than that of the diagrammatic approach in the region of photon energies greater than 60 MeV, but this was later attributed (Myhrer, 1999) to unwarranted approximations made in the phase space evaluation. A similar  $\mathcal{O}(p^2)$  calculation was done by Bernard *et al.* (2001b) who however used the so called small scale expansion which allows one to put the  $\Delta$  in explicitly. Such an approach is not fundamentally different from the usual HBChPT approach. It just allows one to extract explicitly the contribution of the  $\Delta$  to the various LEC's. In the usual approach the  $\Delta$  degrees of freedom are integrated out and their effects absorbed in the LEC's. These authors found results similar to those of earlier diagrammatic calculations and specifically that the  $\Delta$  contribution was only of order of a few percent, consistent with the findings of Beder and Fearing (1987, 1989).

### 3. Model calculations

Recently there has been a somewhat different model calculation of RMC (Truhlik and Khanna, 2001) based on a  $\pi\rho\omega a_1$  Lagrangian which also includes  $\Delta$ 's (Smejkal *et al.*, 1999). This is basically a diagrammatic approach, but based on a Lagrangian which has a number of additional pieces, and which thus results in an explicitly gauge invariant expression, which also satisfies CVC and PCAC and which generates some of the higher order terms analogous to those derived by Adler and Dothan (1966). For the best values of the parameters the  $\Delta$  contributions range from about 3-7% which can be increased to roughly 7-11% at the extreme edge of the allowed parameter space. Thus their results are very similar to those obtained by Beder and Fearing (1987, 1989), and so this model would seem to give a result only a few percent different from the ChPT result or from the standard diagrammatic approach including the  $\Delta$ .

### 4. Spin effects

For RMC, just as for OMC, there are fairly dramatic differences in the capture rate from singlet and triplet initial states, and likewise in sensitivities to  $g_p$ . Figure 5 shows the integrated photon spectrum above 60 MeV plotted versus  $g_p$  for RMC on the proton. Now it is the triplet state which dominates and the singlet which is most sensitive to  $g_p$ , just the opposite situation from OMC. Furthermore, if one looks at the RMC photon spectrum before integration (Beder and Fearing, 1989) one sees that variations in  $g_p$  about the PCAC value tend to affect the singlet rate more at the upper end of the spectrum than at the lower end, whereas for the triplet state the change is more uniform across the spec-

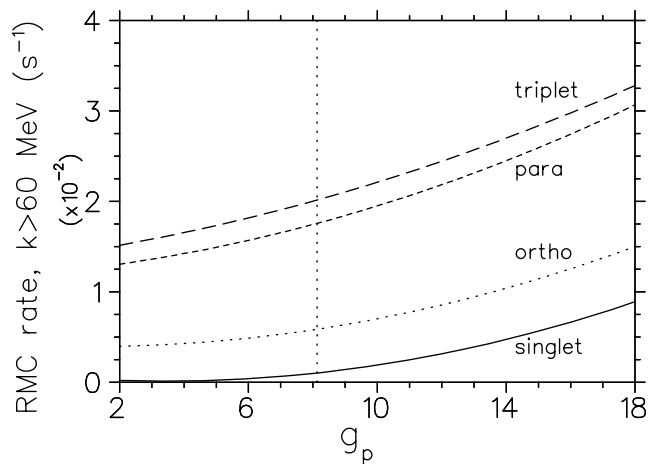


FIG. 5 The photon spectrum for RMC on a proton, integrated from 60 MeV to the upper end point, shown as a function of  $g_p(-0.88m_\mu^2)$ . Shown separately are the rates for the muon initially in the singlet or triplet state of the  $\mu p$  atom or in the ortho or para state of the  $p\mu p$  molecule. The vertical line corresponds to the PCAC value of  $g_p = 8.13$ , as defined in Eq. (9), which includes the constant term. Details of the model used are described in Sec. V.D

trum. This further enhances the sensitivity to  $g_p$ , since it is the upper end of the spectrum which is experimentally accessible.

Finally one should note that the effects which change the relative proportion of singlet and triplet states work in different directions for OMC and RMC. This is because triplet capture is most important for RMC whereas singlet capture is most important for OMC. Thus for example, some effect which increases the proportion of the triplet state relative to the singlet will decrease the OMC rate and increase the RMC rate, for a given value of  $g_p$ .

### C. Experimental methods for hydrogen and deuterium

Herein we discuss the experimental methods for muon capture on hydrogen and deuterium. They include measurements of ordinary capture via neutron detection, Sec. V.C.3, Michel electron detection, Sec. V.C.2, and radiative capture via  $\gamma$ -ray detection, Sec. V.C.4.

#### 1. Bubble chamber studies

The first observations of OMC on hydrogen were reported by Hildebrand (1962), Bertolini *et al.* (1962) and Hildebrand and Doede (1962). In these early bubble chamber experiments the muons were identified by range and curvature and neutrons were identified via their knock-on protons. An attractive feature of bubble chamber studies is the determination of the neutron energy from the measurement of the proton kinematics. This is helpful in distinguishing the neutrons from OMC

in  $H_2$  from combinatorial backgrounds of uncorrelated muons and knock-on protons. Recall the neutrons from OMC in  $H_2$  are mono-energetic  $E_n = 5.2$  MeV. However the bubble chamber studies were limited by statistics.

#### 2. Lifetime method

The ‘lifetime method’ involves comparing the negative muon lifetime and positive muon lifetime when stopped in hydrogen or deuterium. For positive muons the lifetime is the inverse of the  $\mu$  decay rate, whereas for negative muons the lifetime is the inverse of the sum of the  $\mu$  decay rate and the  $\mu$  capture rate. The lifetime difference thus determines the capture rate. This approach was used at Saclay to determine the  $\mu$  capture rate in liquid  $H_2$  (Bardin *et al.*, 1981a) and liquid  $D_2$  (Bardin *et al.*, 1986).

The Saclay experiments used a pulsed beam with typically a 3000 Hz repetition rate and typically a 3.0  $\mu s$  pulse width. The beam entered via a lead collimator and a copper degrader, stopping in a 24 cm diameter Cu-walled target. The target was filled with  $LH_2$  or  $LD_2$  with high elemental and isotopic purity. The target was viewed by six Michel electron telescopes each comprising a three-ply plastic scintillator sandwich. A quartz oscillator was used to determine the time between the beam pulse start signal and the decay electron stop signal. Note that the stop signals were recorded in time windows of about  $1 \mu s < t < 16 \mu s$  following the end of the beam pulse.

The major challenge in the lifetime experiment is the required accuracy. Since the  $\mu$  decay rate is about 1000 times the  $\mu$  capture rate, the  $\mu^+ - \mu^-$  lifetime difference is only about 0.1%. Consequently a determination of the capture rate  $\Lambda$  to about 5% requires a measurement of the lifetime  $\tau$  to about  $5 \times 10^{-5}$ . Therefore both high statistics and low systematics are important.

One concern is muon stops in non-hydrogen materials. Detection of decay electrons from extraneous materials will alter the time spectrum and distort the measured lifetime. Note that the degrader, collimator, and target cell were all constructed from high- $Z$  materials, so muon stops were rapidly absorbed. Also special care was taken to avoid the occurrence of muon stops in plastic scintillator. Lastly,  $H_2$  or  $D_2$  of ultra-high elemental and isotopic purity was used. For  $\mu p$  experiments a small quantity of  $D_2$  in  $H_2$  will result in  $\mu$ -transfer (see Sec. IV.C). For  $\mu d$  experiments, where muons are quickly recycled from  $d\mu d$  molecules to  $\mu d$  atoms (see Sec. IV.B), the effects of muon transfer to high- $Z$  contaminants are especially troublesome.

Another concern is a time distortion due to rate effects, *i.e.* distortion arising from finite resolving time and electron pulse pile-up. Bardin *et al.* (1981a) found the main effect of pulse pile-up is an additional time component with an effective lifetime  $\tau/2$ . They corrected for this effect by measuring lifetimes at different rates and

extrapolating to zero. The correction to  $\tau$  was roughly  $\sim 0.1$  ns. Additionally time dependent and time independent physical backgrounds were accounted for.

In  $\mu d$  experiments a correction is also necessary for  $\mu$  capture on  ${}^3\text{He}$  nuclei. The  $\mu{}^3\text{He}$  atoms are produced via  $d\mu d$  formation and  $dd$  fusion (see Sec. IV.B). The  ${}^3\text{He}$  background, which was monitored by the detection of the 2.5 MeV neutrons from the  $dd$  fusion, was a 10% correction in the Saclay  $\mu d$  experiment.

Finally we note that although the Saclay group measured both the  $\mu^+$  and  $\mu^-$  lifetimes they employed the then available world average values for  $\tau_+$  in order to extract the capture rates in  $\text{LH}_2$  and  $\text{LD}_2$ . The earlier hydrogen experiment used  $\tau_+ = 2197.148 \pm 0.066$  ns (Bardin *et al.*, 1981a), though this was later updated by Martino (1982, 1984). The later deuterium measurement (Bardin *et al.*, 1986) used  $\tau_+ = 2197.03 \pm 0.04$  ns. This point is discussed in detail in Sec. V.D.

### 3. Neutron method

The ‘neutron method’ involves directly detecting the recoil neutrons from muon capture in  $\text{H}_2$  or  $\text{D}_2$ . For hydrogen capture the neutrons are mono-energetic with  $E_n = 5.2$  MeV while for deuterium capture the neutrons are peaked at  $E_n \sim 1.5$  MeV. Hydrogen data is available on liquid targets from Bleser *et al.* (1962) and Rothberg *et al.* (1963) and on gas targets from Alberigi-Quaranta *et al.* (1969) and Bystritskii *et al.* (1974). Deuterium data is available in pure  $\text{D}_2$  from Cargnelli *et al.* (1989) and  $\text{H}_2/\text{D}_2$  mixtures from Wang *et al.* (1965) and Bertin *et al.* (1973).

The ‘neutron method’ involves (i) counting the incoming muons and outgoing neutrons and (ii) determining their corresponding detection efficiencies. In a typical set-up the  $\mu$ -beam is directed into the target vessel via a scintillator telescope and the neutrons are detected in a liquid scintillator counter array. Pulse-shape analysis enables the separation of neutrons from  $\gamma$ -rays and veto counters enable the separation of neutrons from electrons. Both electrons and gammas from  $\mu$ -decay are intense backgrounds. Typically the detection of neutrons is initiated about 1  $\mu\text{s}$  after  $\mu$  arrival.

The low yield of capture neutrons from OMC in  $\text{H}_2$  or  $\text{D}_2$  means neutron backgrounds from  $\mu$  capture in surrounding materials,  $\mu$  transfer to target impurities, and other sources, are troublesome. By using high- $Z$  materials for the collimator, vessel, etc., the neutron backgrounds from  $\mu$  stops in extraneous materials are short-lived.<sup>5</sup> By using high-purity gas/liquid with small  $Z > 1$

contamination the problem of transfer is minimized. Additionally a neutron background generated by the combination of Michel bremsstrahlung and  $(\gamma, n)$  reactions is observed. These photo-neutrons have the 2.2  $\mu\text{s}$  lifetime of the  $\mu$  stops. Therefore studies with  $\mu^+$  stops, yielding photo neutrons without capture neutrons, are necessary to subtract this background.

Also the accurate determination of the neutron detection efficiency is a difficult problem. Calibration via the 8.9 MeV neutrons from the  $\pi^- p \rightarrow \gamma n$  reaction is helpful, but careful simulations of neutron interactions in counters, target, etc., are necessary.

Note that the deuterium experiment using the neutron method is especially challenging. First the deuterium neutrons form a continuous distribution peaking at 1.5 MeV. Second a large background is produced by  $dd$  fusion following  $d\mu d$  formation.

### 4. Radiative capture

RMC on  $\text{H}_2$  has a yield per muon stop of  $\sim 10^{-8}$  and a continuum gamma-ray spectrum with  $E_\gamma \leq 99.2$  MeV. The first measurement of RMC on  $\text{H}_2$  was recently accomplished at TRIUMF (Jonkmans *et al.*, 1996; Wright *et al.*, 1998).

The experiment detected photons from  $\mu$  stops in liquid  $\text{H}_2$ . An ultra-pure muon beam ( $\pi/\mu = 10^{-3}$ ) was directed into a liquid  $\text{H}_2$  target via a scintillator telescope. The target flask and vacuum jacket were constructed from Au and Ag in order to ensure wall stops in high- $Z$  materials. The flask contained pure hydrogen with a  $\text{D}_2$  contamination of about 1 ppm and a  $Z > 1$  contamination of less than 1 ppb. The  $\gamma$ -ray detector was a high acceptance, medium resolution, pair spectrometer and comprised a lead cylinder for  $\gamma$ -ray conversion, cylindrical multiwire and drift chambers for  $e^+e^-$  tracking, and axial B-field for momentum analysis. The photon detection efficiency was  $\epsilon\Omega \sim 10^{-2}$  and photon energy resolution was  $\Delta E/E \sim 10\%$ .

The major difficulty in RMC on  $\text{H}_2$  is the tiny yield. Consequently photon backgrounds from pion stops in liquid hydrogen, muon capture in nearby materials, and  $\mu$  decay are dangerous.

Pion stops in liquid  $\text{H}_2$  undergo both charge exchange,  $\pi^- p \rightarrow \pi^0 n$ , and radiative capture,  $\pi^- p \rightarrow \gamma n$ . The resulting photons comprise a Doppler spectrum of 55–83 MeV and monoenergetic peak at 129 MeV, thus endangering the region of interest for RMC on  $\text{H}_2$ . Wright *et al.* (1998) suppressed this background via an ultra-high purity muon beam, prompt photon timing cut, and the difference in the  $\pi/\mu$  ranges. Additionally the authors determined the residual background from the 55–83 MeV photons via the residual signal from the 129 MeV  $\gamma$ -ray peak.

The bremsstrahlung of electrons from  $\mu$ -decay yields a continuum background with  $E_\gamma < m_\mu/2$ . It prevents the measurement of the RMC spectrum below 53 MeV

<sup>5</sup> Further, the experiments of Alberigi-Quaranta *et al.* (1969), Bertin *et al.* (1973), and Bystritskii *et al.* (1974) used a counter arrangement in the target vessel to define the  $\mu$ -stops in hydrogen.

and threatens the measurement of the RMC spectrum above 53 MeV, because of the finite resolution of the pair spectrometer. Wright *et al.* (1998) designed their spectrometer to minimize the contribution of the high-energy tail in the response function. Additionally the remaining background from Michel bremsstrahlung was measured by stopping a  $\mu^+$  beam in liquid H<sub>2</sub>, yielding the photon background from  $\mu$  decay without the photon signal from  $\mu$  capture.

In addition the backgrounds from  $\mu$  stops in extraneous materials and  $\mu$  transfer to target impurities were minimized by (i) using high-Z materials in the target vicinity and (ii) using high isotopic purity H<sub>2</sub> as the target material. Also ancillary measurements were employed to determine the photon backgrounds from accelerator sources and cosmic-ray interactions.

The experiment recorded  $397 \pm 20$  photons with energies  $E_\gamma > 60$  MeV and times  $t > 365$  ns. After subtracting the backgrounds from  $\mu$ -decay bremsstrahlung ( $48 \pm 7$ ), Au/Ag radiative  $\mu$  capture ( $29 \pm 11$ ), and other sources, a total of  $279 \pm 26$  photons from RMC in liquid H<sub>2</sub> was obtained. The resulting partial branching ratio for RMC on liquid H<sub>2</sub>, *i. e.* the integrated photon spectrum for  $k > 60$  MeV divided by the sum of the muon decay and capture rates, was  $R_\gamma(k > 60 \text{ MeV}) = (2.10 \pm 0.21) \times 10^{-8}$ . Note this value corresponds to the particular occupancy of the  $\mu p$  spin-states in the TRIUMF experiment, *i. e.* with  $t > 365$  ns at liquid H<sub>2</sub> densities.

#### D. Comparison of experiment and theory

In Table II we summarize the results of the various measurements of muon capture on hydrogen. For each experiment we have shown the density of the target  $n/n_0$ , relative to liquid hydrogen, the approximate time delay from muon stop until counting starts  $\Delta t$ , the time averaged proportion of singlet, ortho and para states relevant for the experiment, and the rate obtained under these conditions. Note that the singlet/ortho/para ratios depend on the muon chemistry, and the underlying parameters determining that chemistry, and the delay time  $\Delta t$ . In Table II we used a  $p\mu p$  molecular formation rate  $\Lambda_{p\mu p} = 2.5 \times 10^6 \text{ s}^{-1}$ , a ratio of ortho-state formation to para-state formation of 240:1 (Faifman and Men'shikov, 1999; Ponomarev and Faifman, 1976; Zel'dovich and Gershtein, 1959), an ortho-to-para transition rate  $\Lambda_{op} = 4.1 \times 10^4 \text{ s}^{-1}$  (Bardin *et al.*, 1981a), and gamma factors of  $2\gamma^{ortho} = 1.009$  and  $2\gamma^{para} = 1.143$  (Bakalov *et al.*, 1982). Furthermore the rates tabulated correspond to different experimental conditions and so are not directly comparable.

First we stress that the various experiments are sensitive to different combinations of the  $\mu$  atomic and molecular states, *i. e.* the triplet, singlet, ortho and para states. The situation is simplest in the H<sub>2</sub> gas experiments of Alberigi-Quaranta *et al.* (1969) and Bystritskii *et al.*

(1974) where muon capture is almost exclusively from the  $F = 0$  atomic state and  $p\mu p$  molecule formation is a few percent correction. However for experiments in liquid H<sub>2</sub>, while capture from the ortho state is the largest, capture from other states is significant. The precise blend of states is determined by the delay  $\Delta t$  between the muon arrival time and the counting start time. The greater the delay the smaller the contribution from the  $F = 0$  atomic state and the larger the contribution from the para molecular state, as the muon has additional time to form the  $p\mu p$  molecular state and convert from ortho to para state, in accord with the processes described in Sec. IV. Thus for example the bubble chamber experiments, where  $\Delta t = 0$ , have therefore the largest contribution of singlet atom capture and smallest contribution of para molecule capture. In contrast the Saclay lifetime experiment, where  $\Delta t \sim 2.5 \mu\text{s}$ , had the smallest contribution of singlet atom capture and, though still dominated by ortho capture, the largest contribution of capture from the para state.<sup>6</sup>

In the last column of this table is given the value of  $g_p$  corresponding to the experimental rate. To get these numbers the singlet and triplet capture rates were calculated and combined as appropriate for the experimental conditions of the individual experiment. The model used was the standard diagrammatic approach of Fearing (1980) updated to the extent that modern values of the couplings, particularly  $g_a = 1.267$ , were used and form factors were included. These form factors were taken to be of the form  $f(q^2) = 1 + q^2 \langle r^2 \rangle / 6$  with the values of the rms radii squared  $\langle r^2 \rangle$  taken as  $0.59 \text{ fm}^2$  and  $0.80 \text{ fm}^2$  for  $g_v$  and  $g_m$  (Mergell *et al.*, 1996) respectively and  $0.42 \text{ fm}^2$  for  $g_a$  (Ahrens *et al.*, 1988). At the momentum transfer appropriate for OMC these form factors are typically  $0.98 - 0.96$  so that including them reduces the theoretical OMC rate by 2-4%. The constant term appearing in  $g_p$ , as in Eq. (5) or (9), was included and  $g_p$  was parameterized as

$$g_p(q^2) = R \frac{2m_\mu m_N}{(m_\pi^2 - q^2)} g_a(0) - \frac{m_\mu m_N g_a(0) r_A^2}{3}. \quad (25)$$

Here  $R$  is not intended to have physical significance, but just be a conventional way of parametrizing the variation of  $g_p$  from the PCAC value. At the PCAC point,  $R = 1$  and  $g_p(-0.88m_\mu^2) = 8.58 - 0.45 = 8.13$ .

For RMC form factors were included also using the  $1 + q^2 \langle r^2 \rangle / 6$  form and the necessary gauge terms were generated via a minimal substitution. This gives a gauge invariant result which includes most of the terms found by Adler and Dothan (1966). For RMC these form factors make essentially no difference, *e.g.*  $< 1\%$  in the rate corresponding to the TRIUMF experiment, pre-

<sup>6</sup>  $\Delta t \sim 2.5 \mu\text{s}$  is an approximate average value for the Saclay experiment. In analyzing the data the detailed time structure had to be explicitly treated.

TABLE II Summary of world data for OMC and RMC on hydrogen. The columns correspond to the target density in units of liquid hydrogen density  $n_o$ , the time delay between  $\mu$  stop and start of counting, the effective, time averaged, singlet/ortho/para ratio corresponding to the particular experimental conditions, the capture rate corresponding to these ratios, and the value of  $g_p$  implied using the calculation described in the text. For RMC the value given in the rate column corresponds to  $R_\gamma(k > 60MeV)$ , the partial branching ratio obtained by integrating the photon spectrum above  $k = 60MeV$  and dividing by the sum of the  $\mu$  decay and capture rates. Note that the ratios of molecular states in the S:O:P column depend on the parameters, e. g.  $\Lambda_{op}$ , used, and are given only for those experiments that measure the neutron or gamma yield. For the Saclay experiment (Bardin *et al.*, 1981a) the relationship between the measured rate and the ortho capture rate depends on details of the experiment and is given in the original paper.

Ref.	n/n <sub>o</sub>	$\Delta t(\mu s)$	S:O:P	rate ( $s^{-1}$ )	$g_p(-0.88m_\mu^2)$
OMC					
Hildebrand (1962)	1.0	0.0	0.15:0.77:0.07	$420 \pm 120$	$19.5 \pm 11.6$
Hildebrand and Doede (1962)	1.0	0.0	0.15:0.77:0.07	$428 \pm 85$	$18.7 \pm 8.2$
Bertolini <i>et al.</i> (1962)	1.0	0.0	0.15:0.77:0.07	$450 \pm 50$	$16.4 \pm 4.9$
Bleser <i>et al.</i> (1962)	1.0	1.0	0.01:0.88:0.11	$515 \pm 85$	$6.3 \pm 8.7$
Rothberg <i>et al.</i> (1963)	1.0	1.2	0.01:0.88:0.12	$464 \pm 42$	$11.4 \pm 4.2$
Alberigi-Quaranta <i>et al.</i> (1969)	0.014	0.9	1.00:0.00:0.00	$651 \pm 57$	$11.0 \pm 3.8$
Bystritskii <i>et al.</i> (1974)	0.072	1.4	1.00:0.00:0.00	$686 \pm 88$	$8.7 \pm 5.7$
Bardin <i>et al.</i> (1981a)(original $\tau_+$ )	1.0	2.5	–	$460 \pm 20$	$7.9 \pm 3.0$
(new $\tau_+$ )				$435 \pm 17$	$10.6 \pm 2.7$
RMC					
Wright <i>et al.</i> (1998)(original theory)	1.0	0.365	0.06:0.85:0.09	$(2.10 \pm 0.21) \times 10^{-8}$	$12.4 \pm 0.9 \pm 0.4$
(new theory)					$12.2 \pm 0.9 \pm 0.4$

sumedly because both spacelike and timelike momentum transfers contribute and, with the linear approximation for the form factors, tend to cancel. The  $\Delta$  was included as in Beder and Fearing (1987, 1989).

The OMC results obtained from this calculation are in very good agreement with other modern OMC calculations such as those of Ando *et al.* (2000) and Bernard *et al.* (2001b). It is interesting to observe however that the values of  $g_p$  quoted in Table II are 0.3-0.8 higher than those in a similar table given in Bardin *et al.* (1981b). This can be traced to two main effects, namely the increase in  $g_a$  to its modern value, 1.254→1.267, and the use of more modern form factors which fall somewhat less rapidly with  $q^2$  than those used in Bardin *et al.* (1981b). Both of these effects lead to a larger theoretical rate for a given value of  $g_p$  and thus, as can be seen from Fig. 2, to a larger  $g_p$  to fit a given experimental rate.

A further comment is required concerning the value of  $g_p$  obtained from the Saclay experiment (Bardin *et al.*, 1981a,b). In analyzing their data the authors extracted the capture rate from the difference between their measured value for  $\tau_-$  and the world average value for  $\tau_+$ . They used the world average for comparison because their measured value for  $\tau_+$ , although consistent with the world average, had a larger uncertainty. Since the publication of Bardin *et al.* (1981a) the world average of  $\tau_+$

has changed from  $2197.15 \pm 0.07$  ns to  $2197.03 \pm 0.04$  ns (Particle Data Group, 2000). In determining  $g_p$  for Table II we decided it best to update the  $\mu^+$  lifetime in extracting the  $\mu^-$  capture rate,<sup>7</sup> which now becomes  $435 \pm 17s^{-1}$  instead of  $460 \pm 20s^{-1}$ . Therefore the value of  $g_p(-0.88m_\mu^2) = 10.6 \pm 2.7$  in Table II is one standard deviation larger than  $g_p(-0.88m_\mu^2) = 7.9 \pm 3.0$  which is obtained from the original published rate with our theoretical calculation, and even larger than the value  $g_p(-0.88m_\mu^2) = 7.1 \pm 3.0$  given in the original paper (Bardin *et al.*, 1981b).

The values of  $g_p(-0.88m_\mu^2)$  obtained from the five more recent, electronic, OMC experiments are all in general agreement within their errors and result in a world average value  $10.5 \pm 1.8$ . The single determination with the smallest uncertainty is that of Bardin *et al.* (1981b) which gives  $10.6 \pm 2.7$ . Both of these values are somewhat larger than the PCAC prediction  $g_p(-0.88m_\mu^2) = 8.13$ , which includes the constant term, though are consistent with it at the 1 to 1.3 standard deviation level. Note that

<sup>7</sup> This was also done, in a conference proceedings, by one of the members of the original experimental group. See Martino (1984).

if one does not update the  $\mu^+$  lifetime in the Bardin *et al.* (1981b) analysis the Saclay result is  $g_p(-0.88m_\mu^2) = 7.9 \pm 3.0$  and world average is  $g_p(-0.88m_\mu^2) = 9.4 \pm 1.9$ , both of which are also consistent with PCAC, but both still about 0.7 larger than the corresponding numbers,  $7.1 \pm 3.0$  and  $8.7 \pm 1.9$  quoted in the original paper, because of the updates to the parameters of the theory.

However the result  $g_p(-0.88m_\mu^2) = 12.4 \pm 0.9 \pm 0.4$ , or  $12.2 \pm 1.1$  using the updated theory, from the TRIUMF radiative capture experiment (Wright *et al.*, 1998) is 50% larger than, and clearly inconsistent, with PCAC. Note that the RMC result is quite consistent with the world average from OMC or the Saclay result for  $g_p$  if one uses the updated  $\mu^+$  lifetime. However, with the older  $\mu^+$  lifetime that Bardin *et al.* (1981b) have used, the Saclay result and RMC result do not overlap within their uncertainties.

We can thus summarize the situation in hydrogen as follows. The RMC result is several standard deviations larger than the PCAC prediction and clearly inconsistent with it. The OMC results have always been considered to be in agreement with PCAC, based on the results of the Saclay experiment. We have seen though that, as a result of updates to the parameters in the theory and to subsequent measurements of the  $\mu^+$  lifetime, the value of  $g_p$  obtained from the OMC result has increased. The increase is only about one standard deviation, so the result is still marginally consistent with PCAC. The central value however is now also high, and actually somewhat closer to the RMC result than to the PCAC value.

## E. Attempts to resolve the discrepancy

### 1. General comments

In the previous section we saw that the results for  $g_p$  obtained from RMC were significantly higher than the PCAC prediction and in definite disagreement. The new interpretation of the OMC results suggest that they are too high also, being in good agreement with the RMC result, but perhaps only marginally consistent with PCAC. Since the older interpretation of the OMC data seemed to be in good agreement with PCAC, there has been essentially no consideration of possible difficulties with OMC. However the discrepancy between the RMC results and PCAC has generated a lot of discussion and a number of attempts to find additional effects to explain it, some of which will be now discussed.

A first question one asks is it logical to have a different  $g_p$  for RMC and OMC? At a fundamental level the value of  $g_p$  should be the same. However given the present state of analysis, an apparent difference could arise simply because RMC is much more complicated than OMC and involves a lot of additional diagrams. Thus if something is left out of the RMC analysis, a fit to the data using the standard approach may require a different value of  $g_p$  to compensate for the piece left out. In this view a difference

in the values of  $g_p$  extracted from OMC and RMC using current theory may reflect something wrong or missing in the theory rather than a failure of the PCAC relation of Eq. (5). Note however that while a difference between the values of  $g_p$  extracted from OMC and RMC might be rationalized this way, this would not explain any differences between the OMC and PCAC results since for OMC  $g_p$  is a parameter in the most general weak amplitude. It can thus be determined from data largely independently of the details of the weak capture part, as opposed to the molecular and atomic part, of the theory.

A second question to ask is what does it take to bring the RMC result closer to PCAC, and what does that do to OMC? As discussed earlier the rates for both RMC and OMC depend strongly on the proportion of singlet versus triplet components in the initial state. To get the RMC result to agree better with PCAC we need to increase the predicted rate for a given  $g_p$ , which can be done by increasing the amount of triplet capture and reducing the singlet capture. Since OMC is dominated by the singlet rate, this reduces the OMC rate, which also moves the extracted  $g_p$  toward the PCAC value. However the sensitivity of OMC and RMC to increasing triplet is different, and thus it becomes difficult to completely fix one without destroying the agreement of the other.<sup>8</sup>

In any case, in the subsequent paragraphs we will discuss several aspects of the muon chemistry which change the average singlet/ortho/para ratio for each experiment and thus in principle affect the comparison of the results with PCAC. We will also discuss two other suggestions, dealing specifically with the RMC calculation which have been put forward as potentially resolving the discrepancy implied by the RMC results.

### 2. Value of the ortho-para transition rate $\Lambda_{op}$

As has been noted, the experimental combination of singlet and triplet states is important, and this is determined by the various transition rates governing the chemical processes the muon undergoes between stopping and capture. The least certain of these rates is  $\Lambda_{op}$ , the ortho-para transition rate. There is a single theoretical value  $\Lambda_{op} = (7.1 \pm 1.2) \times 10^4 s^{-1}$  (Bakalov *et al.*, 1982)

---

<sup>8</sup> To get simultaneous agreement of both the TRIUMF RMC result and Saclay OMC result with PCAC a larger increase in triplet occupancy is needed for RMC than for OMC. Since the TRIUMF RMC experiment detected the majority of its photons with muon capture times less than a few  $\mu s$ , whereas the Saclay OMC experiment detected the majority of its electrons with muon decay times more than a few  $\mu s$ , in principle such circumstances are possible. For example a long-lived, i.e.  $\sim 1 \mu s$  lifetime, triplet atom component could increase triplet occupancy for the TRIUMF RMC experiment much more than for the Saclay OMC experiment. However, such a long-lived triplet atom is completely at odds with our current knowledge of muon chemistry in liquid hydrogen.



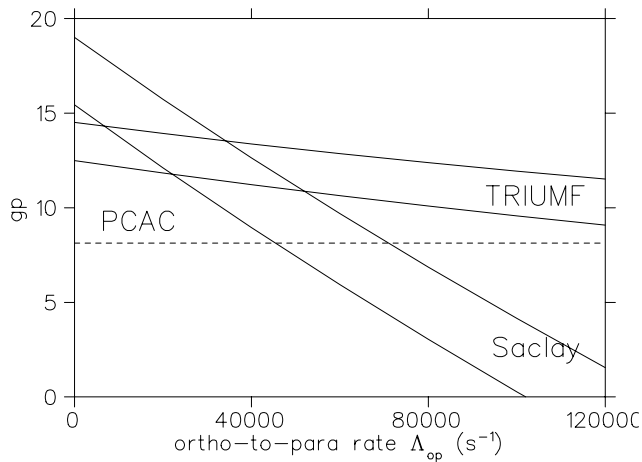


FIG. 6 The region in the  $g_p - \Lambda_{op}$  plane which is allowed by the TRIUMF RMC experiment (Wright *et al.*, 1998) and the Saclay OMC experiment (Bardin *et al.*, 1981a). The dashed line indicates the PCAC value,  $g_p^{PCAC} = 8.13$ , as defined in Eq. (9), which includes the constant term. Details of the model used are described in Sec. V.D. Note that in determining the error bands the uncertainty included in the experimental results due to the uncertainty in  $\Lambda_{op}$  has not been included, as the results are being plotted against  $\Lambda_{op}$ .

which however is nearly a factor of two larger than the experimental value  $(4.1 \pm 1.4) \times 10^4 s^{-1}$  (Bardin, 1982; Bardin *et al.*, 1981b),<sup>9</sup> though another experiment is in progress (Armstrong *et al.*, 1995). A larger value of  $\Lambda_{op}$  increases the relative amount of para state, and thus increases the amount of the triplet component contained in the initial state. Figure 6 shows the region in the  $g_p - \Lambda_{op}$  plane allowed by the TRIUMF RMC experiment (Wright *et al.*, 1998) and the latest OMC experiment (Bardin *et al.*, 1981a).

For these experiments an increase in the value of  $\Lambda_{op}$ , which leads to a greater triplet component in the initial state, increases the predicted RMC rate and decreases the OMC rate for a given value of  $g_p$ . In the vicinity of the PCAC value of  $g_p$ , the RMC rate increases and the OMC rate decreases with increasing  $g_p$ . This means that for fixed value of the rate the extracted value of  $g_p$  decreases with increasing  $\Lambda_{op}$  for both OMC and RMC, as can be seen from the figure. However the Saclay OMC experiment is much more sensitive to  $\Lambda_{op}$  than the TRIUMF RMC experiment.

The updates and improvements we have made in the theory, which raise the OMC band in this figure, make it a little easier to accommodate a larger value of  $\Lambda_{op}$  and still have consistency between OMC and RMC. In fact now a modest increase in  $\Lambda_{op}$  from the experimental value which has normally been used improves the agree-

ment of both OMC and RMC with PCAC while keeping them consistent. However increasing  $\Lambda_{op}$  enough to get agreement of OMC with PCAC or increasing it further to the theoretical value still leaves RMC several standard deviations above the PCAC prediction. Increasing it sufficiently to produce the PCAC value of  $g_p$  from the RMC data would lead to a catastrophic disagreement between the Saclay OMC experiment and the PCAC prediction. Thus while one can envision a value of  $\Lambda_{op}$  which slightly improves the agreement with the PCAC prediction for both OMC and RMC, there still appears to be no value which will simultaneously result in good agreement with PCAC for both cases.

### 3. Admixtures of a $J = 3/2$ ortho-molecular state

It was pointed out in the very early work of Weinberg (1960) that the ortho state could also include a component of total spin angular momentum  $S = 3/2$ . Subsequent theoretical calculations (Bakalov *et al.*, 1982; Halpern, 1964a,b; Wessel and Phillipson, 1964) seemed to indicate that this component was zero or very small. Nevertheless if there were such a component it would effectively increase the amount of triplet state in the initial state. This has been suggested as a possible explanation by Ando *et al.* (2000, 2001a). Their original numbers were not quite right, due to a misinterpretation of the appropriate initial state in the OMC experiment, but the idea is worth examining. Figure 7 shows the region in the  $\eta - g_p$  plane allowed by the TRIUMF RMC experiment and the most recent OMC experiment. Here  $\eta$  is the fraction of the spin 3/2 state present in the ortho state. The OMC calculation here differs slightly from that of Ando *et al.* (2000) by virtue of the fact that form factors have now been included. The theoretical prediction,  $\eta = 0$  corresponding to no additional spin 3/2 component, gives the most consistent result. The updates to the OMC theory, which again raise the band from the Saclay experiment, make it possible to slightly improve both RMC and OMC results with a small non-zero value of  $\eta$ . However analogous to the previous case, a value of  $\eta$  which makes OMC agree with PCAC leaves RMC too high and a value which makes RMC agree leads to dramatic disagreement of OMC. Thus this effect does not appear to resolve the discrepancy.

### 4. Direct singlet - para transitions

As shown in Fig. 1 it is in principle possible for the  $\mu p$  singlet atom to make a direct transition to the para  $p\mu p$  molecule. This also would increase the proportion of the triplet component in the initial state. This transition is governed by the rate  $\Lambda_{p\mu p}^{para}$  which is predicted to be  $\simeq 0.75 \times 10^4 s^{-1}$  for liquid hydrogen, which is two orders of magnitude smaller than the transition rate to the ortho state,  $\Lambda_{p\mu p}^{ortho} \simeq 1.8 \times 10^6 s^{-1}$ , (Faifman and Men'shikov,

<sup>9</sup> This group also obtained a value  $7.7 \pm 2.7 \times 10^4 s^{-1}$  via a measurement of the electron time spectrum. See Martino (1982).

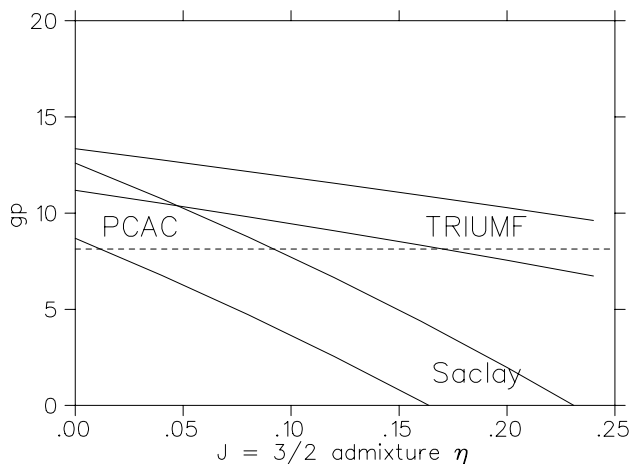


FIG. 7 The region in the  $g_p - \eta$  plane which is allowed by the TRIUMF RMC experiment (Wright *et al.*, 1998) and the Saclay OMC experiment (Bardin *et al.*, 1981a). The dashed line indicates the PCAC value,  $g_p^{PCAC} = 8.13$ , as defined in Eq. (9), which includes the constant term. Details of the model used are described in Sec. V.D.  $\Lambda_{op}$  has been taken as  $4.1 \times 10^4 s^{-1}$  and the uncertainty in its value has not been included in the plotted error bands.

1999), and so should be a negligible effect.

### 5. Large $\Delta$ resonance effects

In a recent calculation of RMC in a Lagrangian based model, described in Section V.B.3 above, Truhlik and Khanna (2001) argue that the discrepancy is at least partially resolved by a contribution coming primarily from the  $\Delta$ . The first observation to be made however is that using their best parameters the  $\Delta$  contribution they obtain is essentially the same size as the contribution obtained earlier (Beder and Fearing, 1987, 1989) which was already included in the analysis of the TRIUMF RMC experiment. Other values of the parameters, but still within the region allowed by other experiments, can raise this  $\Delta$  contribution by 3-4% in the most important part of the spectrum, where the discrepancy is more than 40%. It would appear, as they in fact note, that their primary results really basically agree with previous ones and so do not provide an explanation of the discrepancy. They go on to observe however that one can change one of the parameters corresponding to off-shell properties of the  $\Delta$  and thus fit the experimental spectrum. That is certainly possible, as one can usually arbitrarily change one parameter to get a fit to another. However it requires the  $\Delta$  contribution to be an order of magnitude larger than what they consider most reasonable. Furthermore one would have to reconcile such an explanation with the general result that changing off-shell properties can not change physically measurable quantities. See e. g. Fearing (1998b, 2000); Fearing and Scherer (2000); Scherer and Fearing (2001) and references cited

therein. Although it is clear that there are uncertainties in any attempt to include a  $\Delta$  in a calculation such as this, their best estimate of the  $\Delta$  contribution is quite consistent with the (small) contribution found in the two previous independent calculations which included the  $\Delta$  (Beder and Fearing, 1987, 1989; Bernard *et al.*, 2001b). An enhancement obtained by varying off-shell parameters which is large enough to explain the full discrepancy does not seem too likely.<sup>10</sup>

### 6. Other possibilities

Another suggestion was made by Bernard *et al.* (2001b), namely that the discrepancy between PCAC and the RMC results could be resolved by a series of small effects in RMC which happen to add up. Such effects might include for example those discussed above or perhaps higher order loop effects which have not been included, radiative corrections, or variations in some of the parameters. Clearly one can not test this suggestion without calculating all such effects, which has not been done. We note however that in so far as the molecular effects we have discussed are concerned, they all serve to increase the amount of triplet capture, at least for current liquid  $H_2$  experiments. However in each of these cases, or in some combination of them, as they are somewhat equivalent, it appears that changes sufficient to make RMC agree, lead to drastic disagreement for OMC.

Another particular effect they proposed was an isospin breaking effect. This proposal was based on the observation that the RMC rate changed quite a bit when the charged pion mass in the pion propagator was replaced by the neutral pion mass, thus supposedly showing a sensitivity to the kinds of presumed electromagnetic isospin breaking effects responsible for the pion mass splitting. This sensitivity clearly originates in the fact that some of the momentum transfers in RMC can get quite close to the pion pole. Thus changing the position of the pole, even by a few MeV, can change the results significantly. One should note however that the pion exchanged is in fact a charged one. Thus in an ideal theory which properly incorporated all electromagnetic effects, after all the renormalizations, and after all the terms which lead to mass splittings were included, the pion mass appearing in the propagator would in fact be the physical charged pion mass, not the neutral one. Thus this particular argument for sensitivity to isospin effects is spurious. In such a complete theory one would probably expect terms in the numerator of the amplitude proportional to the pion mass splitting, and likewise the neutron-proton mass

<sup>10</sup> There was also a suggestion by Cheon and Cheoun (1998, 1999) of an additional term in the Lagrangian which could contribute, but it was shown that such a term was already included in standard calculations, and so was not an additional effect (Fearing, 1998a; Smejkal and Truhlik, 1998).

splitting. But the scale in the denominator would likely be something like the pion mass, so these terms should be small. Nevertheless, there could be accidental enhancements, so this is a calculation which should be done.

One might also want to consider radiative corrections to both OMC and RMC. Typically these might be expected to be  $O(\alpha/\pi)$ , and this was what was found by the one such calculation we are aware of (Goldman, 1972). This is too small an effect to be relevant now, but might be important in the interpretation of future, high precision, OMC experiments.

## F. Summary and outlook for hydrogen

It is thus possible to summarize the situation in hydrogen as follows. From the theory side, all calculations of OMC in hydrogen are in essential agreement, as they must be as all couplings and form factors except  $g_p$  are fixed by generally well accepted principles such as CVC or by other experiments. The several calculations of RMC, which in principle could differ, e.g. via the extra loop contributions included in the ChPT calculation relative to the standard diagrammatic calculation, are in fact in general agreement at the few percent level.

On the experimental side, all modern OMC experiments now generally lead to values of  $g_p$  which are consistent with each other within the errors. The perception that OMC agrees with PCAC has changed somewhat however with updates to the theoretical calculations and to the  $\mu^+$  lifetime. These updates have increased the world average from OMC by only about one standard deviation, but result in a value which is now higher than the PCAC value by about 1.3 standard deviations and which is in fact in better agreement with the RMC result than with PCAC. The one existing RMC experiment gives a value of  $g_p$  which is 50% larger than the PCAC prediction and with uncertainties small enough that it is in clear disagreement with that prediction. Though there have been a number of suggestions and attempts to explain the discrepancy indicated by the RMC result, none so far have been successful, and the difference remains a puzzle.

So what needs to be done next to resolve this situation? Specifically a high precision measurement of the OMC rate in gaseous hydrogen would be very helpful. By using gas rather than liquid the muon chemistry uncertainties are greatly reduced. Indeed a new measurement of the singlet capture rate for OMC in  $H_2$  gas at  $P \simeq 10$  bar using the lifetime method is currently under way at PSI (Kammel *et al.*, 2000). The goal is a precision of about 1% in the singlet rate and about 6% in the coupling  $g_p$ . Note that the experiment will use a novel hydrogen time projection chamber that enables direct monitoring of muon stops, muon transfer and  $\mu$ -atom diffusion.

Also useful would be a new measurement of OMC in liquid hydrogen with significantly improved uncertain-

ties. Such a measurement might distinguish between two possible scenarios. In one, both OMC and RMC may give values of  $g_p$  which are too high and inconsistent with PCAC, which would suggest that the problem is something common to OMC and RMC, perhaps some difficulty with our understanding of the molecular or atomic effects. In the other OMC might clearly agree with PCAC and disagree with RMC, which would suggest that the problem is something wrong with our understanding of RMC.

It would also help to confirm some aspects of the muon chemistry, particularly the value of  $\Lambda_{op}$  which is important in determining the initial muonic state and for which the existing experimental (Bardin, 1982; Bardin *et al.*, 1981b) and theoretical (Bakalov *et al.*, 1982) values differ by almost a factor of two. Such an experiment is under way (Armstrong *et al.*, 1995) and should have results soon.

Another alternative is to try to measure some other quantity which is especially sensitive to  $g_p$ . One such quantity is the triplet capture rate for OMC in  $H_2$ . Here the central problem is that the triplet rate is about thirty times smaller than the singlet rate. Further during the time evolution of the  $\mu p$  system following atomic capture, the singlet state is always present, so the singlet capture dominates the OMC rate at all times. However some suggestions have surfaced for isolating the triplet capture from the much larger singlet capture. One possibility suggested by Deutsch (1983) is to measure the time dependence of the neutron polarization. Neutrons following capture from the singlet state have polarization -1, while those from the triplet state have a polarization depending on the weak dynamics and  $g_p$ . Measuring as a function of time allows one to determine a relative neutron polarization, rather than an absolute one, which is more difficult. Such a measurement of the neutron polarization could, in principle, help in identifying the triplet capture and isolating the  $g_p$  contribution. Another suggestion (Bailey *et al.*, 1983) notes that the triplet  $\mu p$  atoms, unlike the singlet  $\mu p$  atoms, will precess in a magnetic field. Consequently the time spectra of decay electrons or capture neutrons will be modulated by this precession when muons are stopped in  $H_2$  gas at low pressures, where triplet atoms are relatively long-lived, thus enabling isolation of triplet capture. While interesting and worth reconsidering, such experiments are of course extremely difficult.

For RMC, it is clear that a new experiment in liquid hydrogen, where triplet capture is largest, would also be both interesting and useful to check the TRIUMF result. Further a new RMC experiment in gaseous hydrogen, where singlet capture is largest, would be very interesting. However an RMC experiment in gaseous hydrogen is extraordinarily difficult since the muon stopping rate is much less and the singlet RMC rate is much smaller than the triplet RMC rate.

Since for RMC the triplet rate is by far the largest, it is possible, by utilizing both a gas target, where capture

is primarily from the singlet state, and a liquid target, where there can be significant captures from the triplet state, to obtain as the dominant contribution to the RMC rate either singlet capture or triplet capture. This is different from the situation for OMC since there the singlet rate is the largest and so in both gas and liquid experiments the singlet capture will dominate the total rate.

In principle it is possible to measure spin degrees of freedom in RMC as well and a suggestion of this type has also been made recently by Ando *et al.* (2002). Such experiments would be extremely difficult because of the low rates and the necessity of either starting with a polarized muonic atom or measuring the polarization of the outgoing photon, but they are more sensitive to  $g_p$  than the rate and are sensitive to a different combination of amplitudes and so give independent information on the process (Fearing , 1975).

## VI. MUON CAPTURE IN DEUTERIUM

We next want to consider OMC on deuterium, *i.e.* the reaction  $\mu + d \rightarrow n + n + \nu$ , which involves many of the same ingredients as OMC on the proton, but also some additional complications.

### A. Theory of muon capture in deuterium

Since there are now two nucleons involved in the capture process, several new ingredients appear which were not relevant for capture on the proton. In particular the process now depends on the two nucleon interaction, which is reflected in the properties of the initial state deuteron, such as the wave function, percentage D state, etc., and also in the final state interaction between the two outgoing neutrons. Furthermore now meson exchange corrections (MEC's) can contribute.

There have been many calculations of the OMC rate in deuterium.<sup>11</sup> Some of the more recent ones include Tataro *et al.* (1990), Adam *et al.* (1990), Doi *et al.* (1990, 1991), Morita and Morita (1992), Hwang and Lin (1999) and Ando *et al.* (2001b). Originally the main emphasis was on using this process to extract the neutron-neutron scattering length  $a_{nn}$ . In the kinematics in which the two neutrons have low relative momentum, the neutron spectrum peaks at a value several orders of magnitude larger than that for kinematics with large relative momentum. Such a measurement of this low energy neutron spectrum, while extremely difficult, is still interesting, but

perhaps less so than originally in view of the advances in our knowledge of the nucleon-nucleon force from other sources. However the sensitivity to  $a_{nn}$  means that it must be well known to have any hope of using this process to extract  $g_p$ , at least if one focuses on the region of low relative neutron momentum where the rate is largest.

Furthermore the total OMC rate, which is dominated by the doublet rate, is only moderately sensitive to  $g_p$ . A 50% change in  $g_p$  produces only about a 10% change in the rate (Doi *et al.*, 1991).

The total rate is also affected by MEC's which have been calculated using specific diagrams involving pion or rho exchange (Doi *et al.*, 1990) or using a more elaborate hard pion Lagrangian involving  $\pi$ 's,  $\rho$ 's,  $\omega$ 's and  $a_1$ 's (Adam *et al.*, 1990; Ivanov and Truhlik , 1979b; Tataro *et al.*, 1990). Generally these MEC's are about a 10% correction to the total rate.

The results of modern calculations now generally agree. For example the doublet capture rate obtained by Tataro *et al.* (1990) is 398-400 s<sup>-1</sup> of which 31-33 s<sup>-1</sup> comes from MEC's and where the range corresponds to different nucleon-nucleon potentials. Doi *et al.* (1990) obtained 402 s<sup>-1</sup> and Adam *et al.* (1990) found 416±7 s<sup>-1</sup>.

It is interesting to note that since this is a three body final state, just like RMC in the proton case, it is possible to get timelike momentum transfers approaching  $+m_\mu^2$  and thus get near the pion pole, where in principle the sensitivity to  $g_p$  is enhanced. To our knowledge sensitivity to  $g_p$  in that region has not been investigated, although Mintz (1983) considered some effects of timelike form factors and Doi *et al.* (1990) and Goulard *et al.* (1982) showed that meson exchange currents are an important effect there. Unfortunately this kinematic region occurs when the two neutrons go out back to back and the  $\nu$  has relatively low energy, which is a region which is strongly suppressed relative to the region where the neutron-neutron final state scattering is important, thus making experiments difficult.

There is a very strong hyperfine effect in the capture rate on deuterium. The quartet rate is only 10-15 s<sup>-1</sup> (Doi *et al.*, 1990; Ho-Kim *et al.*, 1976; Sotona and Truhlik , 1974). It has been suggested (Doi *et al.*, 1991; Morita and Morita , 1992; Morita *et al.*, 1993) that the ratio of quartet to doublet rate is much more sensitive to  $g_p$  than the doublet rate and thus that a measurement of the quartet rate, or directly of the ratio, would give a better value of  $g_p$ .

In principle RMC in deuterium should also be an interesting process, giving information on  $g_p$ . However one might expect that MEC's would be even more important here, since at the least the photon would have to couple to all of the intermediate states which generate the MEC's in OMC. To our knowledge there have not been calculations of RMC in deuterium.

<sup>11</sup> Some representative earlier ones include those of Wang (1965b), Pascual *et al.* (1972), Truhlik (1972), Sotona and Truhlik (1974), Dogotar *et al.* (1979), Ivanov and Truhlik (1979b), Nguyen (1975), Ho-Kim *et al.* (1976), Švarc *et al.* (1978), Švarc (1979), Švarc and Bajzer (1980), Goulard *et al.* (1982), and Mintz (1973, 1983).

## B. Experiments on muon capture in deuterium

A summary of available data for  $\mu d$  total capture rates is given in Table III. It lists experiments with mixed  $H_2/D_2$  targets by Wang *et al.* (1965) and Bertin *et al.* (1973) and pure  $D_2$  targets by Bardin *et al.* (1986) and Cargnelli *et al.* (1989). A  $H_2/D_2$  target is helpful in reducing the neutron background from  $d\mu d$  fusion. The Bardin *et al.* (1986) result was obtained using the ‘lifetime method’ (see Sec. V.C.2) and the other results were obtained using the ‘neutron method’ (see Sec. V.C.3). Note the neutron measurements give partial rates for muon capture with neutron energies  $> E_{thres}$  and require some input from theory to determine the total rate of  $\mu d$  capture.

The measurement by Wang *et al.* (1965) used a liquid  $H_2$  target with a 0.32%  $D_2$  admixture. Under these conditions the  $\mu$  capture is dominantly from  $p\mu d$  molecules, since muon transfer yields  $\mu d$  atoms in roughly 20 ns and proton capture yields  $p\mu d$  molecules in roughly 200 ns. See Sec. IV.C for details. Consequently the neutron signal in Wang *et al.* (1965) involves a superposition of capture on protons, deuterons and  $^3He$ , the latter being produced via  $pd$  fusion in  $p\mu d$  molecules. Note that in analyzing their results the authors assumed a statistical mixture of the  $\mu d$  spin-states in the  $p\mu d$  molecules, as would be expected if hyperfine depopulation by spin-flip collisions is much slower than  $p\mu d$  formation. Also the different time dependence of  $\mu^3He$  neutrons and  $\mu d$  neutrons was employed in separating their contributions.<sup>12</sup> Their final result for doublet capture was  $\Lambda_{1/2} = 365 \pm 96 s^{-1}$ .

The measurement by Bertin *et al.* (1973) used a 7.6 bar  $H_2$  gas target with a 5%  $D_2$  admixture. Under these conditions the  $\mu d$  atom formation is rapid but  $p\mu d$  molecule formation is negligible, thus avoiding the complication of contributions from protons, deuterons, and  $^3He$ . Strangely they found that under the assumption of a statistical mix of the  $\mu d$  spin-states their extracted rate for doublet capture was 1100–1500  $s^{-1}$ , *i.e.* three times the theoretical value. Therefore, in order to understand their results, they postulated a much faster hyperfine depopulation rate than assumed by Wang *et al.* (1965). Thus assuming a pure doublet mix of  $\mu d$  spin states the authors obtained a doublet rate of  $445 \pm 60 s^{-1}$ . However the subsequent studies of hyperfine depopulation in  $H_2/D_2$  systems, *e.g.* Breunlich (1981), have failed to support this claim and therefore the Bertin *et al.* (1973) result is extremely puzzling.

The more recent experiments of Cargnelli *et al.* (1989) and Bardin *et al.* (1986) were conducted in pure deuterium. In these circumstances the  $\mu d + d$  collision rate is sufficient to fully depopulate the  $F_+$  state. Note any

$d\mu d$  formation is followed by prompt fusion and muon recycling into  $\mu d$  atoms. The resulting rates for doublet capture were  $\Lambda_{1/2} = 409 \pm 40 s^{-1}$  from Cargnelli *et al.* (1989), using a gas target and the neutron method, and  $\Lambda_{1/2} = 470 \pm 29 s^{-1}$  from Bardin *et al.* (1986), using a liquid target and the lifetime method. Using the calculation of Doi *et al.* (1991), the Cargnelli *et al.* (1989) result implies  $g_p = 8 \pm 4$  and the Bardin *et al.* (1986) result implies  $g_p = 2 \pm 3$ , which are in disagreement at the level of about 1-1.5  $\sigma$ . Although one experiment used a gas target and the other experiment used a liquid target, in both cases it is believed that capture is from the doublet atomic state, so that muon chemistry in pure deuterium is unlikely to account for the different results. However both experiments were challenging and faced different experimental difficulties. Therefore at present we conclude the two results simply indicate a rather large uncertainty in the value of the coupling  $g_p$  extracted from the  $\mu d$  system.

There has also been one measurement of the high energy neutron spectrum following muon capture in deuterium (Lee *et al.*, 1987) using neutron time of flight methods. In this kinematic situation the neutrons come out back to back, so the direction is well defined, but there is no start signal for time of flight measurements. This group used a novel technique to overcome this, by using the detection of one of the neutrons in a counter placed close to the target as a start signal for the time of flight measurement of the other neutron in a counter placed further away from the target. The results suggest the enhancement due to meson exchange corrections found by Goulard *et al.* (1982) and are in qualitative agreement with the calculations of Doi *et al.* (1990) at least as far as the shape of the spectrum is concerned, but are not precise enough to give any real information on  $g_p$ . In view of the potentially increased sensitivity to  $g_p$  however, such a measurement of high energy neutrons is worth re-examining.

A new higher precision measurement of the  $\mu d$  doublet capture rate would be useful in resolving the possible discrepancy between the current results of Bardin *et al.* (1986) and Cargnelli *et al.* (1989). However in deuterium, unlike in hydrogen, the uncertainties in calculating the contributions of exchange currents may ultimately limit the achievable accuracy in extracting  $g_p$ . We also remark that in pure deuterium and hydrogen-deuterium mixtures the hyperfine depopulation rate is much slower than in pure hydrogen. Consequently measuring either the quartet rate or hyperfine dependence in  $\mu d$  capture, which are strongly dependent on  $g_p$ , may be experimentally easier in  $\mu d$ . It would be worthwhile to reconsider this source of information on  $g_p$ , as has been suggested by Morita and Morita (1992) and Doi *et al.* (1991).

<sup>12</sup> The neutrons from  $\mu d$  capture build-up quickly with the nanosecond timescale of the  $\mu$  transfer process. The neutrons from  $\mu^3He$  capture build-up slowly with the microsecond timescale of the  $pd$  fusion process.

TABLE III Summary of world data for the  $\mu d$  doublet capture rate. The columns correspond to the target density in units of liquid hydrogen density  $n_o$ , target temperature, the time delay between  $\mu$  stop and start of counting, the neutron energy threshold, the deuterium concentration, and the doublet capture rate.

Ref.	$n/n_o$	T(K)	$\Delta t(\mu s)$	$E_n(\text{MeV})$	$c_d$	rate ( $s^{-1}$ )
Wang <i>et al.</i> (1965)	1.0	18	0.8	1.4	0.0032	$365 \pm 96$
Bertin <i>et al.</i> (1973)	0.013	293	0.5	1.5	0.05	$445 \pm 60^a$
Bardin <i>et al.</i> (1986)	1.0	18	2.5	-	1.00	$470 \pm 29$
Cargnelli <i>et al.</i> (1989)	0.04	40	1.9	1.5, 2.5	1.00	$409 \pm 40$

<sup>a</sup> Note that the Bertin *et al.* (1973) doublet capture rate was obtained assuming a much faster hyperfine depopulation rate than is consistent with our current understanding of muon chemistry in  $H_2/D_2$  mixtures. See text for details.

## VII. MUON CAPTURE IN $^3\text{He}$

We now want to consider both OMC and RMC on  $^3\text{He}$ . Since it is possible to break up the final state there are several processes possible,

$$\mu^- + ^3\text{He} \rightarrow ^3\text{H} + \nu \quad (26)$$

$$\mu^- + ^3\text{He} \rightarrow ^2\text{H} + n + \nu \quad (27)$$

$$\mu^- + ^3\text{He} \rightarrow p + n + n + \nu \quad (28)$$

with analogous processes involving a photon in the case of RMC.

Of these, most work has been done on the triton final state, Eq. (26). Like the deuteron, since there is more than one nucleon, the complications of exchange currents must be addressed. Additionally three-body forces are now possible. However there has been a tremendous amount of work done on three-body wave functions in recent years and these wave functions are now extremely well known. Thus the wave function complications which plague interpretation of capture in heavier nuclei really do not enter here. Furthermore the rate is significantly higher than in capture on protons and deuterons and the atomic and molecular processes which make the interpretation of capture in hydrogen or deuterium difficult are not present here. Thus  $^3\text{He}$  is an ideal compromise, and we will see that one of the best measurements of  $g_p$  to date comes from OMC in  $^3\text{He}$ .

### A. Theory of ordinary muon capture in $^3\text{He}$

There have been two major approaches to the theory of muon capture in  $^3\text{He}$ , the elementary particle model (EPM) and the impulse approximation (IA), supplemented by explicit calculations of meson exchange corrections. The EPM exploits the fact that the  $^3\text{He}$

-  $^3\text{H}$  system is a spin 1/2 isodoublet just like the proton-neutron system. Thus one can carry over directly the calculations done for capture on the proton. The couplings and form factors now apply to the three-body system as a whole, rather than the nucleon. However they can be obtained in many cases directly from other processes such as electron scattering on  $^3\text{He}$  or tritium  $\beta$ -decay or from theory, i.e., by applying PCAC to the nuclear pseudoscalar form factor. This approach has the advantage that it already includes effects of MEC's, which are buried in the form factors, and that it can be done relativistically. However it is difficult to relate the nuclear form factors to the fundamental couplings and form factors of the weak current, e. g.  $g_p$ . Some sort of microscopic model is necessary to make this connection.

One of the first such EPM calculations was that of Kim and Primakoff (1965). The idea was later applied to  $^3\text{He}$  by Beder (1976), Fearing (1980), Klieb and Rood (1981), and Klieb (1982). A more modern and very careful calculation with particular attention to the form factors and the various uncertainties was carried out by Congleton and Fearing (1993), and their results were confirmed by Govaerts and Lucio-Martinez (2000) and by Ho *et al.* (2002). The final result is a prediction from the EPM for the statistical capture rate of  $1497 \pm 21s^{-1}$  (Congleton and Fearing, 1993), using the standard PCAC value for  $g_p$ .

The IA on the other hand treats the capture process as capture on an essentially free proton. This one nucleon interaction is then expanded in powers of  $1/m$  and used as an effective interaction in a matrix element between nuclear wave functions. The information specific to the nucleus comes in only via the nuclear wave functions. Early applications of this approach applied to  $^3\text{He}$  include Peterson (1968), Phillips *et al.* (1975), Klieb and Rood (1981), and Klieb (1982). Again a very careful calculation was done by Congleton and Fearing (1993) using the variational wave functions of Kameyama *et al.* (1989) with the result for the rate  $1304 s^{-1}$ . This was essentially confirmed by Ho *et al.* (2002) using for the

wave functions momentum space Faddeev solutions for a variety of potentials. They found however about a  $\pm 3\%$  spread among the results using the various wave functions. The fact that the IA result is about 15% lower than the EPM is characteristic of the IA and indicates the effect of the MEC's. Congleton and Truhlik (1996) refined these IA calculations by including explicitly the MEC's, based on a specific Lagrangian involving  $\pi$ ,  $\rho$ ,  $a_1$ ,  $\Delta$  couplings. The end result, which also included some effects of three-body forces, was  $1502 \pm 32 \text{ s}^{-1}$ . This is in excellent agreement with the EPM result. Finally, very recently Marcucci *et al.* (2001) repeated the calculation of Congleton and Truhlik (1996) using wave functions arising from the Argonne  $v_{14}$  or  $v_{18}$  potentials with some three-body forces. They also made some refinements to the weak current and reduced the size of the uncertainty by fixing the  $\Delta$  contribution to the exchange current corrections via a fit to tritium beta decay. They obtained  $1494 \pm 9 \text{ s}^{-1}$ .

Thus to summarize, the capture rate for OMC on  ${}^3\text{He}$  is well determined by both EPM and IA+MEC calculations with an accuracy of 1-3%. We note that at this level of accuracy radiative corrections might be important and should be evaluated.

Finally it is worth mentioning that there have also been calculations of various spin correlations in OMC (Congleton, 1994; Congleton and Fearing, 1993; Congleton and Truhlik, 1996; Govaerts and Lucio-Martinez, 2000; Marcucci *et al.*, 2001). Generally these correlations are more sensitive to  $g_p$  and less sensitive to the MEC's than the rate is. There have also been calculations of some breakup channels (Phillips *et al.*, 1975; Skibinski *et al.*, 1999; Wang, 1965a).

## B. Experiments on OMC in ${}^3\text{He}$

The  ${}^3\text{H}$  channel in OMC on  ${}^3\text{He}$  yields a muon neutrino with momentum 100 MeV/c and triton recoil with energy 1.9 MeV. The triton yield per  $\mu$  stop is roughly 0.3%. Contrary to muon capture on complex nuclei, the recoil triton has a relatively high energy and a relatively small charge, and is therefore directly detectable. In Sec. VII.B.1 below we discuss the current status of the  ${}^3\text{He} \rightarrow {}^3\text{H}$  capture rate experiments and in Sec. VII.B.2 the  ${}^3\text{He} \rightarrow {}^3\text{H}$  recoil asymmetry experiments.

### 1. ${}^3\text{He}$ capture rate experiments

So far several measurements of the  ${}^3\text{He} \rightarrow {}^3\text{H}$  rate have been performed. They comprise the early work of Auerbach *et al.* (1967), Clay *et al.* (1965), Falomkon *et al.* (1963), Zaimidoroga *et al.* (1963), and recent work of Ackerbauer *et al.* (1998).

The basic method involves counting the numbers of  $\mu$ -stops and  ${}^3\text{He}$ -recoils when a beam of muons is stopped in  ${}^3\text{He}$ . In Auerbach *et al.* (1967) and Ackerbauer *et al.*

(1998) a  ${}^3\text{He}$  gas ionization chamber was used whereas in Falomkon *et al.* (1963) and Clay *et al.* (1965) a  ${}^3\text{He}$  liquid scintillator was used. One advantage of a liquid scintillation counter is the higher muon stopping rate in the liquid helium target. However one advantage of a gas ionization chamber is the better separation of the  $\mu$  and  ${}^3\text{He}$  signals via its tracking capabilities.

The recent experiment of Ackerbauer *et al.* (1998) employed an  ${}^3\text{He}$  ionization chamber with a  $15 \text{ cm}^3$  active volume and a 20 Torr gas pressure. The anode plane was segmented to permit the tracking of the incoming muons, the isolation of the recoil tritons, and the definition of the fiducial volume. The anode strips were read out into flash ADCs for measurement of the drift time and the energy loss. Separate triggers were employed to count the incoming muons or recoil tritons with full efficiency.

One experimental difficulty is muon-triton pile-up, *i.e.* overlapping of the prompt  $\mu^-$  ionization and the delayed  ${}^3\text{He}$  ionization. Ackerbauer *et al.* (1998) addressed this problem by both (i) ignoring pile-up events and extrapolating to  $t = 0$  the non pile-up  $\mu^-{}^3\text{H}$  time spectrum, and (ii) keeping pile-up events and using the anode pulse-shapes for computing  $\mu^-{}^3\text{H}$  time differences. The consistency of (i) and (ii) was helpful in demonstrating the correct treatment of pulse pile-up.

Another experimental difficulty is background processes. The 1.9 MeV triton energy-loss peak is superimposed on backgrounds that include  ${}^3\text{H}$  break-up channels, thermal neutron capture, and  $\mu$ -decay electrons. Ackerbauer *et al.* (1998) employed various fitting procedures in order to separate the triton peak and continuum background and estimate the uncertainties. Their signal-to-background ratio was roughly 20:1.

The Ackerbauer *et al.* (1998) experiment yielded a  ${}^3\text{He} \rightarrow {}^3\text{H}$  rate, corresponding to a statistical hyperfine initial population, of  $1496.0 \pm 4.0 \text{ s}^{-1}$ , with the largest systematic uncertainty being the subtraction of the background. The  $\pm 0.2\%$  accuracy is a ten-fold improvement over the earlier experiments of Falomkon *et al.* (1963)  $1410 \pm 140 \text{ s}^{-1}$ , Clay *et al.* (1965)  $1467 \pm 67 \text{ s}^{-1}$ , and Auerbach *et al.* (1967)  $1505 \pm 40 \text{ s}^{-1}$ . In addition Ackerbauer *et al.* (1998) utilized their time spectrum to establish that transfer from the  $F_-$  to the  $F_+$  hyperfine state as well as capture from the 2S metastable state can be safely neglected.<sup>13</sup>

Taken together the measurement of Ackerbauer *et al.* (1998) and the calculation of Congleton and Truhlik (1996) give  $g_p(-0.954m_\mu^2) = 8.53 \pm 1.54$  which implies  $g_p(-0.88m_\mu^2) = 8.77 \pm 1.58 = (1.02 \pm 0.18)g_p^{PCAC}$ , or  $(1.08 \pm 0.19)g_p^{PCAC}$  if we use the value of  $g_p^{PCAC}$  which includes the constant term. These results are in nice

<sup>13</sup> For the hyperfine transition rate Ackerbauer *et al.* (1998) obtained  $(0.006 \pm 0.008) \mu\text{s}^{-1}$  and for the 2S state lifetime they obtained  $< 50 \text{ ns}$ .

agreement with the PCAC prediction for the coupling  $g_p$ . Here the dominant uncertainty originates from the theoretical calculation and not the experimental data. Clearly the key question is the exact size of the theoretical uncertainty. We have quoted the theoretical error of Congleton and Truhlik (1996) which originates mainly from the  $\Delta$  contribution to the exchange currents. Subsequently Marcucci *et al.* (2001) have suggested this uncertainty can be reduced by fixing some of the parameters using results from exchange current effects in tritium beta decay. However Ho *et al.* (2002) found significant theoretical uncertainty arising from different choices of the nuclear wave functions, though some of this may be due to the fact that three-body forces were not included and tuned to give the same binding energies for all choices. Further efforts on establishing and reducing the theoretical uncertainty in calculating the rate for  ${}^3\text{He} \rightarrow {}^3\text{H}$  capture are definitely worthwhile.

Lastly we note that there have been some recent measurements of partial capture rates and energy spectra for the breakup channels following muon capture in  ${}^3\text{He}$  (Cummings *et al.*, 1992; Kuhn *et al.*, 1994). Comparisons with a recent calculation (Skibinski *et al.*, 1999) indicate that a good treatment of final state effects is necessary to describe the data. However at the present stage these channels give no information on  $g_p$ .

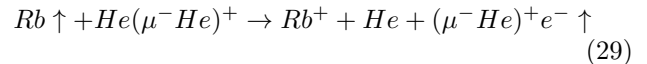
## 2. ${}^3\text{He}$ recoil asymmetry experiments

As discussed for nuclei in general in Sec. IX.B.2 below, the recoil asymmetry in muon capture can be very sensitive to the coupling  $g_p$ . Unfortunately production of a measurable  ${}^3\text{H}$  asymmetry requires production of a large  $\mu^{-3}\text{He}$  polarization, which has proven to be difficult.

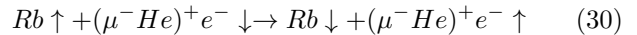
Early attempts to polarize  $\mu^{-3}\text{He}$ , using a polarized beam on a unpolarized target and an unpolarized beam on a polarized target, were unsuccessful. For example, Souder *et al.* (1975) obtained a  $\mu^{-}$  polarization of only  $\sim 6\%$  when stopping polarized muons in unpolarized  ${}^3\text{He}$  gas and Newbury *et al.* (1991) obtained a  $\mu^{-}$  polarization of only  $\sim 7\%$  when stopping unpolarized muons in polarized  ${}^3\text{He}$  gas.<sup>14</sup> The breakthrough was made at LAMPF by Barton *et al.* (1993) by repolarizing the  $\mu^{-3}\text{He}$  system with a laser-pumped Rb vapor after the atomic cascade.

How does repolarization work? Following the  $\mu^{-3}\text{He}$  atomic cascade a  $(\mu^{-3}\text{He})^+$  positive ion is produced. However the  $(\mu^{-3}\text{He})^+$  ion is short lived, forming either  $(\mu^{-3}\text{He})^+{}^3\text{He}$  molecules via collisions with surrounding He atoms or  $(\mu^{-3}\text{He})^+e^-$  atoms after collisions with electron-donor impurities. The repolarization technique developed by Barton *et al.* (1993) employs both spin transfer in the dissociation of the  $(\mu^{-3}\text{He})^+{}^3\text{He}$

molecules



and spin transfer in the collisions of the  $(\mu^{-3}\text{He})^+e^-$  atoms



where the arrows denote the polarization state of transferred electrons. Following the dissociation process of Eq. (29) and collision process of Eq. (30) the polarization of the electron is shared with the muon via their spin-spin interaction. Barton *et al.* (1993) discovered at high Rb $\uparrow$  densities both processes contribute to muon repolarization on the time scale of the muon lifetime, and produced a  $\mu^{-}$  polarization in  ${}^3\text{He}$  gas of 26%.

Recently the first measurement of the recoil asymmetry in the  ${}^3\text{He} \rightarrow {}^3\text{H}$  transition was accomplished by Souder *et al.* (1998) at TRIUMF. The experiment utilized a  ${}^3\text{He}$  ionization chamber to stop the incoming muons, repolarize the  $\mu^{-3}\text{He}$  system, and track the triton recoils. For experimental details see Bogorad *et al.* (1997) and Souder *et al.* (1998). The chamber had an instrumented volume of 140 cm<sup>3</sup> and a gas pressure of 8 bar. Anode segmentation assisted the definition of the fiducial volume and pulse-shape read-out assisted the separation of the  $\mu/{}^3\text{He}$  pulses. Running the chamber at high voltage, high temperature, and high Rb density was a great achievement.

Souder *et al.* (1998) employed an interesting approach in determining  $\cos\theta$ , the direction between the  ${}^3\text{H}$  recoil and  $\mu/{}^3\text{He}$  polarization. First the magnitude of  $\cos\theta$  was determined from the anode signal width. If the recoil travels perpendicular to the anode plane the drift time range and anode pulse width are large. If the recoil travels parallel to the anode plane the drift time range and anode pulse width are small. Second the sign of  $\cos\theta$  was determined from the anode pulse shape. For a recoil traveling towards the anode the early-arriving Bragg peak yields a fast rise time pulse. For a recoil traveling away from the anode the late-arriving Bragg peak yields a slow rise time pulse.

The  $\mu/{}^3\text{He}$  polarization was determined by detecting the  $\mu$ -decay electrons and using the well known correlation between the electron momentum and the muon spin in the  $\mu \rightarrow e\nu\bar{\nu}$  decay. The electrons were detected using a telescope consisting of wire chambers and plastic scintillators, which permitted ray tracing into the ionization chamber. The asymmetry in the electron counts, on reversing the laser polarization, gave  $P_\mu$ .

Souder *et al.* (1998) achieved a muon polarization of  $P_\mu = 30 \pm 4\%$ . By normalizing the observed triton asymmetry with measured muon polarization the authors obtained a preliminary value for the vector asymmetry for  ${}^3\text{He} \rightarrow {}^3\text{H}$  capture of  $A_v = 0.63 \pm 0.09(\text{stat.}) \pm 0.11^{0.14}(\text{sys.})$ . The largest uncertainty was the systematic error in the experimental determination of the muon polarization.

<sup>14</sup> In both cases the polarizations were smaller than expected from atomic cascade calculations (Reifenröther *et al.*, 1987).



Taking the preliminary result of Souder *et al.* (1998) and the model calculation of Congleton and Truhlik (1996) we obtain, at  $q^2 = -0.954m_\mu^2$ ,  $g_p/g_p^{PCAC} = 0.40 \pm_{0.73}^{0.89}$ , which implies that  $g_p(-0.88m_\mu^2) = 3.3 \pm_{6.1}^{7.4}$ . This result is consistent with PCAC and the  $\mu^3\text{He}$  capture data, but the experimental uncertainties are quite large.

### C. Radiative muon capture in $^3\text{He}$

#### 1. Theoretical calculations

Much less has been done on RMC in  $^3\text{He}$  than on OMC, though there have been calculations of the exclusive rate both in IA and EPM. Calculations in the EPM were made by Hwang and Primakoff (1978), who however made an incorrect assumption, and thus obtained incorrect results, and also by Fearing (1980), Klieb and Rood (1981), Klieb (1982) and Ho *et al.* (2002). For RMC however the EPM seems to be less reliable than for OMC. The nuclear form factors are more rapidly varying than the nucleon form factors so that the gauge terms involving derivatives of the form factors (Adler and Dothan, 1966; Christillin and Servadio, 1977; Ho *et al.*, 2002; Klieb, 1985) are somewhat larger. Furthermore, as emphasized by Klieb and Rood (1984a,b), some important terms involving intermediate state excitations are missed in the EPM.

The RMC rate has also been calculated in IA by Klieb and Rood (1981), Klieb (1982), and Ho *et al.* (2002). The earlier calculations used wave functions from the Reid soft core potential and made a number of approximations in evaluating the nuclear matrix elements. The later calculation of Ho *et al.* (2002) improved on a number of these approximations, kept some additional terms, and used a variety of nuclear wave functions obtained from modern momentum space Faddeev calculations. The end results for the photon spectrum however were about the same as those of Klieb (1982), though the photon polarization was somewhat different, apparently because of the higher order terms kept.

Typical results for the RMC statistical capture rate for photons with energies greater than 57 MeV are  $0.17 \text{ s}^{-1}$  in the IA and  $0.25 \text{ s}^{-1}$  in the EPM (Ho *et al.*, 2002). Just as for OMC, the IA result is significantly below that obtained in the EPM, and presumably the difference is again at least partially explained by MEC's, which will be much more complicated here than they were for OMC, and have not yet been calculated in detail. In view however of the problems with the EPM applied to  $^3\text{He}$ , as noted above, it is not possible to simply ascribe the difference just to MEC's. Such corrections will have to be calculated explicitly to finally obtain a reliable rate.

In principle the various breakup channels would give additional information, but to our knowledge there have not been any calculations of such channels for RMC.

## 2. Experimental results

In  $^3\text{He}$  RMC the  $^3\text{H}$ -channel has a strong peaking at the recoil energy corresponding to the kinematic limit 1.9 MeV. In contrast the energy spectra of charged particles from break-up channels are a broad continua reaching to 53 MeV and therefore are straightforwardly distinguished from  $^3\text{He} \rightarrow ^3\text{H}$ .

While the  $^3\text{He} \rightarrow ^3\text{H}$  transition following  $^3\text{He}$  RMC and the  $p \rightarrow n$  transition following  $^1\text{H}$  RMC are spin-isospin analogs, the  $^3\text{He} \rightarrow ^3\text{H}$  process is experimentally easier. First the  $^3\text{He}$  rate is much larger and consequently the background difficulties are greatly reduced. Second the  $\mu^3\text{He}$  atom circumvents the various chemical processes that confound muonic hydrogen. Of course for  $^3\text{He}$  RMC the presence of exchange currents and the contribution of break-up channels have to be considered.

The  $^3\text{H}$  channel in  $^3\text{He}$  RMC has recently been measured by Wright *et al.* (2000) at TRIUMF. In the experiment a  $\mu^-$  beam was stopped in liquid  $^3\text{He}$  and gamma-triton coincidences recorded. The photons were detected using a pair spectrometer and the tritons were detected via their scintillation light in the liquid helium. Pulse-shape read out permitted the discrimination of the incoming muon from the recoil triton. The detection efficiency was calibrated via  $\pi$  stops in liquid  $^3\text{He}$ , *i.e.* with the well-known branching ratios for  $\pi^-^3\text{He} \rightarrow \gamma^3\text{H}$  and  $\pi^-^3\text{He} \rightarrow \pi^0^3\text{H}$ .

In the  $^3\text{He}$  RMC experiment the major photon backgrounds originate from muon decay in the target material, muon capture in the nearby materials, and pion contamination in the muon beam. However energy cuts, *i.e.*  $E_\gamma > 57 \text{ MeV}$ , and timing cuts, *i.e.*  $t_\gamma > 440 \text{ ns}$ , together with the gamma-triton coincidence requirement, were effective in discriminating the  $^3\text{He}$  signal from background processes. Note the potential background from random coincidences of photons from RMC and tritons from OMC was negligible.

Only preliminary results are presently available for the  $^3\text{He}$  RMC experiment (Wright *et al.*, 2000). The results indicate that the shape of the measured  $^3\text{He}$  RMC energy spectrum is consistent with the theoretical prediction of Klieb and Rood (1981), but that the overall magnitude is 20-30% smaller than the impulse approximation prediction. To get agreement in magnitude Wright *et al.* (2000) stated that one needs  $g_p = 3.4$ , which is much smaller than the PCAC value.

We stress that the  $^3\text{He} \rightarrow ^3\text{H}$  radiative capture rate is potentially a very valuable data-point for the determination of  $g_p$ . We therefore urge the publication of the final result from the TRIUMF experiment and the undertaking of a modern impulse approximation plus exchange current calculation for the process.

## VIII. OTHER FEW BODY PROCESSES

There have also been attempts to extract  $g_p$  from other processes, notably pion electroproduction. To do this Choi *et al.* (1993) measured the near threshold  $\pi^+$  electroproduction at several momentum transfers. The connection to  $g_p$  was made via a low energy theorem described by Vainshtein and Zakharov (1972) and reviewed by Drechsel and Tiator (1992). The theorem is valid in the limit of vanishing pion mass, so it had to be assumed that higher order corrections were in fact small. Nevertheless Choi *et al.* (1993) obtained results which they interpreted as  $g_p(t)$  over a range of four-momentum transfer squared  $0.07 < t < 0.18 \text{ GeV}^2$ . These results agreed quite well with the predicted pion pole dominance and with the PCAC value near  $t = 0$ .

It is clear that such an approach to ‘measuring’  $g_p$  is quite different than that described for OMC and RMC above. In fact there has been a quite heated disagreement over the question of whether or not pion electroproduction does give new information about either  $g_p$  or  $g_a$  (Bernard *et al.*, 2001c; Guichon, 2001; Haberzettl, 2000, 2001; Truhlik, 2001).

In OMC  $g_p$  is defined as a parameter in the most general form of the amplitude, so that a measurement of the rate gives directly information about  $g_p$ . In RMC this same amplitude appears directly, albeit with one leg off shell and with additional gauge terms, some of which probe the interior structure of the amplitude. To the extent these are small, one again in RMC has an almost direct measurement of  $g_p$ .

In other processes however, such as pion electroproduction, one needs to make a number of assumptions in order to make the connection to  $g_p$ . For example, the low energy theorem approach is based on chiral symmetry, which implies the usual PCAC relation between  $g_a$  and  $g_p$ , which in turn allows one to eliminate one or the other from the expressions for the amplitude. Alternatively in a Born approximation diagram approach, which is often used, a pion pole diagram is included. This is the diagram which is assumed to be responsible for  $g_p$ . Thus in such cases is one measuring  $g_p$  or just the importance of a pion exchange diagram?

It thus appears that there is a degree of circularity in trying to use processes such as pion electroproduction to ‘measure’  $g_p$ . To make the interpretation, one has to assume something nearly equivalent to the PCAC relation between  $g_a$  and  $g_p$ , which is what is being tested. In our view then processes such as pion electroproduction are very interesting, and very worth measuring, but primarily as consistency checks on our understanding of the underlying theory, rather than as independent measurements of  $g_p$ .

Finally one should note that in the context of ChPT the calculations of OMC give a relation between  $g_p$  and some of the low energy constants (Ando *et al.*, 2000; Bernard *et al.*, 1998; Fearing *et al.*, 1997). Thus any process which contains these same low energy constants

could be considered as a way of ‘measuring’  $g_p$ , but only within the context of ChPT.

## IX. EXCLUSIVE OMC ON COMPLEX NUCLEI

Determining  $g_p$  from exclusive OMC on complex nuclei is not easy. First, the reaction products are a  $\sim 100 \text{ MeV}$  neutrino and a  $\sim 0.1 \text{ MeV}$  recoil, and therefore the  $\beta$ -rays or  $\gamma$ -rays from the recoil’s decay must be detected. Second, the effects of  $g_p$  in OMC are small and subtle, and therefore measurements of spin observables are usually required. Last, the observables are functions of both the weak couplings and the nuclear wave functions, and disentangling these contributions is unavoidably model dependent.

In allowed transitions on  $J_i = 0$  targets the  $0p$  transition  $^{12}\text{C}(0^+, 0) \rightarrow ^{12}\text{B}(1^+, 0)$  and  $1s-0d$  transition  $^{28}\text{Si}(0^+, 0) \rightarrow ^{28}\text{Al}(1^+, 2201)$  have attracted the most attention. In order to isolate the coupling  $g_p$ , the  $^{12}\text{C}$  experiments have measured recoil polarizations via the  $^{12}\text{B}$   $\beta$ -decay and the  $^{28}\text{Si}$  experiments have measured  $\gamma$ -ray correlations via the  $^{28}\text{Al}$   $\gamma$ -decay. In allowed transitions on  $J_i \neq 0$  targets the  $0p$  nucleus  $^{11}\text{B}$  and  $1s-0d$  nucleus  $^{23}\text{Na}$  have been studied. These experiments measured the hyperfine effect in  $3/2^\pm \rightarrow 1/2^\pm$  transitions to extract the coupling  $g_p$ . Last, the capture rate of the  $^{16}\text{O}(0^+, 0) \rightarrow ^{16}\text{N}(0^-, 120)$  transition has been measured by several groups; since the  $0^+ \rightarrow 0^-$  spin sequence offers special sensitivity to  $g_p$ .

The material on exclusive OMC is organized as follows. In section IX.B we describe the physical observables in partial transitions. In Sec. IX.C we discuss the dynamical content of the physical observables in OMC and in Sec. IX.D we describe the specific manifestations of the coupling  $g_p$  in OMC. The experimental work on exclusive transitions is covered in Sec. IX.E. In Secs. IX.F and IX.G respectively we review the theoretical framework and nuclear models for exclusive OMC on complex nuclei. In Sec. IX.H we discuss the results for  $g_p$ .

One goal is a unified discussion and comparison of the different experiments and calculations. Another goal is a critical assessment of the current ‘best values’ and model uncertainties in the extraction of the coupling  $g_p$ .

We don’t discuss the related topic of total OMC rates on complex nuclei. Although a large body of accurate data is nowadays available on total OMC rates, because the total rate is weakly dependent on  $g_p$  and the model uncertainties in total rates are large, extracting  $g_p$  isn’t feasible. We point out though that total OMC rates are employed in analyzing the total rate of radiative capture on complex nuclei (see Sec. X).

### A. Free couplings versus effective couplings

We first wish to comment on the meaning of the coupling  $g_p$  that’s extracted from partial transitions on com-

plex nuclei, and specifically the issue of free nucleon coupling constants versus effective nucleon coupling constants.

Suppose one performed an exact calculation of the initial-final wave functions and the weak transition, that is, incorporating all components that contribute significantly to the wave functions and all currents that contribute significantly to the transition. Naturally it would require a large number of basis states, a realistic interaction between nucleons, and the contribution of nucleonic excitations, such as the  $\Delta$  resonance, and exchange currents, such as pion exchange. However such a calculation would involve the free nucleon values of the weak couplings  $g_a$ ,  $g_p$ , etc.

However, in practice only for few-body systems are such highly accurate calculations feasible. Rather in complex nuclei a common practice is to consider only a handful of active nucleons and a truncated model space, and to omit both exchange currents and nucleonic excitations. In such calculations the free coupling constants are replaced by effective coupling constants, with their renormalization accounting for the overall effects of the missing components of the nuclear model. The use of effective electric charges and an effective axial coupling are well known examples of this approach to the problem.

In this article our interest is in the coupling  $g_p$  of the free nucleon. We therefore have tried to use the most sophisticated models available, in order to extract the coupling  $g_p$ . In almost every case we discuss there are full-shell model calculations with perturbation theory computations of core polarization effects, *i.e.* the effects of truncating the model space, and exchange current effects, *e.g.* the effects of pion exchange and  $\Delta$  excitations. In this way we believe we come as close as possible to extracting the free nucleon value for the induced coupling  $g_p$ .

## B. Physical observables

In muon capture the initial state is the 1S ground state of the muonic atom. Capture then yields a muon neutrino with momentum  $\vec{\nu}$  and recoil nucleus with momentum  $-\vec{\nu}$ , *i.e.*

$$\mu^- + [A, Z] \longrightarrow [A, Z - 1] + \nu. \quad (31)$$

For  $J_i = 0$  targets the total spin of the  $\mu$ -atom is  $F = 1/2$ , and for  $J_i > 0$  targets the possible spins of the  $\mu$ -atom are  $F_{\pm} = J_i \pm 1/2$ . On  $J_i = 0$  targets the necessary variables for describing capture are the  $\mu$ -atom orientation, the recoil orientation and the neutrino direction. On  $J_i > 0$  targets the capture process is further dependent on the  $F$ -state.

### 1. Capture rates

The easiest observable to experimentally determine is the capture rate of the partial transition. For  $J_i = 0$

targets we shall denote the capture rate by  $\Lambda$  and for  $J_i > 0$  targets we shall denote the hyperfine rates by  $\Lambda_{\pm}$ . In addition on  $J_i > 0$  targets it's useful to define the statistical rate

$$\Lambda_S = \left(\frac{J_i + 1}{2J_i + 1}\right)\Lambda_+ + \left(\frac{J_i}{J_i + 1}\right)\Lambda_- \quad (32)$$

where  $(J_i + 1)/(2J_i + 1)$  and  $J_i/(2J_i + 1)$  are the statistical populations of the  $F_{\pm}$  hyperfine states.

### 2. Recoil asymmetries

Generally the direction of emission of recoils after capture is anisotropic about the  $\mu$ -atom orientation axis.<sup>15</sup> For  $J_i = 0$  targets the angular distribution for recoil emission is (Bernabeu , 1975; Ciechanowicz and Oziewicz , 1984; Mukhopadhyay , 1977)

$$\frac{d\Lambda}{d\Omega} = \frac{\Lambda}{4\pi} [1 + \alpha |\vec{P}_{\mu}| P_1(\hat{P}_{\mu} \cdot \hat{\nu})] \quad (33)$$

where  $\vec{P}_{\mu}$  is the muon polarization,  $\hat{\nu}$  is the neutrino direction,  $P_1$  is the  $\ell = 1$  Legendre polynomial, and  $\alpha$  is the asymmetry coefficient. Note that the recoil asymmetry is a pseudoscalar quantity, and therefore an example of parity violation in muon capture.

For  $J_i > 0$  targets the angular distribution for recoil emission is generally more complicated. For example a  $F = 1$   $\mu$ -atom may possess both a vector polarization, *i.e.* non-statistical populations of the  $m_F = +1$  and  $m_F = -1$  sub-states, and a tensor polarization, *i.e.* non-statistical populations of the  $|m_F| = 1$  and  $m_F = 0$  sub-states. Consequently for  $F = 1$  capture the angular distribution of recoil emission is (Ciechanowicz and Oziewicz , 1984; Congleton and Fearing , 1993; Galindo and Pascual , 1968)

$$\frac{d\Lambda}{d\Omega} = \frac{\Lambda}{4\pi} [1 + A_v |\vec{P}_{\mu}| P_1(\hat{P}_{\mu} \cdot \hat{\nu}) + A_t |\vec{P}_{\mu}| P_2(\hat{P}_{\mu} \cdot \hat{\nu})] \quad (34)$$

where  $A_v$  is the vector asymmetry coefficient and  $A_t$  is the tensor asymmetry coefficient. Note for  $F > 1$  atoms even higher ranks of  $\mu$ -atom orientation are possible in principle.

We stress that  $\vec{P}_{\mu}$  in Eq. (33) and Eq. (34) is the muon's residual polarization in the  $\mu$ -atom ground state. Unfortunately in all targets the muon-nucleus spin-orbit interaction leads to substantial depolarization during the atomic cascade. For example for  $J_i = 0$  targets the residual polarization is typically 17%. Further in  $J \neq 0$  targets the muon-nucleus spin-spin interaction

<sup>15</sup> An exception is the isotropic distribution of the recoil emission from a  $F = 0$   $\mu$ -atom.

leads to additional depolarization during the atomic cascade. The degree of depolarization is dependent on  $J_i$  and  $F$ . For further details see Favart *et al.* (1970); Hambro and Mukhopadhyay (1975, 1977); Kuno *et al.* (1987); Mukhopadhyay (1977).

### 3. Recoil orientations

Generally after muon capture the recoil nucleus is oriented, where orientation along both the  $\nu$ -momentum axis and the  $\mu$ -spin axis is possible. For a  $J_f = 1/2$  recoil the orientation is described by its recoil polarization  $P$ , where  $P = (p_{+1/2} - p_{-1/2}) / \sum p_m$  with  $p_m$  denoting the population of each magnetic sub-state  $m$ . For a  $J_f = 1$  recoil the orientation is described by its polarization  $P$  and its alignment  $A$ , where  $A = (p_{+1} + p_{-1} - 2p_0) / \sum p_m$ . For  $J_f > 1$  recoils even higher ranks of orientation are possible in principle. Conventionally the recoil orientation along the  $\nu$ -momentum axis is designated the longitudinal polarization  $P_L$  and longitudinal alignment  $A_L$ , and the recoil orientation along the  $\mu$ -spin axis is designated the average polarization  $P_{av}$  and average alignment  $A_{av}$ . The recoil polarizations, *i.e.*  $P_L$  and  $P_{av}$ , are pseudoscalar quantities and additional examples of parity violation in muon capture. For further details see Bernabeu (1975); Devanathan *et al.* (1972); Mukhopadhyay (1977); Subramanian *et al.* (1976).

Additionally triple correlations of the recoil orientation with the  $\mu$ -spin direction and the  $\nu$ -momentum direction are possible. Of experimental importance are the so-called forward hemisphere and backward hemisphere polarizations. Defining the hemispheres relative to the  $\mu$ -spin axis,  $P_F$  is the polarization along the  $\mu$ -axis for the ‘forward hemisphere’ recoils, and  $P_B$  is the polarization along the  $\mu$ -axis for the ‘backward hemisphere’ recoils. Note that  $P_F$  and  $P_B$  are related to  $P_L$  and  $P_{av}$  via

$$P_F = \frac{1}{2}(P_{av} + \frac{1}{2}P_L) \quad (35)$$

$$P_B = \frac{1}{2}(P_{av} - \frac{1}{2}P_L) \quad (36)$$

which demonstrates their dependence on both the  $\mu$ -spin direction and the  $\nu$ -momentum direction.

### 4. Gamma-ray correlations

Gamma-ray directional correlations with the  $\nu$ -momentum axis and the  $\mu$ -spin axis in the sequence

$$\mu^- + [Z, A] \longrightarrow [Z - 1, A]^* + \nu \longrightarrow [Z - 1, A]^{**} + \gamma \quad (37)$$

are additional observables in partial transitions. Such correlations originate from the recoil orientation and the

recoil asymmetry in the capture process. For unpolarized muons a  $\gamma$ - $\nu$  directional correlation is possible and for polarized muons a  $\gamma$ - $\nu$ - $\mu$  triple correlation is also possible. In discussing the correlations we shall denote the spin sequence in Eq. (37) by  $J_i \rightarrow J_f \rightarrow j$  where  $J_i$ ,  $J_f$  and  $j$  are the angular momenta of the three nuclear states. Note that below we consider only unpolarized targets and  $J_f \leq 1$  recoils. For further details see Ciechanowicz and Oziewicz (1984).

For unpolarized muons  $\vec{P}_\mu = 0$  the  $\gamma$ - $\nu$  directional correlation is given by <sup>16</sup>

$$W = 1 + a_2 P_2(\hat{k} \cdot \hat{\nu}) \quad (38)$$

where  $\hat{k}$  is the  $\gamma$ -ray direction,  $\hat{\nu}$  is the neutrino direction,  $P_2$  is the  $\ell = 2$  Legendre polynomial, and  $a_2$  is the  $\gamma$ - $\nu$  correlation coefficient. Note that this directional correlation  $a_2$  is a consequence of the longitudinal alignment  $A_L$  of the recoil nucleus in the capture process.

For polarized muons  $\vec{P}_\mu \neq 0$  the  $\gamma$ - $\nu$ - $\mu$  triple correlation is given by

$$W = 1 + (\alpha + \frac{2}{3}c_1) \vec{P}_\mu \cdot \hat{k} \cdot \hat{\nu} + (a_2 + b_2 \vec{P}_\mu \cdot \hat{\nu} \hat{k} \cdot \hat{\nu}) P_2(\hat{k} \cdot \hat{\nu}) \quad (39)$$

and contains three distinct correlation terms involving  $(\alpha + \frac{2}{3}c_1)$ ,  $a_2$  and  $b_2$ . Note in Eq. (39) that (i)  $\hat{k}$  enters only quadratically because of parity conservation in  $\gamma$ -decays, (ii)  $\vec{P}_\mu$  enters only linearly because the muon is spin- $1/2$ , and (iii)  $\hat{\nu}$  enters in powers of two or less for  $J_f \leq 1$ . In Eq. (39) the correlation involving  $\alpha$  is a consequence of the recoil asymmetry and the correlation involving  $a_2$  is a consequence of the longitudinal alignment. The remaining terms, *i.e.*  $c_1$  and  $b_2$ , originate from the triple correlation of the recoil alignment with  $\vec{P}_\mu$  and  $\hat{\nu}$ . If either unpolarized muons, *i.e.*  $\vec{P}_\mu = 0$ , or perpendicular geometry, *i.e.*  $\vec{P}_\mu \cdot \hat{k} = 0$ , is employed the only non-vanishing correlation is  $a_2$ , and Eq. (39) becomes Eq. (38).

It's important to recognize that  $c_1$ ,  $a_2$  and  $b_2$  are functions of both the  $\mu$ -capture process and the  $\gamma$ -decay process. For example the coefficient  $a_2$  may be written in the form of a product  $A_L B_2$ , where the alignment  $A_L$  is governed by the  $\mu$  capture process and the parameter  $B_2$  is governed by the  $\gamma$ -decay process. A handy compilation of the coefficients  $B_2$  for various  $J_f \rightarrow j$  spin-parities, multipolarities, and mixing ratios is given in Table 1 of Ciechanowicz and Oziewicz (1984). Note that in certain cases, *e.g.* for M1 emission in a  $1^+ \rightarrow 0^+$  decay,

<sup>16</sup> The theory of  $\gamma$ -ray correlations was developed by Popov and co-workers in Bukat and Popov (1964); Bukhvostov and Popov (1967a,b,c, 1970); Oziewicz and Popov (1965); Popov (1963). See also Parthasarathy and Sridhar (1978) and Ciechanowicz and Oziewicz (1984).

$B_2$  is large, but in other cases, *e.g.* for M1 emission in a  $1^+ \rightarrow 2^+$  decay,  $B_2$  is small. This makes the former  $1^+ \rightarrow 0^+$  case more favorable, and the latter  $1^+ \rightarrow 2^+$  case less favorable, for  $\gamma$ -ray correlation experiments.

### C. Helicity representation

Herein we consider the overall dynamical content of exclusive muon capture. Utilizing the helicity representation we discuss the constraints imposed on  $\mu$  capture by  $\nu$ -handedness and T-invariance. We shall denote the corresponding helicity amplitudes by  $T_\lambda^F$ , where  $\lambda$  is the recoil helicity and  $F$  is the  $\mu$ -atom hyperfine state. We use the superscript ‘+’ for  $F = J_i + 1/2$  capture, the superscript ‘-’ for  $F = J_i - 1/2$  capture, and no superscript for  $J_i = 0$  atoms. Assuming the absence of T violation in  $\mu$  capture the helicity amplitudes are real numbers.

Further details on the helicity representation in the  $(\mu, \nu)$  reaction are given in Bernabeu (1975), Mukhopadhyay (1977) and Ciechanowicz and Oziewicz (1984).

#### 1. Capture on zero-spin targets

For  $J_i = 0$  targets the helicity representation depicts muon capture as the two-body decay of a spin-1/2  $\mu$ -atom into a left-handed neutrino and a spin- $J_f$  recoil. Choosing the  $z$ -axis along the  $\nu$ -axis, the definite neutrino helicity of  $\lambda_\nu = -1/2$  means the allowable recoil helicities are  $\lambda_f = 0, +1$ . The corresponding helicity amplitudes, denoted by  $T_0$  and  $T_1$ , are the underlying dynamical variables in  $\mu$  capture on  $J_i = 0$  targets.

In Table IV we compile explicit formulas for various physical observables in  $0 \rightarrow J_f$  transitions in terms of  $T_0, T_1$  and their ratio  $X = \sqrt{2}T_0/T_1$ . The  $\gamma$ -ray correlation coefficients also involve the quantity  $B_2$  that is governed by the  $\gamma$ -decay. With the exception of  $\Lambda$ , the reaction dynamics are completely determined by  $X$ , and consequently there exist numerous relations between observables in  $0 \rightarrow J_f$  transitions, for example see Bernabeu (1975) and Mukhopadhyay (1977). Clearly although different observables offer alternative possibilities for experimental measurements, the dynamical content of  $0 \rightarrow J_f$  transitions is somewhat limited.

Note that the  $0 \rightarrow 0$  sequence is a special case. Compared to  $J_f > 0$ , where the  $\lambda_f = 0, +1$  helicity states are allowable, for  $J_f = 0$ , only the  $\lambda_f = 0$  helicity state is possible. Consequently a single amplitude  $T_0$  is the sole dynamical quantity for physical observables in  $0 \rightarrow 0$  transitions.

#### 2. Capture on nonzero-spin targets

For  $J_i > 0$  targets the helicity representation depicts capture as a two-body decay of the  $F = J_i \pm 1/2$   $\mu$ -atom. Based on definite neutrino handedness and angu-

TABLE IV Helicity decomposition of physical observables in  $0 \rightarrow 1$  transitions. We give the capture rate  $\Lambda$ , recoil asymmetry  $\alpha$ , longitudinal polarization and alignment  $P_L$  and  $A_L$ , average polarization and alignment  $P_{av}$  and  $A_{av}$ , and  $\gamma$ -ray correlation coefficients  $a_2, b_2$  and  $(\alpha + \frac{2}{3}c_1)$ . The helicity amplitudes for recoil helicities of  $\lambda_f = 0, +1$  are denoted by  $T_0$  and  $T_1$  and  $X = \sqrt{2}T_0/T_1$ . The parameter  $B_2$  involved in the  $\gamma$ -ray correlations depends on the spin-parities of the initial-final states and the multipolarity of the gamma-radiation in the  $\gamma$ -decay.

Observable	Helicity decomposition
$\Lambda$	$ T_1 ^2(2 + X^2)$
$\alpha$	$(X^2 - 2)/(X^2 + 2)$
$P_L$	$-2/(2 + X^2)$
$A_L$	$2(1 - X^2)/(2 + X^2)$
$P_{av}$	$2/3(1 + 2X)/(2 + X^2)$
$A_{av}$	0
$\alpha + \frac{2}{3}c_1$	$B_2\sqrt{2}(2 + 2X - X^2)/(2 + X^2)$
$a_2$	$B_2\sqrt{2}(1 - X^2)/(2 + X^2)$
$b_2$	$B_2\sqrt{2}(1 - 2X + X^2)/(2 + X^2)$

lar momentum coupling the total number of recoil helicity states  $\lambda_f$  and contributing helicity amplitudes  $T_\lambda^F$  is the lesser of either  $2J_f + 1$  or  $2F + 1$  (Ciechanowicz and Oziewicz, 1984; Mukhopadhyay, 1977).

For concreteness let’s consider the example of a  $1/2 \rightarrow 1/2$  transition, where the  $\mu$ -atom spin is either  $F = 0$  or  $F = 1$ . For  $F = 1$  both the  $\lambda_f = -1/2, +1/2$  recoil helicity states are populated, but for  $F = 0$  only the  $\lambda_f = +1/2$  recoil helicity state is populated because of the single magnetic sub-state of the  $F = 0$   $\mu$ -atom. Consequently one helicity amplitude governs the  $F = 0$  capture, two helicity amplitudes govern the  $F = 1$  capture, and three dynamical variables underlie  $1/2 \rightarrow 1/2$  transitions. By comparison in  $3/2 \rightarrow 1/2$  transitions a total of four helicity amplitudes contribute, two for  $F_+$  capture and two for  $F_-$  capture.

In summary for  $J_i > 0$  targets many independent quantities are experimentally accessible. In principle the increased number of variables allows an increased number of cross checks on model calculations for  $J_i > 0$  transitions.

## D. Induced currents

Most often in partial transitions the leading contributions originate from the axial coupling  $g_a$ . This subsection concerns ‘where to find the coupling  $g_p$ ?’

To answer this question we shall examine capture in (i) the  $q/M \rightarrow 0$  limit, where  $q$  is the three-momentum transfer and  $M$  is the nucleon mass, and (ii) in the Fujii–Primakoff (FP) approximation (Fujii and Primakoff, 1959). In the  $q/M \rightarrow 0$  limit the effects of  $g_p$  are absent. However in the FP approximation, which keeps  $q/M$  terms involving allowed operators, but drops  $\ell$ -forbidden and gradient operators, the leading effects of induced currents are present. Therefore comparison of the capture process in the  $q/M \rightarrow 0$  limit and the FP approximation is helpful in understanding the manifestation of  $g_p$  in capture.

At this point it is helpful to recall the Fujii–Primakoff effective Hamiltonian for muon capture (Fujii and Primakoff, 1959; Primakoff, 1959). Its form is

$$\tau^+ \frac{\mathbf{1} - \boldsymbol{\sigma} \cdot \hat{\boldsymbol{\nu}}}{2} \sum_{i=1}^A \tau_i^- (G_V \mathbf{1} \cdot \mathbf{1}_i + G_A \boldsymbol{\sigma} \cdot \boldsymbol{\sigma}_i + G_P \boldsymbol{\sigma} \cdot \hat{\boldsymbol{\nu}} \boldsymbol{\sigma}_i \cdot \hat{\boldsymbol{\nu}}) \delta(\mathbf{r} - \mathbf{r}_i) \quad (40)$$

where  $\mathbf{1}$ ,  $\mathbf{1}_i$ ,  $\boldsymbol{\sigma}$  and  $\boldsymbol{\sigma}_i$  are the  $2 \times 2$  unit and spin matrices and  $\mathbf{r}$  and  $\mathbf{r}_i$  are the spatial coordinates of the lepton and the  $i^{\text{th}}$  nucleon respectively,  $\hat{\boldsymbol{\nu}}$  is the  $\nu$ -momentum unit vector, and  $\tau^+$ ,  $\tau_i^-$  convert the muon into a neutrino and a proton into a neutron. Last,  $G_V$ ,  $G_A$  and  $G_P$  are the so-called Fujii–Primakoff effective couplings

$$G_V = g_v \left(1 + \frac{q}{2M}\right) \quad (41)$$

$$G_A = -(g_a + \frac{q}{2M}(g_v + g_m)) \quad (42)$$

$$G_P = -\frac{q}{2M}(g_p - g_a + g_v + g_m) \quad (43)$$

Note that, when  $q/M \rightarrow 0$ , the coupling  $G_P$  vanishes and  $G_V$  and  $G_A$  are determined by  $g_v$  and  $g_a$  respectively. Furthermore the induced currents are order  $q/M$ , and  $g_p$  appears in  $G_P$  only. For the canonical values of the weak couplings, as given in Table I (see Sec. II),  $G_V = 1.00$ ,  $G_A = -1.27$  and  $G_P = 0.00$  in the  $q/M \rightarrow 0$  limit, and  $G_V = 1.03$ ,  $G_A = -1.52$  and  $G_P = -0.62$  in the FP approximation and with  $q = 100$  MeV/c.

### 1. Asymmetries, orientations and correlations

To understand the  $g_p$  sensitivity of orientations, correlations, etc., we compare the terms with  $G_A$  and  $G_P$  in Eq. (40). Observe the operator corresponding to the  $G_P$  term, *i.e.*  $(\mathbf{1} - \boldsymbol{\sigma} \cdot \hat{\boldsymbol{\nu}}) \boldsymbol{\sigma} \cdot \hat{\boldsymbol{\nu}} \boldsymbol{\sigma}_i \cdot \hat{\boldsymbol{\nu}}$ , cannot change the spin projection of either the lepton or the nucleon along

the  $\nu$ -momentum axis. However this limitation does not apply to the  $G_A$  term and the operator  $(\mathbf{1} - \boldsymbol{\sigma} \cdot \hat{\boldsymbol{\nu}}) \boldsymbol{\sigma} \cdot \boldsymbol{\sigma}_i$ . Consequently in Eq. (40) the  $G_P$  term admits only a longitudinal coupling of the weak currents whereas the  $G_A$  term admits also a transverse coupling of the weak currents. This makes correlations, orientations, etc., sensitive to  $g_p/g_a$ . For further details see Grenacs (1985).

To further illustrate the  $g_p$  sensitivity we consider the example of a  $0^+ \rightarrow 1^+$  transition. In the  $q/M \rightarrow 0$  limit the two helicity amplitudes, *i.e.*  $T_0$  and  $T_1$ , are both determined by the product of the coupling  $g_a$  and the allowed Gamow–Teller operator, and  $X = 1$ . However in the FP approximation, the amplitude  $T_0$  is proportional to  $(G_A - G_P)$  and involves a longitudinal coupling of the weak currents, and the amplitude  $T_1$  is proportional to  $G_A$  and involves a transverse coupling of the weak currents, and  $X = (G_A - G_P)/G_A \simeq 0.59$  for  $q = 100$  MeV/c. Therefore the asymmetries, correlations and orientations, which are governed by  $X$ , permit the determination of  $g_p/g_a$ . For further details see Mukhopadhyay (1977).

In Table V we compile FP approximation expressions for physical observables in  $0^+ \rightarrow 1^+$  transitions in terms of  $G_A$  and  $G_P$ . Note in the  $q/M \rightarrow 0$  limit the recoil polarizations are  $P_L = -2/3$  and  $P_{av} = +2/3$  and the recoil alignments are  $A_L = 0$  and  $A_{av} = 0$ , thus indicating that the recoil is ‘highly polarized’ but ‘not aligned’. Most strikingly, in the FP approximation the longitudinal alignment  $A_L = +0.55$  is very large and highly sensitive to  $g_p/g_a$ . This occurs because the alignment measures the difference in population of the  $\lambda_f = 0$  recoil sub-state, which is populated by  $G_P$ , and the  $\lambda_f = 1$  recoil sub-state, which is not populated by  $G_P$ . It therefore represents a golden observable for the spin structure of the induced coupling  $g_p$ .

### 2. Hyperfine dependences

The hyperfine dependence  $\Lambda_+/\Lambda_-$  of  $\Delta J^\pi = J_f - J_i = \pm 1^+$  transitions in muon capture on  $J_i \neq 0$  targets is also sensitive to the coupling  $g_p$ . Specifically in the multipole expansion of the Fujii–Primakoff Hamiltonian the  $G_A$ -term makes allowed contributions to neutrino waves with total angular momentum  $j^\pi = 1/2^+$  only, whereas the  $G_P$ -term makes allowed contributions to neutrino waves with total angular momentum  $j^\pi = 3/2^+$  also. This difference is because of *hatv* in Eq. (40). In  $\Delta J^\pi = +1^+$  transitions, neutrinos with  $j = 1/2^+$  may be emitted in  $F_+$  capture, but neutrinos with  $j = 3/2^+$  must be emitted in  $F_-$  capture. This makes  $\Lambda_+/\Lambda_- \gg 1$  and a strong function of the ratio  $g_p/g_a$ . However in  $\Delta J^\pi = -1^+$  transitions, neutrinos with  $j = 1/2^+$  may be emitted in  $F_-$  capture, but neutrinos with  $j = 3/2^+$  must be emitted in  $F_+$  capture. This makes  $\Lambda_+/\Lambda_- \ll 1$  and a strong function of the ratio  $g_p/g_a$ .

For example, we consider the important case of  $3/2^+ \rightarrow 1/2^+$  transitions. In the  $q/M \rightarrow 0$  limit, cap-

TABLE V Expressions and values of observables for  $0^+ \rightarrow 1^+$  transitions in the  $q/M \rightarrow 0$  limit and the Fujii-Primakoff approximation.  $G_A$  and  $G_P$  are the Fujii-Primakoff effective constants defined in Eqs. (42) and (43) and the common denominator is  $\Gamma = (3G_A^2 + G_P^2 - 2G_A G_P)$ . We tabulate the  $\gamma$ -ray directional correlations for the  $0^+ \rightarrow 1^+ \rightarrow 0^+$  sequence.

Observable	FPA Eq.	$q/M \rightarrow 0$ value	FPA value
$\alpha$	$(3G_A^2 + G_P^2 - 2G_A G_P)/\Gamma$	-0.33	-0.70
$P_L$	$-2G_A^2/\Gamma$	-0.67	-0.85
$A_L$	$(-2G_P^2 + 4G_A G_P)/\Gamma$	0.00	-0.55
$P_{av}$	$(2G_A^2 - \frac{4}{3}G_A G_P)/\Gamma$	+0.67	+0.61
$A_{av}$	0	0	0
$\alpha + \frac{2}{3}c_1$	$(3G_A^2 - G_P^2)/\Gamma$	1.0	1.21
$a_2$	$(-G_P^2 + 2G_P G_A)/\Gamma$	0.00	0.28
$b_2$	$G_P^2/\Gamma$	0.00	0.07

ture from the  $F_- = 1$  hyperfine state is governed by  $g_a$  but capture from the  $F_+ = 2$  hyperfine state is forbidden. Therefore  $\Lambda_+/\Lambda_- = 0$ . However in the FP approximation, the two  $F_+$  helicity amplitudes are proportional to  $G_P$  while the two  $F_-$  helicity amplitudes are proportional to either  $(4G_A - G_P)$  or  $(2G_A - G_P)$ . Consequently the hyperfine dependence  $\Lambda_+/\Lambda_-$  is highly dependent on  $g_p/g_a$ .

The FP approximation expressions for various observables in  $3/2^+ \rightarrow 1/2^+$  transitions are given in Table VI. In passing we mention that the asymmetries, correlations and orientations in  $F_-$  capture for  $3/2^+ \rightarrow 1/2^+$  transitions are also sensitive to the coupling  $g_p$ , for the same reasons as described for the  $0^+ \rightarrow 1^+$  transitions in the preceding Sec. IX.D.1. This is not true for the case of asymmetries, correlations and orientations for  $F_+$  capture in  $3/2^+ \rightarrow 1/2^+$  transitions, because only  $j^\pi = 3/2^+$  neutrino emission is possible.

Related FP approximation expressions for other  $\Delta J^\pi = \pm 1^+$  transitions are given for example by Mukhopadhyay (1977) and Ciechanowicz and Oziewicz (1984).

TABLE VI Equations and values for selected observables in  $3/2^+ \rightarrow 1/2^+$  transitions in the  $q/M \rightarrow 0$  limit and Fujii-Primakoff approximation. The common denominator is  $\Gamma = (24G_A^2 - 16G_A G_P + 3G_P^2)$ .

Observable	FPA Eq.	$q/M \rightarrow 0$ value	FPA value
$\Lambda_+/\Lambda_-$	$3G_P^2/\Gamma$	0.00	0.027
$\alpha^-$	$-\frac{1}{3}(4G_A - G_P)^2/\Gamma$	-0.22	-0.24
$\alpha^+$	$\frac{2}{5}$	+0.60	+0.60
$P_L^-$	$(8G_A^2 - G_P^2)/\Gamma$	+0.33	+0.44
$P_L^+$	$\frac{1}{5}$	+0.20	+0.20

### 3. Capture rates

In general in  $\mu$  capture the rate  $\Lambda$  has a fairly weak dependence on the coupling  $g_p$ . For example in  $0^+ \rightarrow 1^+$  transitions the contribution of  $g_p$  is typically 10%. However an exception is the capture rate of the first-forbidden  $0^+ \leftrightarrow 0^-$  transition.

To understand the sensitivity it is instructive to assume the dominance of the  $\ell = 1$  retarded Gamow-Teller operator in the first-forbidden  $0^+ \rightarrow 0^-$  transition, *i.e.* ignoring the contribution from the axial charge operator. For details see Towner and Khanna (1981). The capture rate in  $0^+ \rightarrow 0^-$  transitions is then governed by the coupling constant combination  $(G_A - G_P)$ , which is strongly dependent on  $g_p$ . For example in going from  $g_p = 0$  to  $g_p = 6.7g_a$  the rate is increased by roughly 50%. In short, the quantum numbers of the  $\Delta J^\pi = 0^-$  multipole are effective in isolating the longitudinal contributions to weak currents, such as  $g_p$ .

### E. Experimental studies of partial transitions

This subsection concerns the experimental work on exclusive OMC. We discuss two allowed transitions on  $J_i = 0$  targets,  $^{12}\text{C}(0^+, 0) \rightarrow ^{12}\text{B}(1^+, 0)$  and  $^{28}\text{Si}(0^+, 0) \rightarrow ^{28}\text{Al}(0^+, 2201)$ , two allowed transitions on  $J_i \neq 0$  targets,  $^{11}\text{B}(3/2^-, 0) \rightarrow ^{11}\text{Be}(1/2^-, 320)$  and  $^{23}\text{Na}(3/2^+, 0) \rightarrow ^{23}\text{Ne}(1/2^+, 3458)$ , and the first-forbidden transition  $^{16}\text{O}(0^+, 0) \rightarrow ^{16}\text{N}(0^-, 120)$ . The experiments include measurements of capture rates, recoil orientations,  $\gamma$ -ray correlations, and hyperfine dependences.

1.  $^{12}\text{C}(0^+, 0) \rightarrow ^{12}\text{B}(1^+, 0)$ 

The  $^{12}\text{C}(0^+, 0) \rightarrow ^{12}\text{B}(1^+, 0)$  reaction is an allowed Gamow-Teller transition between the spin-0, isoscalar  $^{12}\text{C}$  ground state and the spin-1 isovector  $^{12}\text{B}$  ground state. The transition was first observed in cosmic-ray data by Godfrey (1953) via the identification of the Godfrey-Tiomino cycle, *i.e.*  $\mu$  capture on  $^{12}\text{C}$  followed by  $\beta$ -decay of  $^{12}\text{B}$ .

The first investigation of the recoil polarization in the  $^{12}\text{C}(0^+, 0) \rightarrow ^{12}\text{B}(1^+, 0)$  transition was conducted by Love *et al.* (1959) in order to measure the  $\mu^-$  helicity in  $\pi^-$  decay. The application of polarization measurements to induced currents was pioneered by Possoz *et al.* (1977, 1974) at Saclay and extended by Roesch *et al.* (1981a,b) and Truttman *et al.* (1979) at PSI. Using ingenious techniques these researchers have amassed impressive data on several polarization observables in  $^{12}\text{C}(0^+, 0) \rightarrow ^{12}\text{B}(1^+, 0)$  capture. More recently Kuno *et al.* (1984, 1986) at the BOOM facility have polished some techniques and re-measured the polarization  $P_{av}$ .

The procedure for measuring the polarization  $P_{av}$  of  $^{12}\text{B}$  recoils from  $^{12}\text{C}$  capture is straightforward in principle. First one makes polarized  $\mu^-^{12}\text{C}$  atoms by stopping polarized muons in carbon-containing material. Next the polarized  $\mu^{12}\text{C}$  atoms produce the polarized  $^{12}\text{B}$  recoils via muon capture. Then one measures the  $^{12}\text{B}$   $\beta$ -ray asymmetry to determine the recoil polarization  $P_{av}$ . Note that the method relies on the known correlation of the ejected  $\beta$ -rays with the  $^{12}\text{B}$  orientation. Also note that this method gives the average polarization  $P_{av}$ , *i.e.* along the  $\mu$ -axis, not the longitudinal polarization  $P_L$ , *i.e.* along the  $\nu$ -axis.

Unfortunately the measurement of  $P_{av}$  is difficult in practice. First the muon polarization is largely destroyed via the spin-orbit interaction in the atomic cascade. Second the  $^{12}\text{B}$  polarization is easily destroyed by the spin-spin interaction in the host material. Third only about 1% of  $\mu$  stops in  $^{12}\text{C}$  undergo the  $^{12}\text{C}(0^+, 0) \rightarrow ^{12}\text{B}(1^+, 0)$  transition (Maier *et al.*, 1964; Reynolds *et al.*, 1963). Consequently, the beta-ray asymmetries are small, the target choices are limited, and backgrounds are troublesome. Fortunately the short 29 ms lifetime and high 15 MeV end point for  $^{12}\text{B}$  beta-decay are ideally suited to a measurement of the polarization.

Average polarization measurements have been performed by Possoz *et al.* (1977, 1974) at Saclay and Kuno *et al.* (1984, 1986) at BOOM. The basic set-up comprises a beam telescope for detecting incoming muons, beta-ray counters for detecting  $^{12}\text{B}$  decays, and Michel counters for detecting  $\mu$ -decays. Possoz *et al.* (1977, 1974) found a  $\geq 0.3$  kG longitudinal B-field and a graphite target were sufficient to preserve the  $^{12}\text{B}$  polarization for  $t > 29$  ms. Note that the distinctive lifetime/end point are used to identify the  $^{12}\text{B}$   $\beta$ -rays and their forward/backward count rates are used to determine the  $^{12}\text{B}$   $\beta$ -asymmetry. Pulsed-beam operation allows beta-ray detection under beam-off conditions and reduces the

backgrounds. Transverse-field precession of the  $\mu$  spin is used to measure the muon polarization  $P_\mu$ .

One challenge is the experimental determination of a small  $\beta$ -ray asymmetry ( $\sim 3\%$ ) with a reasonable accuracy ( $\pm 10\%$ ). Consequently false asymmetries, such as geometrical and instrumental effects, must be minimized and then measured. Possoz *et al.* (1977, 1974) used a polarization preserving target material (graphite) and a polarization destroying target (polyethylene) to determine false asymmetries. Kuno *et al.* (1984, 1986) used a novel magnetic resonance technique to periodically destroy the muon polarization.

In summary the resulting values of the average polarization were  $P_{av} = 0.38 \pm 0.07$  from Possoz *et al.* (1974),  $P_{av} = 0.452 \pm 0.042$  from Possoz *et al.* (1977),  $P_{av} = 0.462 \pm 0.053$  from Kuno *et al.* (1984, 1986). We discuss the extraction of  $g_p$  from  $P_{av}$  in Sec. IX.H.1.

Additionally the forward ( $P_F$ ) and backward ( $P_B$ ) polarizations, defined in Eqs. (35) and (36), for the  $^{12}\text{C}(0^+, 0) \rightarrow ^{12}\text{B}(1^+, 0)$  transition have been measured by Truttman *et al.* (1979) and Roesch *et al.* (1981b). These experiments are masterpieces of ingenuity and technique.

The experiments employed a novel target with recoil direction sensitivity. The targets comprised a multi-layer sandwich of ‘triple-foils’ with each triple-foil comprising a carbon target foil (C), a polarization preserving foil (P), and a polarization destroying foil (D). Arranging the P-foil upstream and D-foil downstream of the carbon foil, *i.e.* DCP, permits selective retention of the forward hemisphere recoil polarization. Arranging the D-foil upstream and P-foil downstream of the carbon foil, *i.e.* PCD, permits selective retention of the backward hemisphere recoil polarization. Thereby  $\beta$ -ray asymmetry measurements for the DCP configuration yield  $P_F$  and the PCD configuration yield  $P_B$ . Additionally a PCP sandwich enables the measurement of the average polarization and a DCD sandwich enables the measurement of the false asymmetries.

One advantage of measuring  $P_{F/B}$  is a larger recoil polarization and a larger beta-ray asymmetry.<sup>17</sup> Another advantage is that combining both  $P_F$  and  $P_B$  to deduce  $P_{av}/P_L$  where

$$\frac{P_{av}}{P_L} = 2 \frac{P_F + P_B}{P_F - P_B} \quad (44)$$

reduces the sensitivity to false asymmetries and systematic uncertainties. Note that the measurements of  $P_F$  and  $P_B$  are achieved by simply rotating the multi-layer target by 180 degrees.

However a major challenge in measuring  $P_{F/B}$  is the small quantity of the  $^{12}\text{C}$  material in the multi-layer tar-

<sup>17</sup> Recall from Sec. IX.B.3 that  $P_{F/B}$  have contributions from both  $P_{av}$ , which is decreased by  $\mu$  depolarization, and from  $P_L$ , which is unchanged by  $\mu$  depolarization.



get, since the carbon foils must be thin enough for recoils to emerge and the P/D foils must be thick enough for recoils to stop. Consequently any  $^{12}\text{B}$  background from  $\mu^-$  stops in nearby carbon is especially perilous. Therefore Truttman *et al.* (1979) and Roesch *et al.* (1981b) took great care to avoid using any carbon-containing materials in the neighborhood of the experiment. Based on these data the authors obtained  $P_{av}/P_L = -0.516 \pm 0.041$ .

In Table VII we summarize the various measurements of recoil polarizations in  $^{12}\text{C}(0^+, 0) \rightarrow ^{12}\text{B}(1^+, 0)$ . Note we quote all results in terms of the helicity amplitude ratio  $X$  so as to facilitate their comparison. The experimental results are mutually consistent.

We stress the experimental results for  $P_{av}$  and  $P_{F/B}$  are for muon capture to all bound states in the  $^{12}\text{B}$  nucleus. Therefore a correction is necessary to obtain the interesting ground state polarization from the observed bound state polarization. Measurements of the total rate to bound states (Maier *et al.*, 1964; Reynolds *et al.*, 1963) and the individual rates to excited states (Budyashov *et al.*, 1970; Giffon *et al.*, 1981; Miller *et al.*, 1972a; Roesch *et al.*, 1981a) are employed to determine this correction.

Unfortunately the  $\gamma$ -ray measurements of  $\mu$  capture to individual  $^{12}\text{B}$  excited states are complicated by near equal energies of several Doppler broadened  $\gamma$ -rays.<sup>18</sup> Furthermore the latest results of Roesch *et al.* (1981a) and earlier results of Budyashov *et al.* (1970), Miller *et al.* (1972a) and Giffon *et al.* (1981) are in disagreement, and consequently there exists some uncertainty in the correction for the capture to the  $^{12}\text{B}$  excited states. For a detailed discussion of the experimental data see Measday (2001). Using the  $\gamma$ -ray yields from Giffon *et al.* (1981) and the model calculations of Fukui *et al.* (1987), the world average for  $X$  in  $^{12}\text{C}(0^+, 0) \rightarrow ^{12}\text{B}(1^+, 0)$  is  $0.23 \pm 0.06$ . However using the  $\gamma$ -ray yields from Roesch *et al.* (1981a) and the model calculations of Fukui *et al.* (1987), the world average for  $X$  in  $^{12}\text{C}(0^+, 0) \rightarrow ^{12}\text{B}(1^+, 0)$  is  $0.20 \pm 0.06$ . Fortunately the corrections are not too large.

## 2. $^{11}\text{B} \rightarrow ^{11}\text{Be}$ and $^{23}\text{Na} \rightarrow ^{23}\text{Ne}$

Historically studies of the hyperfine effect in nuclear muon capture reaction were important in demonstrating the  $V - A$  structure of weak interactions. These experiments were performed in muonic  $^{19}\text{F}$  by Culligan *et al.* (1961) and Winston (1963). The first application of the hyperfine effect to the induced coupling  $g_p$  was conducted by Deutsch *et al.* (1968) in muonic  $^{11}\text{B}$ . Recently Wiaux *et al.* (2002) at PSI have improved the data on  $^{11}\text{B}$ , and

Johnson *et al.* (1996) at TRIUMF have extended the data to  $^{23}\text{Na}$ .

Recall from Sec. IX.B.1 that the 1S ground state of a  $J_i \neq 0$   $\mu$ -atom is a hyperfine doublet with a spin  $F_{\pm} = J_i \pm 1/2$ . These states are split by the spin-spin interaction of the muon-nucleus magnetic moments. For a positive nuclear magnetic moment the  $F_-$  state is the true atomic ground state and for a negative nuclear magnetic moment the  $F_+$  state is the true atomic ground state.

The two hyperfine state are initially populated with statistical weights, *i.e.*  $n_+ = (J_i + 1)/(2J_i + 1)$  and  $n_- = J_i/(2J_i + 1)$ .<sup>19</sup> Thereafter hyperfine transitions from the upper F-state to the lower F-state occur by M1-Auger emission, changing the relative occupancies of the hyperfine states. The rate  $\Lambda_h$  of hyperfine conversion by Auger emission is governed by (i) the wave function overlap of the electron and the  $\mu$ -atom and (ii) the relative sizes of the electron binding and the hyperfine splitting. The wave function overlap leads to a systematic increase in  $\Lambda_h$  with  $Z$  whereas the electron binding leads to sudden decreases in  $\Lambda_h$  at  $Z \sim 6$ , where K-shell emission is forbidden, and  $Z \sim 18$ , where L-shell emission is forbidden. A detailed account of hyperfine conversion by Auger emission is given by Winston (1963) and experimental determinations of conversion rates have generally confirmed the calculated rates (Gorrington *et al.*, 1993; Measday, 2001; Suzuki *et al.*, 1987). Most importantly for investigating  $g_p$ , there exist a handful of  $\mu$ -atoms with comparable hyperfine transition and muon disappearance rates, *e.g.*  $^{11}\text{B}$ ,  $^{19}\text{F}$ ,  $^{23}\text{Na}$  and  $^{35}\text{Cl}$ .

Telegdi (1959) was first to recognize that the hyperfine conversion during the  $\mu$ -atom lifetime would alter the muon occupancy of the  $F$ -states, and modify the time spectrum of the capture products, and thus permit the determination of the hyperfine dependence  $\Lambda_+/\Lambda_-$ . Formulas for the time evolution of capture products in the presence of hyperfine conversion have been published by several authors. For the case of a positive nuclear magnetic moment, *e.g.*  $^{11}\text{B}$  and  $^{23}\text{Na}$ ,

$$\frac{dN}{dt} \propto e^{-\Lambda_D^- t} \left[ \left( \frac{n_-^-}{n^+} + \frac{\Lambda_h}{\Lambda_h + \Delta\Lambda_D} \right) + \left( \frac{\Lambda^+}{\Lambda^-} - \frac{\Lambda_h}{\Lambda_h - \Delta\Lambda_D} \right) e^{-(\Lambda_h + \Delta\Lambda_D)t} \right] \quad (45)$$

where  $n^+$ ,  $n^-$  and  $\Lambda_+$ ,  $\Lambda_-$  are the initial populations and the capture rates of the  $F_+$ ,  $F_-$  hyperfine states,  $\Lambda_D^-$  is the  $F_-$  state disappearance rate,  $\Delta\Lambda_D = \Lambda_D^+ - \Lambda_D^-$  is the hyperfine disappearance increment, and  $\Lambda_h$  the hyperfine conversion rate. In almost all cases of interest  $\Lambda_h \gg \Delta\Lambda_D$  and therefore the factor  $\Lambda_h/(\Lambda_h \pm \Delta\Lambda_D)$  is close to unity.

<sup>18</sup> Specifically (i) the 947 keV (2620  $\rightarrow$  1674) and 953 keV (953  $\rightarrow$  0) gamma-ray lines and (ii) the 1668 keV (2620  $\rightarrow$  953) and 1674 keV (1674  $\rightarrow$  0) gamma-ray lines

<sup>19</sup> The exception is the use of a polarized target and a polarized beam (Hambro and Mukhopadhyay, 1977; Mukhopadhyay, 1977).

TABLE VII Compilation of results from the recoil polarization experiments for the transition  $^{12}\text{C}(0^+, 0) \rightarrow ^{12}\text{B}(1^+, 0)$ . The results are presented in terms of the dynamical parameter  $X = \sqrt{2}T_0/T_1$ . They incorporate the corrections for capture to  $^{12}\text{B}$  bound excited states using the  $\gamma$ -ray data from Giffon *et al.* (1981) in column three and (Roesch *et al.*, 1981a) in column four. The experimental observable is listed in column two.

Ref.	obs.	$X$ using Giffon <i>et al.</i> (1981)	$X$ using Roesch <i>et al.</i> (1981a)
Possoz <i>et al.</i> (1974)	$P_{av}$	$0.10 \pm 0.11$	$0.08 \pm 0.11$
Possoz <i>et al.</i> (1977)	$P_{av}$	$0.22 \pm 0.07$	$0.20 \pm 0.07$
Roesch <i>et al.</i> (1981b)	$P_{F/B}$	$0.27 \pm 0.07$	$0.24 \pm 0.07$
Kuno <i>et al.</i> (1984)	$P_{av}$	$0.23^{+0.10}_{-0.08}$	$0.21^{+0.10}_{-0.08}$
FPA		0.59	0.59

As discussed in Sec. IX.D.2 the hyperfine dependence  $\Lambda_+/\Lambda_-$  of partial transitions with  $\Delta J^\pi = \pm 1^+$  spin-sequences is especially sensitive to  $g_p$ . Eq. (45) demonstrates clearly that the hyperfine dependence  $\Lambda_+/\Lambda_-$  in such capture is encoded in the time spectrum of the reaction products.

The  $^{11}\text{B}(3/2^-, 0) \rightarrow ^{11}\text{Be}(1/2^-, 320)$  reaction is a  $\Delta J^\pi = 1^+$  allowed transition from the  $^{11}\text{B}$  ground state to the 320 keV  $^{11}\text{B}$  first-excited state. The 320 keV,  $1/2^-$   $^{11}\text{Be}$  excited state decays by  $\gamma$ -emission ( $\tau = 115 \pm 10$  fs) to the  $^{11}\text{Be}$  ground state, and the  $^{11}\text{Be}$   $1/2^+$  ground state decays by  $\beta$ -emission ( $\tau = 13.81 \pm 0.08$  s) to the  $^{11}\text{B}$  ground state. For reference, the  $^{11}\text{B}$  disappearance rate is  $\Lambda_D = (0.4787 \pm 0.0008) \times 10^6 \text{s}^{-1}$  (Wiaux *et al.*, 2002) and the  $^{11}\text{B}$  hyperfine transition rate is  $\Lambda_h = (0.181 \pm 0.016) \times 10^6 \text{s}^{-1}$  (Wiaux *et al.*, 2002).

One nice feature in the experimental study of the hyperfine effect in the  $^{11}\text{B}(3/2^-, 0) \rightarrow ^{11}\text{Be}(1/2^-, 320)$  transition is the level structure of the  $^{11}\text{Be}$  nucleus. Since the only particle-stable states are the  $1/2^+$  ground state and the  $1/2^-$  excited state this minimizes any concerns of cascade feeding from muon capture to higher-lying  $^{11}\text{Be}$  states. However one difficulty is the very low rate for the  $^{11}\text{B}(3/2^-, 0) \rightarrow ^{11}\text{Be}(1/2^-, 320)$  transition, with only about 0.2% of  $\mu$  stops in  $^{11}\text{B}$  undergoing this reaction.

Two  $^{11}\text{B}(3/2^-, 0) \rightarrow ^{11}\text{Be}(1/2^-, 320)$  measurements, the pioneering work by Deutsch *et al.* (1968) at CERN and the recent work by Wiaux *et al.* (2002) at PSI, have been performed. Both counted incoming muons in a plastic scintillator beam telescope, detected outgoing  $\gamma$ -rays in a high resolution Ge detector, and used a natural isotopic abundance boron target. The 320 keV  $\gamma$ -ray signal-to-noise ratio was 1:2 in the earlier Deutsch *et al.* (1968) experiment and 5:1 in the later Wiaux *et al.* (2002) ex-

periment.

Both experiments fit their 320 keV  $\gamma$ -ray time spectra to the time dependence of Eq. (45) in order to extract  $\Lambda_+/\Lambda_-$ . The instrumental time resolutions were determined via muonic x-rays and the continuum backgrounds were subtracted via neighboring energy windows. Wiaux *et al.* (2002) analyzed both the 320 keV  $\gamma$ -ray time spectrum and the Michel time spectrum in order to reduce the correlations between  $\Lambda_D^-$ ,  $\Lambda_h$  and  $\Lambda_+/\Lambda_-$ . For  $^{11}\text{B}(3/2^-, 0) \rightarrow ^{11}\text{Be}(1/2^-, 320)$  the Deutsch *et al.* (1968) experiment yielded  $\Lambda_+/\Lambda_- < 0.26$  and the Wiaux *et al.* (2002) experiment yielded  $\Lambda_+/\Lambda_- = 0.028 \pm 0.021$ . These experiments clearly demonstrate the strong dependence of the capture process on the hyperfine state.

In allowed capture on  $^{23}\text{Na}$  nuclei a large fraction of Gamow-Teller strength is to several levels in the energy region 1–4 MeV (Siebels *et al.*, 1995). In particular two  $\Delta J^\pi = -1^+$  reactions,  $^{23}\text{Na}(3/2^+, 0) \rightarrow ^{23}\text{Ne}(1/2^+, 1017)$  and  $^{23}\text{Na}(3/2^+, 0) \rightarrow ^{23}\text{Ne}(1/2^+, 3458)$ , exhaust a sizable fraction of GT strength. For reference, the  $^{23}\text{Na}$  disappearance rate is  $\Lambda_D = (0.831 \pm 0.002) \times 10^6 \text{s}^{-1}$  (Suzuki *et al.*, 1987) and the  $^{23}\text{Na}$  hyperfine conversion rate is  $\Lambda_h = (15.5 \pm 1.1) \times 10^6 \text{s}^{-1}$  (Gorringe *et al.*, 1994).

Compared to  $^{11}\text{B}$ , in  $^{23}\text{Na}$  (i) the capture rates are considerably larger and (ii) the hyperfine rate and disappearance rate are more readily distinguished, thus making the measurement more straightforward. However the large number of  $^{23}\text{Ne}$  states, and greater fragmentation of Gamow-Teller strength, means cascade feeding from higher-lying levels to lower-lying levels is a worry.

The study of the hyperfine effect in the  $\mu^{23}\text{Na}$  atoms was conducted at TRIUMF (Gorringe *et al.*, 1994; Johnson *et al.*, 1996). Incident muons were counted in a plastic scintillator telescope and stopped in a

sodium metal target. Emerging  $\gamma$ -rays were detected in high purity Ge detectors with surrounding NaI Compton suppressors. For  $^{23}\text{Na}(3/2^+, 0) \rightarrow ^{23}\text{Ne}(1/2^+, 1017)$  and  $^{23}\text{Na}(3/2^+, 0) \rightarrow ^{23}\text{Ne}(1/2^+, 3458)$  the measurement yielded  $\Lambda_+/\Lambda_- = 0.18 \pm 0.03$  and  $\Lambda_+/\Lambda_- \leq 0.19$  and revealed a very large hyperfine effect. Note that in analyzing their data the authors had to account for the direct production and the indirect production of the 1017 keV  $\gamma$ -rays. For more details on the interpretation of their data see Johnson *et al.* (1996).

### 3. $^{16}\text{O}(0^+, 0) \rightarrow ^{16}\text{N}(0^-, 120)$

The  $^{16}\text{O}(0^+, 0) \rightarrow ^{16}\text{N}(0^-, 120)$  transition is a first forbidden transition from the  $J_i^\pi = 0^+$ ,  $^{16}\text{O}$  ground state to the  $J_f^\pi = 0^-$ ,  $^{16}\text{N}$  metastable state. As discussed in Sec. IX.D.3 the capture rates of  $\Delta J^\pi = 0^-$  transitions are especially sensitive to the longitudinal component of the axial current, and hence to  $g_p$ . The  $^{16}\text{N}$  level structure comprises four particle-stable bound states: the  $(2^-, 0)$  ground state and  $(0^-, 120)$ ,  $(3^-, 298)$ , and  $(1^-, 397)$  excited states. Note that the  $^{16}\text{N}(0^-, 120)$  state decays, with a half-life  $t_{1/2} = 5.25\mu\text{s}$ , both by  $\gamma$ -ray emission to the  $^{16}\text{N}(2^-, 0)$  ground state and by  $\beta$ -ray emission to the  $^{16}\text{O}(0^+, 0)$  ground state. Also note that the dominant decay of the  $1^-$ ,  $^{16}\text{N}$  state is via  $\gamma$ -ray cascade through the  $0^-$ ,  $^{16}\text{N}$  state.

One experimental difficulty is the low rate of the  $^{16}\text{O}(0^+, 0) \rightarrow ^{16}\text{N}(0^-, 120)$  transition. This difficulty is compounded by the low energy of the de-excitation  $\gamma$ -ray, resulting in large backgrounds from Michel bremsstrahlung and Compton scattering. Furthermore because of the meta-stability of the  $^{16}\text{N}(0^-, 120)$  state the 120 keV  $\gamma$ -ray time spectrum is a convolution of the  $1.8\mu\text{s}$   $\mu^{16}\text{O}$  lifetime and the  $5.2\mu\text{s}$   $^{16}\text{N}(0^-, 120)$  lifetime. Consequently some care is needed in applying  $\mu$ -stop timing gates as the 120 keV  $^{16}\text{N}$   $\gamma$ -ray and other  $^{16}\text{N}$   $\gamma$ -rays are impacted differently. Last the feeding of the  $^{16}\text{N}(0^-, 120)$  level from the  $^{16}\text{N}(1^-, 398)$  level also complicates the extraction of  $\Lambda$ .

The first experimental studies of  $^{16}\text{O} \rightarrow ^{16}\text{N}$  partial transitions were conducted by Cohen *et al.* (1963), Cohen *et al.* (1964) and Astbury *et al.* (1964) in the early sixties. The experiments detected the de-excitation  $\gamma$ -rays from  $^{16}\text{N}$  excited states using NaI detectors. Unfortunately, because of the limited resolution of the NaI detectors, they suffered from poor signal-to-noise and unidentified background lines. Consequently from the late sixties to the late seventies a further series of  $\gamma$ -ray experiments were conducted using Ge detectors by Deutsch *et al.* (1969), Kane *et al.* (1973) and Guichon *et al.* (1979).

The experimental results for  $\mu$  capture rates to  $^{16}\text{N}$  bound states are summarized in Table VIII. All experiments indicate substantial capture to the  $2^-$  ground state, some capture to the  $0^-$  and  $1^-$  excited states, and negligible capture to the  $3^-$  excited state. Unfortu-

nately measurement-to-measurement discrepancies of a factor of two are apparent for  $^{16}\text{O}(0^+, 0) \rightarrow ^{16}\text{N}(0^-, 120)$ . Probably one should reject the early measurements with NaI detectors due to poor resolution and thus uncertain backgrounds. Further the peculiar time dependence of the interesting 120 keV  $\gamma$ -ray is probably the origin of disagreement between the early studies of Deutsch *et al.* (1969) and later studies of Kane *et al.* (1973) and Guichon *et al.* (1979). In the later experiments special efforts was made to tackle this difficulty. Kane *et al.* (1973) employed a continuous beam without a  $\mu$ -stop time gate and Guichon *et al.* (1979) employed a pulsed beam with a long  $\mu$ -stop time gate. These experiments, using different timing techniques and yielding consistent results, give a mean value for the  $^{16}\text{O}(0^+, 0) \rightarrow ^{16}\text{N}(0^-, 0)$  rate of  $\Lambda = 1520 \pm 100\text{s}^{-1}$ .

TABLE VIII Muon capture rates in  $^{16}\text{O}$  to the  $(0^-, 120)$  and  $(1^-, 397)$  excited states of  $^{16}\text{N}$  from the published results of Cohen *et al.* (1963), Astbury *et al.* (1964), Deutsch *et al.* (1969), Kane *et al.* (1973) and Guichon *et al.* (1979) in units of  $\times 10^3\text{s}^{-1}$ . No evidence was found for production of the  $^{16}\text{N}(3^-, 298)$  excited state.

Ref.	$0^+ \rightarrow 0^-$	$0^+ \rightarrow 1^-$
Cohen <i>et al.</i> (1963)	$1.1 \pm 0.2$	$1.7 \pm 0.1$
Astbury <i>et al.</i> (1964)	$1.6 \pm 0.2$	$1.4 \pm 0.2$
Deutsch <i>et al.</i> (1969)	$0.85_{-0.060}^{+0.15}$	$1.85_{-0.17}^{+0.36}$
Kane <i>et al.</i> (1973)	$1.56 \pm 0.03$	$1.31 \pm 0.11$
Guichon <i>et al.</i> (1979)	$1.50 \pm 0.11$	$1.27 \pm 0.09$

### 4. $^{28}\text{Si}(0^+, 0) \rightarrow ^{28}\text{Al}(1^+, 2201)$

The study of  $g_p$  by measurement of  $\gamma$ -ray angular correlations in  $\mu^- [A, Z] \rightarrow \nu [A, Z-1]^* \rightarrow \gamma [A, Z-1]**$  transitions was originally proposed by Popov and co-workers.<sup>20</sup> The authors examined  $\gamma$ -ray correlations in allowed and forbidden transitions on  $J = 0$  and  $J \neq 0$  targets, and emphasized the  $g_p$  sensitivity of the  $0^+ \rightarrow 1^+ \rightarrow 0^+$  spin sequence.

An experimental method for  $\gamma$ -ray correlation measurements was subsequently suggested by Grenacs *et al.*

<sup>20</sup> See Bukat and Popov (1964); Bukhvostov and Popov (1967a,b,c, 1970); Oziewicz and Popov (1965); Popov (1963).

(1968). The method exploits the Doppler energy shift of nuclear  $\gamma$ -ray from in-flight decay. To illustrate the method we consider a recoil nucleus with a  $\gamma$ -decay lifetime denoted by  $\tau$  and a stopping time denoted by  $\tau_S$  (the stopping time is typically  $\sim 0.5$  ps in medium-weight nuclei). If  $\tau \ll \tau_S$  the recoil is in motion as it decays and consequently the  $\gamma$ -ray energy is Doppler shifted by

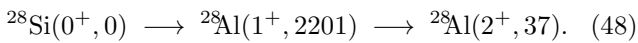
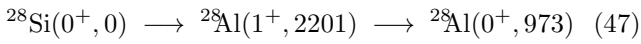
$$\frac{\Delta E}{E_o} = \frac{E - E_o}{E_o} = \beta \cos \theta \quad (46)$$

where  $E_o$  is the  $\gamma$ -ray energy in the recoil reference frame,  $E$  is the  $\gamma$ -ray energy in the laboratory reference frame,  $\beta = v/c$  is the velocity of the recoil in the laboratory, and  $\theta$  is the angle between the  $\gamma$ -ray and the recoil momentum. As a consequence of Eq. (46) the energy spectra of nuclear  $\gamma$ -rays from muon capture are Doppler broadened when  $\tau \ll \tau_S$ . Further the exact lineshape of the Doppler spectrum is a function of the correlations between the  $\gamma$ -ray, recoil and  $\mu$ -spin directions. As recognized by Grenacs *et al.* (1968), this permits a determination of the  $\gamma$ -ray correlation coefficients by measurement of the  $\gamma$ -ray Doppler energy spectrum.

Two experimental configurations for correlation measurements have special significance. In the first arrangement, the  $\gamma$ - $\nu$  configuration, the experiment is conducted with either unpolarized muons or perpendicular geometry, so that  $\vec{P}_\mu \cdot \hat{k} = 0$  where  $\hat{k}$  is the  $\gamma$ -ray direction. From Eq. (39) this configuration yields sensitivity to the correlation coefficient  $a_2$  only. In the second arrangement, the  $\gamma$ - $\nu$ - $\mu$  configuration, the experiment is conducted with both polarized muons and non-perpendicular geometry, so that  $\vec{P}_\mu \cdot \hat{k} \neq 0$ . From Eq. (39) this configuration yields sensitivity to the correlation coefficients  $\alpha + \frac{2}{3}c_1$  and  $b_2$  also. Note that, due to different powers of  $\hat{k}$  in Eq. (39), the Doppler lineshape arising from  $a_2$  is symmetric about  $E_o$  whereas the Doppler lineshapes arising from  $\alpha + \frac{2}{3}c_1$  and  $b_2$  are asymmetric about  $E_o$ .

Measurements of  $\gamma$ - $\nu$  and  $\gamma$ - $\nu$ - $\mu$  correlations have pros and cons. One disadvantage of  $\gamma$ - $\nu$ - $\mu$  correlation measurements is the small  $\mu$  polarization in the  $\mu$ -atom ground state. However one advantage is that the Doppler lineshape may be manipulated by varying the  $\mu$ -spin direction or  $\gamma$ -detector position, which is helpful in separating the Doppler signal from the continuum background. Furthermore distortion of the  $\gamma$ -ray lineshape due to slowing-down of the recoil nucleus is more straightforwardly separated from the asymmetric effects of  $\gamma$ - $\nu$ - $\mu$  correlations than from the symmetric effects of  $\gamma$ - $\nu$  correlations.

Two  $\mu^- [A, Z] \rightarrow \nu [A, Z-1]^* \rightarrow \gamma [A, Z-1]**$  transitions have attracted the most attention,



They involve a common GT transition from the  ${}^{28}\text{Si}(0^+, 0)$  ground state to the  ${}^{28}\text{Al}(1^+, 2201)$  excited state. Note

that the  $0^+ \rightarrow 1^+ \rightarrow 0^+$  sequence involves a pure M1  $\gamma$ -decay whereas the  $0^+ \rightarrow 1^+ \rightarrow 2^+$  sequence involves a mixed E2/M1  $\gamma$ -decay with mixing ratio  $\delta(E2/M1) = 0.37 \pm 0.11$  (Kudoyarov *et al.*, 1998). Additionally the 2201 keV state lifetime is  $59 \pm 6$  fs and slowing-down effects are non-negligible. Although at first glance the two sequences involve six correlations, *i.e.*  $(\alpha + \frac{2}{3}c_1)^{1229}$ ,  $a_2^{1229}$  and  $b_2^{1229}$  for the 1229 keV  $\gamma$ -ray and  $(\alpha + \frac{2}{3}c_1)^{2170}$ ,  $a_2^{2170}$  and  $b_2^{2170}$  for the 2170 keV  $\gamma$ -ray, these coefficients are related to a single underlying dynamical parameter, the helicity amplitude ratio  $X$ , as described in Sec. IX.C.1.

The ground-breaking work on the  $\gamma$ -ray correlations in these spin sequences was conducted at SREL by Miller *et al.* (1972b). They measured the  $\gamma$ -ray lineshapes from  $\mu$  stops in both natural Si and enriched  ${}^{28}\text{SiO}_2$  targets. Unfortunately the statistics were limited and the authors were forced to assume the absence of distortions of the Doppler lineshape due to slowing-down of the recoil ion.

More recently an improved measurement of the  $a_2$  coefficient was conducted at TRIUMF by Moftah *et al.* (1997). The experiment was performed in perpendicular geometry, *i.e.* with  $\vec{P}_\mu \cdot \hat{k} = 0$ , and utilized a coincidence technique with Compton suppression to improve the 1229 keV  $\gamma$ -ray signal-to-noise. In analyzing the data the authors treated the  $a_2$  coefficients for 1229 keV and 2170 keV  $\gamma$ -rays as independent, since the 2170 keV multipolarity was not measured at the time. However they included recoil slowing-down effects in the fit of the lineshapes.

Also recently a new measurement of all the coefficients has been performed at the Dubna phasotron by Brudanin *et al.* (1995) and Briançon *et al.* (2000). To identify both  $(\alpha + \frac{2}{3}c_1)$  and  $b_2$  the authors recorded the Doppler spectra for different values of  $\vec{P}_\mu \cdot \hat{k}$ . In Brudanin *et al.* (1995) they used forward/backward positioned Ge detectors to vary  $\vec{P}_\mu \cdot \hat{k}$  and in Briançon *et al.* (2000) they used  $\mu$  spin precession to vary  $\vec{P}_\mu \cdot \hat{k}$ . In analyzing their data the authors enforced the dynamical relations between correlation coefficients and fit the 2201 keV lifetime and 2170 keV mixing ratio.

Note that a concern in all experiments is the production of the  ${}^{28}\text{Al}(1^+, 2201)$  state by either (i)  $(\mu, n\nu)$  or  $(\mu, nn\nu)$  capture on  ${}^{29}\text{Si}$  or  ${}^{30}\text{Si}$  isotopes, or (ii)  $(\mu, \nu)$  capture to higher-lying  ${}^{28}\text{Si}$  levels. Such contributions would distort the lineshapes and impact the extraction of  $(\alpha + \frac{2}{3}c_1)$ ,  $a_2$  and  $b_2$ . Note that Miller *et al.* (1972a) obtained constraints on contributions from  ${}^{29}\text{Si}(\mu, n\nu)$  and Moftah *et al.* (1997) and Briançon *et al.* (2000) obtained limits on cascade feeding from higher levels. However a small contribution from (i) or (ii) is not excluded.

In Table IX we summarize the various measurements of  $\gamma$ -ray correlations for  ${}^{28}\text{Si}(0^+, 0) \rightarrow {}^{28}\text{Al}(1^+, 2201)$ . The experimental configurations are denoted by  $\vec{P}_\mu \cdot \hat{k} = 0$  or  $\vec{P}_\mu \cdot \hat{k} \neq 0$  and indicate the absence or presence of sensitivity to  $(\alpha + \frac{2}{3}c_1)$  and  $b_2$ . To assist the comparison of experiments we quote all results in terms of the helicity amplitude ratio  $X$ . The ‘world data’ weighted mean is

$$X = 0.554 \pm 0.042.$$

TABLE IX Compilation of recent results from the  $\gamma$ -ray correlation experiments for the transition  $^{28}\text{Si}(0^+, 0) \rightarrow ^{28}\text{Al}(1^+, 2201)$ . The results are presented in terms of the dynamical parameter  $X = \sqrt{2}T_0/T_1$ . The analyzed gamma-rays are listed in column two and the experimental technique is listed in column three. FPA is the Fujii-Primakoff approximation value.

Ref.	$\gamma$ -ray trans.	$\gamma$ -ray corr.	$X = \sqrt{2}T_0/T_1$
Moftah <i>et al.</i> (1997)	1229	' $\gamma$ - $\nu$ '	$0.454^{+0.12}_{-0.11}$
Brudanin <i>et al.</i> (1995)	1229, 2171	' $\gamma$ - $\nu$ - $\mu$ '	$0.543 \pm 0.052$
Briançon <i>et al.</i> (2000)	1229, 2171	' $\gamma$ - $\nu$ - $\mu$ '	$0.566 \pm 0.045$
FPA			0.59

## F. Theoretical framework for exclusive OMC

Herein we describe the theoretical treatment of physical observables in  $(\mu, \nu)$  reactions. Our main goals are to outline the steps and assumptions in calculating the observables and provide some details of work on  $^{11}\text{B}$ ,  $^{12}\text{C}$ ,  $^{16}\text{O}$ ,  $^{23}\text{Na}$  and  $^{28}\text{Si}$ . In Sec. IX.F.1 we describe the operators that contribute to  $\mu$  capture. In Sec. IX.F.2 we discuss the application of the impulse approximation and in Sec. IX.F.3 we discuss the effects due to exchange currents. The detailed discussion of nuclear models is left to Sec. IX.G.

### 1. Multipole operators

The model calculation of partial transitions on complex nuclei is generally conducted via a multipole expansion of the Fujii-Primakoff effective Hamiltonian of Eq. (40). We refer the reader who is interested in the details of the formalism to the articles by Primakoff (1959), Morita and Fujii (1960), Luyten *et al.* (1963), Walecka (1975), Mukhopadhyay (1977) and Ciechanowicz and Oziewicz (1984). Herein we briefly describe the specific operators that contribute to transitions of interest for  $g_p$ , *i.e.* the transitions  $0^+ \rightarrow 0^-$ ,  $0^+ \rightarrow 1^+$  and  $3/2^\pm \rightarrow 1/2^\pm$ . We employ the notation of Walecka (1975) for the contributing electroweak operators,  $(\mathcal{L}_J - \mathcal{M}_J$  and  $\mathcal{T}_J^{el} - \mathcal{T}_J^{mag}$ ), and notation of Donnelly and Haxton (1979, 1980) for the contributing multipole operators,  $M_J(qx)$ ,  $M_{JL}(qx) \cdot \sigma$ ,  $M_{JL}(qx) \cdot \nabla$  and  $M_J(qx) \sigma \cdot \nabla$ . Note that

$\mathcal{L}_J - \mathcal{M}_J$  involves a longitudinal coupling to the lepton field and is dependent on  $g_p$ , while  $\mathcal{T}_J^{el} - \mathcal{T}_J^{mag}$  involves a transverse coupling to the lepton field and is independent of  $g_p$ .

$0^+ \rightarrow 0^-$  transitions, *e.g.*  $^{16}\text{O}$ , involve a unique  $J^\pi = 0^-$  multipole, a single electroweak weak operator,  $L_0^5 - M_0^5$ , and two multipole operators,  $M_{01} \cdot \sigma$  and  $M_0 \sigma \cdot \nabla$ . The  $M_{01} \cdot \sigma$  operator is the  $\ell = 1$  retarded Gamow-Teller operator originating from the space component of the axial current. The  $M_0 \sigma \cdot \nabla$  operator is the axial charge operator originating from the time component of the axial current. Note that the contribution of  $g_p$  in  $0^+ \rightarrow 0^-$  transitions is via  $M_{01} \cdot \sigma$ .

$0^+ \rightarrow 1^+$  transitions, *e.g.*  $^{12}\text{C}$  and  $^{28}\text{Si}$ , involve a unique  $J^\pi = 1^+$  multipole, two electroweak weak operators,  $L_1^5 - M_1^5$  and  $T_1^{el5} - T_1^{mag}$ , and four multipole operators,  $M_{10} \cdot \sigma$ ,  $M_{12} \cdot \sigma$ ,  $M_1 \sigma \cdot \nabla$  and  $M_{11} \cdot \nabla$ . The  $M_{10} \cdot \sigma$  operator is the allowed GT operator. The remaining contributions include the axial current's time-component, *i.e.*  $M_1 \sigma \cdot \nabla$ , and second-forbidden corrections, *i.e.*  $M_{12} \cdot \sigma$ . Note that the leading contribution of  $g_p$  in  $0^+ \rightarrow 1^+$  transitions is via  $M_{10} \cdot \sigma$ .

For transitions on  $J_i \neq 0$  targets a range of multipoles are involved, *i.e.*  $|J_i - J_f|$  to  $(J_i + J_f)$ . For example, a  $1/2^+ \rightarrow 1/2^+$  transition, *e.g.*  $^1\text{H}$  or  $^3\text{He}$ , involves  $J^\pi = 0^+, 1^+$  multipoles and a  $3/2^+ \rightarrow 1/2^+$  transition, *e.g.*  $^{11}\text{B}$  or  $^{23}\text{Na}$ , involves  $J^\pi = 1^+, 2^+$  multipoles. For  $1/2^+ \rightarrow 1/2^+$  transitions the  $L_0 - M_0$  operator yields an additional contribution from the allowed Fermi operator. For  $3/2^+ \rightarrow 1/2^+$  transitions the  $L_2 - M_2$  and  $T_2^{el} - T_2^{mag5}$  operators yield additional contributions from the  $\ell$ -forbidden multipole operators  $M_2$  and  $M_{22} \cdot \sigma$  and the gradient multipole operators  $M_{21} \cdot \nabla$  and  $M_{23} \cdot \nabla$ . However the leading contribution of  $g_p$  in  $1/2^+ \rightarrow 1/2^+$  transitions and  $3/2^+ \rightarrow 1/2^+$  transitions is still via  $M_{10} \cdot \sigma$ . Note that the multipoles with  $J^\pi = 0^+$  and  $J^\pi = 2^+$  are independent of  $g_p$ .

### 2. Impulse approximation

In principle the weak amplitudes in muon capture have one-, two- and many-body contributions. However in practice the starting point for most calculations is to approximate the weak nuclear amplitude by a summation of A one-body amplitudes, *i.e.* the impulse approximation. This amounts to ignoring the effects of pion exchange currents,  $\Delta$ -hole excitations, etc.

Assuming a one-body form for nuclear currents, the required multi-particle weak matrix elements  $\langle J_f || O^J || J_i \rangle$  between an initial state  $|J_i \rangle$  and final state  $|J_f \rangle$  may be written in terms of single-particle weak matrix elements  $\langle \alpha' || O^J || \alpha \rangle$  between single-particle states labeled by  $|\alpha \rangle$  and  $|\alpha' \rangle$  as (Donnelly

and Haxton , 1979)

$$\langle J_f || O^J || J_i \rangle = \sum_{\alpha, \alpha'} C(J, \alpha, \alpha', J_f, J_i) \langle \alpha' || O^J || \alpha \rangle \quad (49)$$

where the states  $\alpha \equiv [n, j, \ell]$  and  $\alpha' \equiv [n', j', \ell']$  and in  $\mu$  capture the operator  $O^J$  is  $\mathcal{M}_J - \mathcal{L}_J$  or  $\mathcal{T}_J^{el} - \mathcal{T}_J^{mag}$ . The coefficients  $C(J, \alpha, \alpha', J_f, J_i)$  are called one-body transition densities and determine the contributions of each single-particle matrix element  $\langle \alpha' || O^J || \alpha \rangle$  to the multi-particle matrix element  $\langle J_f || O^J || J_i \rangle$ . Note that the one-body transition densities are determined by the nuclear structure while the single-particle matrix elements are functions of the weak couplings. Eq. (49) therefore represents a convenient separation of nuclear structure and weak dynamics.<sup>21</sup> We stress that in practice in applying Eq. (49) the summation is truncated to a finite number of the single particle transitions.

### 3. Exchange currents

At some level the impulse approximation will break down, and consequently the evaluation of contributions from pion exchange, delta excitation, etc., is important in extracting  $g_p$ . One approach to computing exchange currents is to use low energy theorems to constrain soft pion contributions. Another approach involves enumerating a plausible set of Feynman diagrams that incorporate  $\pi$ 's,  $\Delta$ 's, etc. We shall not attempt to cover in detail the broad topic of exchange currents, but rather we summarize their application to muon capture on complex nuclei.

The work of Kubodera *et al.* (1978) was pivotal in establishing the importance of soft pion exchange currents in various electroweak processes. The authors observed that soft pions produce large effects in the time component of the axial current and the space component of the vector current. Further they recognized that arguments based on chiral symmetry fix the size of these effects, yielding a powerful tool in determining the corrections from 2-body currents. In particular for muon capture the soft-pion corrections to axial charge operators, while substantial, are well determined. Such  $M_J \sigma \cdot \nabla$  operators compete with the leading contributions of  $g_p$  in both allowed and  $0^+ \rightarrow 0^-$  transitions. For further details see Guichon *et al.* (1978); Guichon and Samour (1979) and Towner (1986).

Unfortunately, for the space component of the axial current and the time component of the vector current the constraints dictated by chiral symmetry are ineffective in determining the contributions of 2-body currents. For example for the allowed Gamow-Teller operator and the

allowed Fermi operator this approach is not helpful. Instead the modifying effects of exchange currents must be addressed by explicitly evaluating a specific set of Feynman graphs. An example of such an approach is the  $N\pi\rho A_1$  phenomenological Lagrangian model of Ivanov and Truhlik (1979a). Note that the Feynman graphs and corresponding operators are obviously not unique and the couplings constants and form factors are frequently not well known. Consequently the calculation of 2-body corrections to GT matrix elements and Fermi matrix elements have significant uncertainties. In particular the  $\Delta$ 's contribution is poorly determined. For examples of applications to muon capture see Adam *et al.* (1990).

### G. Nuclear models for partial transitions

Next we consider the specific structure and nuclear models for partial transitions on  $A = 11, 12, 16, 23$  and 28 nuclei. Our focus is on the elements of the models that impact the determination of  $g_p$ .

Nowadays full-space shell model calculations are routinely performed for  $4 < A < 16$ , *i.e.* 0p shell nuclei, and  $16 < A < 40$ , *i.e.* 1s-0d shell nuclei, and the empirical determination of effective interactions from least-squares-fits to nuclear data is well established. For example, the parameters of the 0p shell interaction were obtained by Cohen and Kurath (1967) by fitting  $4 < A < 16$  level energies and the parameters of the 1s-0d interaction were obtained by Wildenthal (1984) by fitting  $16 < A < 40$  level energies. In addition semi-empirical interactions, which incorporate assumptions for the particular form of the effective interaction, are available (Brown *et al.*, 1988). Both empirical and semi-empirical interactions are capable of reproducing many features and phenomena in 0p and 1s-0d nuclei.

Note that an alternative approach is the microscopic derivation of the effective NN interaction from the free NN interaction. The derivation involves a power-series relating the effective interaction and free interaction, but unfortunately the question of convergence is tricky. In general such interactions either give less satisfactory model-data agreement than empirical interactions, *e.g.* the interaction of Kuo and Brown (1966), or need some ad-hoc tuning of model parameters, *e.g.* the interaction of Hauge and Maripuu (1973). However the comparison of results from empirical interactions and realistic interactions is helpful in understanding and evaluating the model uncertainties.

#### 1. $^{11}\text{B}(3/2^-, 0) \rightarrow ^{11}\text{Be}(1/2^-, 320)$

Several calculations of capture rate and hyperfine dependences have been performed for the  $^{11}\text{B}(3/2^-, 0) \rightarrow ^{11}\text{Be}(1/2^-, 320)$  transition (Bernabeu , 1971; Koshigiri *et al.*, 1982, 1984; Kuz'min *et al.*, 1994; Suzuki , 1997). Bernabeu (1971) first discussed the relatively high sensi-

<sup>21</sup> Strictly the radial form of the nuclear wave functions also enters the computation of the single-particle matrix elements.

tivity to  $g_p$  and relatively low sensitivity to nuclear structure of  $\Lambda_+/\Lambda_-$ . More recently Kuz'min *et al.* (1994) assessed the effects of different 0p-shell effective interactions while Suzuki (1997) assessed the effects of a  $^{11}\text{Be}$  neutron halo.

The simplest picture of  $^{11}\text{B}(3/2^-, 0) \rightarrow ^{11}\text{Be}(1/2^-, 320)$  consists of a  $0s_{1/2}^4 0p_{3/2}^7$  initial state,  $0s_{1/2}^4 0p_{3/2}^6 0p_{1/2}^1$  final state, and  $0p_{3/2} \rightarrow 0p_{1/2}$  single particle transition. However in reality the  $^{11}\text{B}(3/2^-, 0)$  initial state has substantial contributions from both  $0s_{1/2}^4 0p_{3/2}^5 0p_{1/2}^2$  and  $0s_{1/2}^4 0p_{3/2}^3 0p_{1/2}^4$  configurations, and interference between the  $0p_{1/2} \rightarrow 0p_{3/2}$  single particle transition and the  $0p_{3/2} \rightarrow 0p_{1/2}$  single particle transition is important. For example the capture rate is grossly over-estimated in a simple  $0p_{3/2} \rightarrow 0p_{1/2}$  picture.

Full 0p-shell model calculations for  $^{11}\text{B}(3/2^-, 0) \rightarrow ^{11}\text{Be}(1/2^-, 320)$  with well established effective interactions confirm the leading transition is  $0p_{3/2} \rightarrow 0p_{1/2}$ , with a substantial contribution from  $0p_{1/2} \rightarrow 0p_{3/2}$  and a significant contribution from  $0p_{3/2} \rightarrow 0p_{3/2}$ . Since the Gamow-Teller matrix elements for  $0p_{3/2} \rightarrow 0p_{1/2}$  and  $0p_{1/2} \rightarrow 0p_{3/2}$  have opposite signs they interfere destructively and dramatically decrease both  $\Lambda_+$  and  $\Lambda_-$ . Typical model-to-model variations in the  $0p_{3/2} \rightarrow 0p_{1/2}$  and  $0p_{1/2} \rightarrow 0p_{3/2}$  densities are roughly  $\pm 10\%$ . Note that the remaining  $0p_{1/2} \rightarrow 0p_{1/2}$  and  $0p_{3/2} \rightarrow 0p_{3/2}$  densities show larger model-to-model variations, however their contributions to capture are smaller.

A unique complication for the  $^{11}\text{B}(3/2^-, 0) \rightarrow ^{11}\text{Be}(1/2^-, 320)$  transition is the  $^{11}\text{Be}$  neutron halo. The halo is interesting in the context of nuclear structure studies but worrisome in the context of extracting  $g_p$ . Recently Suzuki (1997) has assessed the impact of the neutron halo on the capture rate and its hyperfine dependence. Suzuki (1997) reported it tends to reduce both  $\Lambda_+$  and  $\Lambda_-$  but barely changes  $\Lambda_+/\Lambda_-$ .

## 2. $^{12}\text{C}(0^+, 0) \rightarrow ^{12}\text{B}(1^+, 0)$

A large number of model calculation are available for  $^{12}\text{C}(0^+, 0) \rightarrow ^{12}\text{B}(1^+, 0)$ . Early studies of  $\mu$  capture rates and  $\beta$ -decay rates were performed by Flamard and Ford (1959), O'Connell *et al.* (1972), Mukhopadhyay and Macfarlane (1971), Immele and Mukhopadhyay (1975), and Mukhopadhyay and Martorell (1978). More comprehensive studies of rates and polarizations in  $\mu$  capture were published by Morita and co-workers,<sup>22</sup> and by Subramanian *et al.* (1976), Rosenfelder (1979), Ciechanowicz (1981), Hayes and Towner (2000) and Auerbach and Brown (2002). They include investigations of two-body currents and core polarization effects.

The simplest picture of  $^{12}\text{C}(0^+, 0) \rightarrow ^{12}\text{B}(1^+, 0)$  consists of a  $0s_{1/2}^4 0p_{3/2}^8$  initial state,  $0s_{1/2}^4 0p_{3/2}^7 0p_{1/2}^1$  final state, and a  $0p_{3/2} \rightarrow 0p_{1/2}$  single particle transition. Like the  $^{11}\text{B}$  g.s., the  $^{12}\text{C}$  g.s. has substantial contributions from both  $0s_{1/2}^4 0p_{3/2}^6 0p_{1/2}^2$  and  $0s_{1/2}^4 0p_{3/2}^4 0p_{1/2}^4$  configurations, and the interference of amplitudes from  $0p_{3/2} \rightarrow 0p_{3/2}$  transitions and  $0p_{1/2} \rightarrow 0p_{3/2}$  transitions is important. Again the capture rate is grossly over-estimated by a simple  $0p_{3/2} \rightarrow 0p_{1/2}$  picture.

Note that the overall pattern of the transition densities obtained from full 0p-shell model calculations with well established effective interactions is quite similar for  $^{11}\text{B}(3/2^-, 0) \rightarrow ^{11}\text{Be}(1/2^-, 320)$  and  $^{12}\text{C}(0^+, 0) \rightarrow ^{12}\text{B}(1^+, 0)$ . Specifically for  $^{12}\text{C}$  the largest density is  $0p_{3/2} \rightarrow 0p_{1/2}$ , the next-to-largest density is  $0p_{1/2} \rightarrow 0p_{3/2}$ , and the contributions from  $0p_{3/2} \rightarrow 0p_{3/2}$  and  $0p_{1/2} \rightarrow 0p_{1/2}$  are small. As in  $^{11}\text{B}$ , in  $^{12}\text{C}$  the interference of  $0p_{3/2} \rightarrow 0p_{1/2}$  with  $0p_{1/2} \rightarrow 0p_{3/2}$  is important in reducing the Gamow-Teller matrix element.

A nice feature of  $^{12}\text{C}(0^+, 0) \rightarrow ^{12}\text{B}(1^+, 0)$  is that related data on other electroweak processes are available, *e.g.*  $^{12}\text{B}$   $\beta$ -decay,  $^{12}\text{C}(e, e')$  scattering and  $^{12}\text{C}(1^+, 15.1 \text{ MeV})$   $\gamma$ -decay, and are helpful in testing the model calculations. For example the one-body transition densities have been extracted from these data by Doyle and Mukhopadhyay (1995) and Haxton (1978) and generally support the model calculations.

## 3. $^{23}\text{Na}(3/2^+, 0) \rightarrow ^{23}\text{Ne}(1/2^+, 3458)$

Calculations of capture rates and hyperfine dependencies in  $^{23}\text{Na} \rightarrow ^{23}\text{Ne}$  transitions have been performed by Johnson *et al.* (1996), Koshigiri *et al.* (1997) and Siiskonen *et al.* (1998). The calculations have been conducted in the full 1s-0d model space using the Wildenthal empirical interaction (Wildenthal, 1984) and the Kuo-Brown realistic interaction (Kuo and Brown, 1966). A study of 2-body currents and core polarization was made by Koshigiri *et al.* (1997).

The  $^{23}\text{Na}$  ground state is  $J^\pi = 3/2^+$ , indicating the simplest picture of a single unpaired proton in a  $0d_{5/2}$  orbital is wrong. Rather the  $A = 20-24$  mass region is well known for examples of light deformed nuclei and rotational band spectra. Consequently the spherical shell model representation of these nuclei is quite complex, with  $A = 23$  wave functions having small occupancies for the  $(d_{5/2})^7$  configuration and large occupancies of the  $1s_{1/2}$ ,  $1d_{3/2}$  orbitals.

For concreteness we describe the  $^{23}\text{Na}(3/2^+, 0) \rightarrow ^{23}\text{Ne}(1/2^+, 3458)$  transition, which is the strongest transition in the  $\mu$ - $^{23}\text{Na}$  experiment. Full 1s-0d shell model calculations with well tested effective interactions show  $0d_{5/2} \rightarrow 0d_{3/2}$  is the strongest single particle transition and  $0d_{3/2} \rightarrow 0d_{3/2}$  is the next strongest single particle transition. Other contributions are typically 10-20% of  $0d_{5/2} \rightarrow 0d_{3/2}$ . The variations of the one-body transition densities between models are  $\leq 10\%$  for  $0d_{5/2} \rightarrow 0d_{3/2}$

<sup>22</sup> See Ami *et al.* (1981); Fukui *et al.* (1983a,b, 1987); Kobayashi *et al.* (1978); Koshigiri *et al.* (1985); Morita *et al.* (1994).

densities and  $\leq 25\%$  for  $0d_{3/2} \rightarrow 0d_{3/2}$  densities.

#### 4. $^{28}\text{Si}(0^+, 0) \rightarrow ^{28}\text{Al}(1^+, 2201)$

Several authors have calculated the rates and correlations for  $^{28}\text{Si}(0^+, 0) \rightarrow ^{28}\text{Al}(1^+, 2201)$ . The first efforts were made by Ciechanowicz (1976) and Parthasarathy and Sridhar (1978, 1981), but employed relatively crude nuclear wave functions, the 1p–1h wave function of Donnelly and Walker (1970) and the truncated 1s–0d wave function of McGrory and Wildenthal (1971). More recently Kuz'min and Tetereva (2000), Kuz'min *et al.* (2001), Siiskonen *et al.* (1999), and Ciechanowicz *et al.* (1998) have conducted full 1s–0d calculations. Siiskonen *et al.* (1999) and Ciechanowicz *et al.* (1998) also considered both 2–body currents and core polarization in  $^{28}\text{Si}(0^+, 0) \rightarrow ^{28}\text{Al}(1^+, 2201)$ .

In the simplest picture  $^{28}\text{Si}(0^+, 0) \rightarrow ^{28}\text{Al}(1^+, 2201)$  consists of a full  $0d_{5/2}^{12}$  initial state,  $J^\pi = 1^+ (0d_{5/2}^{-1}, 0d_{3/2}^1)$  final state, and  $0d_{5/2} \rightarrow 0d_{3/2}$  single particle transition. However the model calculations show the simple picture is insufficient and configurations with several particles in  $1s_{1/2}$ – $0d_{3/2}$  orbitals are important.

A special remark on the one–body transition densities in the  $^{28}\text{Si}(0^+, 0) \rightarrow ^{28}\text{Al}(1^+, 2201)$  transition is worthwhile. Unlike the previous examples of  $^{11}\text{B}$ ,  $^{12}\text{C}$  and  $^{23}\text{Na}$ , in  $^{28}\text{Si}$  the variations from model to model are large, *e.g.* the densities from Kuo and Brown (1966) and Wildenthal (1984) are quite different. Also no particular single particle transition is dominant, *e.g.* the interaction of Wildenthal (1984) shows  $0d_{5/2} \rightarrow 0d_{3/2}$ ,  $0d_{5/2} \rightarrow 0d_{5/2}$ , and  $1s_{1/2} \rightarrow 0d_{3/2}$  with similar magnitudes. Therefore, as discussed by Kuz'min and Tetereva (2000), the model calculations are especially sensitive to interference effects.

#### 5. $^{16}\text{O}(0^+, 0) \rightarrow ^{16}\text{N}(0^-, 120)$

Because the nucleus  $^{16}\text{O}$  is doubly magic and the transition  $^{16}\text{O}(0^+, 0) \rightarrow ^{16}\text{N}(0^-, 0)$  is first forbidden this case is special. The simple model for  $^{16}\text{O}(0^+, 0) \rightarrow ^{16}\text{N}(0^-, 0)$  comprises a 0p closed shell initial state, and a 1p–1h  $J^\pi = 0^-$  final state, and involves  $1p_{1/2} \rightarrow 2s_{1/2}$  and  $1p_{3/2} \rightarrow 1d_{3/2}$  single particle transitions. Several authors have computed the rates of  $\mu$  capture ( $\Lambda_\mu$ ) and  $\beta$ –decay ( $\Lambda_\beta$ ) for  $^{16}\text{O}(0^+, 0) \leftrightarrow ^{16}\text{N}(0^-, 0)$  within this scheme. For example see Guichon *et al.* (1978) and references therein. They found the rates to be strongly dependent on the  $0p_{3/2}^{-1}$ – $0d_{3/2}$  admixture in the  $^{16}\text{N}$  wave function, but the ratio  $\Lambda_\mu/\Lambda_\beta$  to be near–model independent.

Since the work of Brown and Green (1966) we know the above picture is not complete, and that 2p–2h configurations in the  $^{16}\text{O}$  ground state are important. The effects of 2p–2h configurations on  $\mu$  capture and  $\beta$ –decay were first investigated by Guichon and Samour (1979) who considered  $(2s_{1/2})^2(1p_{1/2})^{-2}$  and  $(1d_{3/2})^2(1p_{3/2})^{-2}$

admixtures. They found the effects of 2p–2h configurations on the axial charge matrix element  $M_0\sigma \cdot \nabla$  and the retarded Gamow–Teller matrix element  $\mathbf{M}_{10} \cdot \sigma$  were opposite in sign, and consequently the near–cancellation of model uncertainties in  $\Lambda_\mu/\Lambda_\beta$  broke down. Subsequently Towner and Khanna (1981) evaluated the effects of 2p–2h configurations in  $^{16}\text{N}(0^-, 120) \leftrightarrow ^{16}\text{O}(0^+, 0)$  transitions with more extensive configurations and various effective interactions. They concluded that 2p–2h configurations decrease the  $\beta$ –decay rate by factors of 2 to 4, decrease the  $\mu$  capture rate by factors of 1.5 to 2, and increase  $\Lambda_\mu/\Lambda_\beta$  by factors of 1.5 to 2, thus confirming the model dependence observed by Guichon and Samour (1979).

Recently Haxton and Johnson (1990) and Warburton *et al.* (1994) have performed full  $4\hbar\omega$  ( $3\hbar\omega$ ) calculation for  $^{16}\text{O}$  ( $^{16}\text{N}$ ) low–lying levels. These calculations nicely reproduce the excitation energies of the  $^{16}\text{O}$  isoscalar positive parity states and the  $^{16}\text{N}$  isovector negative parity states, and indicate significant 4p–4h probabilities in  $^{16}\text{O}$ . In both works the authors stress the large destructive interference between  $M_0\sigma \cdot \nabla$  and  $\mathbf{M}_{10} \cdot \sigma$  in  $\beta$ –decay, and therefore substantial model dependences in  $\Lambda_\beta$  and  $\Lambda_\mu/\Lambda_\beta$ . Consequently the authors argue that  $\Lambda_\mu$ , not  $\Lambda_\mu/\Lambda_\beta$ , is preferable for extracting the coupling  $g_p$ .

The foregoing discussions of  $^{16}\text{O}(0^+, 0) \leftrightarrow ^{16}\text{N}(0^-, 120)$  transitions show a worrisome sensitivity to the multi–particle wave functions. In addition the matrix element  $M_0\sigma \cdot \nabla$  is modified considerably by 2–body currents from soft–pion exchange. These effects are discussed in detail by Guichon *et al.* (1978) and Towner and Khanna (1981). The calculations indicate that they increase the  $\beta$ –decay rate by a factor of about four and increase the  $\mu$  capture rate by a factor of about two. The contribution of  $M_0\sigma \cdot \nabla$  is larger in  $\beta$ –decay than  $\mu$  capture. This further complicates the extraction of  $g_p$  from capture on  $^{16}\text{O}$ .

## H. Coupling $g_p$ from partial transitions

### 1. Recommended values of $g_p/g_a$

In Table X we list our recommended values for  $g_p/g_a$  from exclusive OMC on complex nuclei. By ‘recommended values for  $g_p/g_a$ ’ we mean our assessment of the best values from the current world experimental dataset and the most complete model calculations. In quoting these values we combined the experimental results of Possoz *et al.* (1974), Possoz *et al.* (1977), Roesch *et al.* (1981b) and Kuno *et al.* (1984) to obtain a world average of the helicity amplitude ratio  $X = 0.23 \pm 0.06$  for  $^{12}\text{C}(0^+, 0) \rightarrow ^{12}\text{B}(1^+, 0)$  and combined the experimental results of Brudanin *et al.* (1995), Moftah *et al.* (1997) and Briançon *et al.* (2000) to obtain a world average of the helicity amplitude ratio  $X = 0.55 \pm 0.04$  for



$^{28}\text{Si}(0^+, 0) \rightarrow ^{28}\text{Al}(1^+, 2201)$ .<sup>23</sup> For the hyperfine dependence on  $^{11}\text{B}$  we employ the results of Wiaux *et al.* (2002) and for the hyperfine dependence on  $^{23}\text{Na}$  we employ the results of Johnson *et al.* (1996). For the capture rate of the  $^{16}\text{O}(0^+, 0) \rightarrow ^{16}\text{N}(0^-, 120)$  transition we averaged the experimental results of Kane *et al.* (1973) and Guichon *et al.* (1979). Note that in Table X the quoted errors include only experimental uncertainties. Also note we quote the results in Table X in terms of  $g_p/g_a$  not  $g_p$ . In most cases the measured quantities are recoil polarizations,  $\gamma$ -ray correlations or hyperfine dependences, and therefore are governed by ratios of nuclear matrix elements and of weak coupling constants. Consequently quoting  $g_p/g_a$  is more natural and more appropriate.

In order to extract the coupling  $g_p/g_a$  from experimental data a model is necessary. Our model choices, and arguments for selecting them, are given below.

For  $^{11}\text{B}$  we took the results of Kuz'min *et al.* (1994) yielding  $g_p/g_a = 4.3 \pm_{4.3}^{2.8}$ . These authors used the full 0p space with Cohen–Kurath interaction but omitted the effects of core polarization and exchange currents. Note the earlier calculation of Bernabeu (1971) yields a similar value of  $g_p/g_a = 4 \pm_3^3$ . According to Suzuki (1997) the effects of the  $^{11}\text{Be}$  neutron halo on the hyperfine dependence are small.

For  $^{12}\text{C}$  we used the model calculations of Fukui *et al.* (1987) and excited state yields of Giffon *et al.* (1981) to obtain  $g_p/g_a = 9.8 \pm 1.8$ . These authors used the full 0p space with Hauge–Maripuu interaction and accounted for core polarization and exchange currents. The core polarization effects were computed to second-order in perturbation theory and the exchange currents were computed with contributions from pair currents, pionic currents and  $\Delta$  excitations. Earlier calculations with more rudimentary wave functions and less sophisticated treatments of core polarization and exchange currents gave similar results.

For  $^{16}\text{O}$  a number of determinations of  $g_p/g_a$  are published. We took the value  $g_p/g_a = 6.0 \pm 0.4$  from Warburton *et al.* (1994), which incorporates both 4p–4h  $^{16}\text{O}$  configurations and 3p–3h  $^{16}\text{N}$  configurations and reproduces the  $^{16}\text{N}$   $\beta$ -decay rate. The 4p–4h calculation of Haxton and Johnson (1990) yields a similar value of  $g_p/g_a = 5$ –7. We note, however, that the earlier calculations which omit 4p–4h configurations have generally preferred higher values for  $g_p/g_a$ .

For  $^{23}\text{Na}$  we took the results of Koshigiri *et al.* (1997) yielding  $g_p/g_a = 6.6 \pm_{2.4}^{2.6}$ . The authors used the full 1s–0d space with the Brown–Wildenthal interaction, and accounted for core polarization to first-order and exchange

TABLE X Recommended values of  $g_p/g_a$  from ordinary capture on complex nuclei. The quoted errors are experimental uncertainties, and do not include model uncertainties.

transition	$g_p/g_a$
$^{11}\text{B}(3/2^-, 0) \rightarrow ^{11}\text{Be}(1/2^-, 320)$	$4.3 \pm_{4.3}^{2.8}$
$^{12}\text{C}(0^+, 0) \rightarrow ^{12}\text{B}(1^+, 0)$	$9.8 \pm 1.8$
$^{16}\text{O}(0^+, 0) \rightarrow ^{16}\text{N}(0^-, 120)$	$6.0 \pm 0.4$
$^{23}\text{Na}(3/2^+, 0) \rightarrow ^{23}\text{Ne}(1/2^+, 3458)$	$6.6 \pm_{2.4}^{2.6}$
$^{28}\text{Si}(0^+, 0) \rightarrow ^{28}\text{Al}(1^+, 2201)$	$1.0 \pm_{1.2}^{1.1}$

currents from soft pions and  $\Delta$  excitations. The results of Johnson *et al.* (1996) are similar to Koshigiri *et al.* (1997).

For  $^{28}\text{Si}$  we took the results of Siiskonen *et al.* (1999) yielding  $g_p/g_a = 1.0 \pm_{1.2}^{1.1}$ . The authors used the full 1s–0d space with the Brown–Wildenthal interaction. They included core polarization corrections but omitted exchange current corrections. Note that Ciechanowicz *et al.* (1998) found the effects of soft-pion exchange were negligible. For comparison, the earlier calculations of Ciechanowicz (1976) and Parthasarathy and Sridhar (1981) gave values for  $g_p/g_a$  of  $3.3 \pm 1.0$  and  $1.5 \pm_{1.1}^{0.9}$  respectively.

## 2. Model sensitivities of $g_p/g_a$

The interesting observables in allowed transitions are governed by ratios of nuclear matrix elements. More specifically, in  $0^+ \rightarrow 1^+$  transitions the observables are completely determined by, and in  $3/2^\pm \rightarrow 1/2^\pm$  transitions the observables are strongly dependent on, the helicity amplitude ratio  $X = \sqrt{2}T_0/T_1$ .<sup>24</sup> Therefore understanding the model uncertainties in computing  $X$  is central to tracing the model dependences in recoil polarizations,  $\gamma$ -ray correlations and hyperfine dependences. For example see Junker *et al.* (2000).

Tables XI and XII show the relative contributions of  $\mathbf{M}_{10} \cdot \boldsymbol{\sigma}$ , etc., to  $L_1^5 - M_1^5$  (or  $T_0$ ) and  $T_1^{el5} - M_1^{mag}$  (or  $T_1$ ) for the relevant transitions. The tables show that  $T_1^{el5} - M_1^{mag}$  is entirely dominated by  $\mathbf{M}_{10} \cdot \boldsymbol{\sigma}$ . However,

<sup>23</sup> In the literature both the helicity amplitude ratio, denoted  $X$ , and the neutrino-wave amplitude ratio, denoted  $x$ , have been used in this context. Although both  $X$  and  $x$  are suitable for representing the dynamical content of  $\Delta J^\pi = 1^+$  transitions, they are different, *i.e.*  $X = (-2x + \sqrt{2})/(x + \sqrt{2})$ . Therefore it is important not to confuse the two variables. See Sec. IX.F.1.

<sup>24</sup> Note for  $\Delta J^\pi = 1^+$  multipoles the helicity amplitude ratio  $\sqrt{2}T_0/T_1$  and multipole amplitude ratio  $\sqrt{2}(L_1^5 - M_1^5)/(T_1^{el5} - M_1^{mag})$  are identical

while  $\mathbf{M}_{10} \cdot \boldsymbol{\sigma}$  is the leading piece in the  $L_1^5 - M_1^5$  term, the contributions from  $M_1 \boldsymbol{\sigma} \cdot \nabla$  of about 30–40% and  $\mathbf{M}_{12} \cdot \boldsymbol{\sigma}$  of up to 25% are important. Clearly the leading source of model dependence in computing  $X$  is therefore uncertainties in the ratios of  $M_1 \boldsymbol{\sigma} \cdot \nabla / \mathbf{M}_{10} \cdot \boldsymbol{\sigma}$  and  $\mathbf{M}_{12} \cdot \boldsymbol{\sigma} / \mathbf{M}_{10} \cdot \boldsymbol{\sigma}$ , *i.e.* corrections arising from axial charge and  $2^{nd}$ -forbidden effects.

TABLE XI Comparison of the corrections from the terms involving  $M_1 \boldsymbol{\sigma} \cdot \nabla$ ,  $\mathbf{M}_{12} \cdot \boldsymbol{\sigma}$ , and  $\mathbf{M}_{11} \cdot \nabla$  to the multipole amplitude of  $L_1^5 - M_1^5$  for  $A = 11, 12, 23$  and  $28$  and several effective interactions denoted CKPOT (Cohen and Kurath , 1967), PKUO (Kuo and Brown , 1966), USD (Wildenthal, 1984) and KUOSD (Kuo and Brown , 1966). The values in columns 3–5 correspond to the percentage change in the matrix elements as the correction terms are successively included. Note that  $\mathbf{M}_{11} \cdot \nabla$  doesn't contribute to  $L_1^5 - M_1^5$ .

A	Int.	$L_1^5 - M_1^5$	$M_1 \boldsymbol{\sigma} \cdot \nabla$ corr. (%)	$\mathbf{M}_{12} \cdot \boldsymbol{\sigma}$ corr. (%)	$\mathbf{M}_{11} \cdot \nabla$ corr. (%)
11	CKPOT	-0.103	-30.6	-2.6	0.0
11	PKUO	-0.094	-32.4	0.6	0.0
12	CKPOT	0.107	-34.5	-9.4	0.0
12	PKUO	-0.071	-41.6	-18.4	0.0
23	USD	0.090	-31.8	4.1	0.0
23	KUOSD	-0.071	-44.4	13.1	0.0
28	USD	0.070	-37.2	-27.5	0.0
28	KUOSD	-0.071	-54.5	-18.4	0.0

Uncertainties in one-body transition densities are important sources of model dependencies in  $M_1 \boldsymbol{\sigma} \cdot \nabla / \mathbf{M}_{10} \cdot \boldsymbol{\sigma}$  and  $\mathbf{M}_{12} \cdot \boldsymbol{\sigma} / \mathbf{M}_{10} \cdot \boldsymbol{\sigma}$ . For example let's consider the transitions on boron and carbon which involve the interference of a  $0p_{3/2} \rightarrow 0p_{1/2}$  single particle transition and a  $0p_{1/2} \rightarrow 0p_{3/2}$  single particle transition. Under the interchange of initial and final states the matrix element  $\mathbf{M}_{10} \cdot \boldsymbol{\sigma}$  changes sign but the matrix element  $M_1 \boldsymbol{\sigma} \cdot \nabla$  does not. Consequently  $M_1 \boldsymbol{\sigma} \cdot \nabla / \mathbf{M}_{10} \cdot \boldsymbol{\sigma}$  is quite sensitive to the  $0p_{1/2} \rightarrow 0p_{3/2}$  admixture in these  $A = 11, 12$  transitions. Fortunately the destructive interference of  $0p_{1/2} \leftrightarrow 0p_{3/2}$  amplitudes is also reflected in, and thus calibrated by, the capture rates of  $^{11}\text{B}(3/2^-, 0) \rightarrow ^{11}\text{Be}(1/2^-, 320)$  and  $^{12}\text{C}(0^+, 0) \rightarrow ^{12}\text{B}(1^+, 0)$ .

A special comment is worthwhile for  $^{28}\text{Si}(0^+, 0) \rightarrow ^{28}\text{Al}(1^+, 2201)$ . The calculations indicate this transition involves the destructive interference of numerous single particle transitions with comparable one-body densities. See Sec. IX.G.4 for details. Consequently for  $^{28}\text{Si}$  the calculation of  $X$  may be especially sensitive to the model uncertainties.

The inevitable truncation of model spaces, *e.g.* 0p orbitals for  $A = 11, 12$  and 1s–0d orbitals for  $A = 23, 28$ , is another source of model dependence in  $M_1 \boldsymbol{\sigma} \cdot \nabla / \mathbf{M}_{10} \cdot \boldsymbol{\sigma}$

TABLE XII Comparison of the corrections from the terms involving  $M_1 \boldsymbol{\sigma} \cdot \nabla$ ,  $\mathbf{M}_{12} \cdot \boldsymbol{\sigma}$ , and  $\mathbf{M}_{11} \cdot \nabla$  to the multipole amplitude of  $T_1^{el5} - T_1^{mag}$  for  $A = 11, 12, 23$  and  $28$  and several effective interactions denoted CKPOT (Cohen and Kurath , 1967), PKUO (Kuo and Brown , 1966), USD (Wildenthal, 1984) and KUOSD (Kuo and Brown , 1966). The values in columns 3–5 correspond to the percentage change in the matrix elements as the correction terms are successively included. Note that  $M_1 \boldsymbol{\sigma} \cdot \nabla$  doesn't contribute to  $T_1^{el5} - T_1^{mag}$ .

A	Int.	$T_1^{el5} - T_1^{mag}$	$M_1 \boldsymbol{\sigma} \cdot \nabla$ corr. (%)	$\mathbf{M}_{12} \cdot \boldsymbol{\sigma}$ corr. (%)	$\mathbf{M}_{11} \cdot \nabla$ corr. (%)
11	CKPOT	-0.243	0.0	0.9	0.6
11	PKUO	-0.222	0.0	-0.2	1.7
12	CKPOT	0.249	0.0	3.1	-0.4
12	PKUO	-0.164	0.0	5.4	2.1
23	USD	0.213	0.0	-1.4	-2.2
23	KUOSD	-0.170	0.0	-3.6	-4.8
28	USD	0.171	0.0	8.6	4.7
28	KUOSD	0.106	0.0	4.2	0.7

and  $\mathbf{M}_{12} \cdot \boldsymbol{\sigma} / \mathbf{M}_{10} \cdot \boldsymbol{\sigma}$ . Such core polarization effects have been studied by Fukui *et al.* (1987) for  $^{12}\text{C}$ , Siiskonen *et al.* (1999) for  $^{28}\text{Si}$ , and Koshigiri *et al.* (1997) for  $^{23}\text{Na}$ . For  $^{12}\text{C}$  Fukui *et al.* (1987) found downward renormalizations of 13% for  $\mathbf{M}_{10} \cdot \boldsymbol{\sigma}$ , 33% for  $\mathbf{M}_{12} \cdot \boldsymbol{\sigma}$ , and 22% for  $M_1 \boldsymbol{\sigma} \cdot \nabla$ , and for  $^{28}\text{Si}$  Siiskonen *et al.* (1999) found downward renormalizations of 11% for  $\mathbf{M}_{10} \cdot \boldsymbol{\sigma}$ , 30% for  $\mathbf{M}_{12} \cdot \boldsymbol{\sigma}$ , and 39% for  $M_1 \boldsymbol{\sigma} \cdot \nabla$ . The small effect of core polarization on  $\mathbf{M}_{10} \cdot \boldsymbol{\sigma}$  is because the model spaces are 'complete spaces' for this operator. Note that the renormalization of  $\mathbf{M}_{10} \cdot \boldsymbol{\sigma}$  has strong support from experimental data on allowed  $\beta$ -decay and (p,n)/(n,p) reactions, and the renormalization of  $\mathbf{M}_{12} \cdot \boldsymbol{\sigma}$  has some support from experimental data on second forbidden  $\beta$ -decay. For example see Warburton (1992) and Martínez-Pinedo and Vogel (1998).

The contributions arising from exchange currents in allowed transitions have been studied by Fukui *et al.* (1987) for  $^{12}\text{C}$ , Ciechanowicz *et al.* (1998) for  $^{28}\text{Si}$ , and Koshigiri *et al.* (1997) for  $^{23}\text{Na}$ . For  $^{12}\text{C}$  Fukui *et al.* (1987) found corrections of -4% to  $\mathbf{M}_{10} \cdot \boldsymbol{\sigma}$ , +10% to  $\mathbf{M}_{12} \cdot \boldsymbol{\sigma}$ , and +41% to  $M_1 \boldsymbol{\sigma} \cdot \nabla$ . Recall the large renormalization of the axial charge operator  $M_1 \boldsymbol{\sigma} \cdot \nabla$  arises from large soft-pion contributions in the axial current's time component. This renormalization is supported by experimental data on first-forbidden  $\beta$ -decay.

The assumed form for the radial dependence of the nuclear wave functions is another source of model dependence, *e.g.* at the surface of the nucleus the difference in harmonic oscillator and Wood-Saxon wave functions are large. Such effects were investigated for  $^{12}\text{C}$ ,  $^{23}\text{Na}$

and  $^{28}\text{Si}$  by Kortelainen *et al.* (2000). They found the sensitivity of  $X$  to the radial form of the nuclear wave function was typically 5% or less.

Lastly we consider the determination of  $g_p/g_a$  from the capture rate of the  $^{16}\text{O}(0^+, 0) \rightarrow ^{16}\text{N}(0^-, 120)$  transition. Note that this requires knowing the absolute values of  $\mathbf{M}_{01} \cdot \boldsymbol{\sigma}$  and  $M_1 \boldsymbol{\sigma} \cdot \nabla$ , *i.e.* not ratios like  $M_1 \boldsymbol{\sigma} \cdot \nabla / \mathbf{M}_{10} \cdot \boldsymbol{\sigma}$ . Also the capture rate is highly sensitive to the 2p–2h, 4p–4h structure of the  $^{16}\text{O}$  ground state and the 2–body contributions due to soft–pion exchange. Consequently, as discussed by Warburton *et al.* (1994) and Haxton and Johnson (1990), the extraction of  $g_p/g_a$  from  $^{16}\text{O}(0^+, 0) \rightarrow ^{16}\text{N}(0^-, 120)$  is a formidable challenge. Indeed Warburton *et al.* (1994) have cautioned their result for  $g_p/g_a$  is highly model dependent.

### 3. Conclusions and outlook for $g_p/g_a$

The results in Table X are largely consistent with PCAC and  $g_p/g_a = 6.42$ . Specifically the values obtained from  $^{11}\text{B}$ ,  $^{16}\text{O}$  and  $^{23}\text{Na}$  all support the prediction of PCAC. The situation for  $^{12}\text{C}$  is more borderline, with theory and experiment just under  $2\sigma$  apart, but not enough to cause concern. In contrast however for  $^{28}\text{Si}$  the experiment determination and theoretical prediction are in obvious disagreement.

Ignoring the puzzle of  $^{28}\text{Si}$  for now, we believe the theoretical uncertainties in extracting  $g_p/g_a$  from these data are likely about  $\pm 2$  or so. For example for recoil polarizations and  $\gamma$ –ray correlations the largest contribution to model uncertainties arises via corrections at the 30–40% level from the  $M_1 \boldsymbol{\sigma} \cdot \nabla$  operator. Although the matrix elements for this gradient operator are rather difficult to compute accurately, we note even a 50% uncertainty in  $M_1 \boldsymbol{\sigma} \cdot \nabla$  will produce only a 10–20% uncertainty in extracting  $g_p/g_a$ . A similar situation arises in extracting the coupling  $g_p/g_a$  from hyperfine dependences, although here the additional contributions from  $\Delta J = 2^+$  multipoles may increase somewhat the model uncertainty. However the model uncertainty is probably larger for  $^{16}\text{O}(0^+, 0) \rightarrow ^{16}\text{N}(0^-, 120)$ , since absolute values and not ratios of matrix elements are needed, and those required are quite difficult to accurately compute. See Sec. IX.G.5 for details.

The value of  $g_p/g_a = 1.0 \pm_{1.2}^{1.1}$  from  $^{28}\text{Si}$  is rather puzzling. Interestingly the experimental results for  $^{12}\text{C}$  of  $X = 0.26 \pm 0.06$  and  $^{28}\text{Si}$  of  $X = 0.55 \pm 0.04$  are quite different, while the theoretical predictions for  $^{12}\text{C}$  and  $^{28}\text{Si}$  are not, *i.e.* the calculated corrections arising from axial charge and  $2^{\text{nd}}$ –forbidden operators are similar in  $^{12}\text{C}$  and  $^{28}\text{Si}$ . Inspection of the one–body transition densities for  $^{12}\text{C}$  and  $^{28}\text{Si}$  does indicate a difference in the two cases. Whereas for  $^{12}\text{C}$  the transition is mainly  $0p_{3/2} \rightarrow 0p_{1/2}$  with some  $0p_{1/2} \rightarrow 0p_{3/2}$ , for  $^{28}\text{Si}$  the transition involves numerous single particle transitions of similar magnitudes. Therefore sensitivity to the nuclear model for the  $^{28}\text{Si}(0^+, 0) \rightarrow ^{28}\text{Al}(1^+, 2201)$

transition is likely larger. In addition we observe that the agreement of theory and experiment is good for the  $^{12}\text{C}(0^+, 0) \rightarrow ^{12}\text{B}(1^+, 0)$  capture rate but poor for the  $^{28}\text{Si}(0^+, 0) \rightarrow ^{28}\text{Al}(1^+, 2201)$  capture rate, indicating the GT matrix element is reproduced well for  $^{12}\text{C}$  but reproduced poorly for  $^{28}\text{Si}$ . For further details see Gorringer *et al.* (1999).

Finally what new experimental and theoretical work is worthwhile? For partial transitions on complex nuclei a limiting factor is the small number of the available transitions, *i.e.* four allowed transitions and one first–forbidden transition. Given the unavoidable sensitivity to nuclear structure a larger data–set of partial transitions would be helpful. With more data an improved understanding of contributions from  $M_1 \boldsymbol{\sigma} \cdot \nabla$  and  $\mathbf{M}_{12} \cdot \boldsymbol{\sigma}$  is presumably possible. Unfortunately of course the experimental techniques for measuring recoil polarizations, gamma–ray correlations and hyperfine dependences are often limited to special cases. However new experimental studies of muon capture on  $^{32}\text{S}$  and  $^{35}\text{Cl}$  are under way. Additionally a measurement of the hyperfine dependence in the  $^6\text{Li}(1^+, 0) \rightarrow ^6\text{He}(0^+, 0)$  reaction, where accurate nuclear wavefunctions and related nuclear data are available, is definitely interesting.

## X. INCLUSIVE RMC ON COMPLEX NUCLEI

Several factors have motivated investigations of inclusive RMC on complex nuclei. First the radiative rate on complex nuclei is highly sensitive to  $g_p$ . Second the branching ratios for nuclear RMC are comparatively large, *e.g.* the  $^{12}\text{C}$  rate is about 100 times the  $^1\text{H}$  rate and the  $^{40}\text{Ca}$  rate is about 1000 times the  $^1\text{H}$  rate. Third the early theoretical studies implied the ratio of radiative capture to ordinary capture was only mildly model dependent.

We note comprehensive reviews that cover nuclear RMC were published by Mukhopadhyay (1977) and Gmitro and Truöl (1987). These authors have discussed in detail the formalism and methods for RMC calculations on complex nuclei. Herein we simply outline the major approaches, referring the reader to these reviews for more detail, and focus mainly on recent developments. We update the status of model calculations in Sec. X.A and experimental data in Sec. X.B. We discuss the interpretation of the RMC branching ratio data in Sec. X.C and describe the situation for the RMC photon asymmetry data in Sec. X.D.

### A. Theory of nuclear RMC

The theory of RMC in nuclei has a long history, dating back to Rood and Tolhoek (1965). Although they were not the first to consider the problem, they carefully laid out the approach which has become the standard in subsequent calculations. The standard approach to RMC

in nuclei is to develop a non-relativistic Hamiltonian for the process which is then evaluated in impulse approximation (IA) between nuclear states. There are thus two main ingredients, the Hamiltonian and nuclear structure.

In the usual approach the Hamiltonian is derived from the same five diagrams, Fig. 3(a)-(e), used to describe capture on the nucleon. This Hamiltonian, which originates as a relativistic amplitude, is then expanded in powers of the nucleon momentum either directly, or using a Foldy-Wouthuysen procedure. The leading order is independent of the nucleon momentum and the linear order correction is typically 10-20% and is neglected in many calculations. The correction to the non-relativistic Hamiltonian from the terms quadratic in the nucleon momentum was considered by Sloboda and Fearing (1980) and found to be very small.

This single particle Hamiltonian is then summed over all nucleons and matrix elements of the result are taken between nuclear states. In early calculations very crude nuclear states were used, *e.g.* a simple Slater determinant of harmonic oscillator wave functions. In recent calculations however more modern shell model wave functions have been used which are derived using realistic interactions.

The muon deposits a lot of energy in the nucleus and thus there can be many levels excited in the final nucleus. However all measurements so far are of the inclusive rate, and so a technique must be developed to sum over all final states. In early calculations closure was used. However this introduces a new parameter  $k_{max}$  corresponding to the average maximum photon energy, or equivalently the average nuclear excitation. Unfortunately the rate is just as sensitive to  $k_{max}$  as to  $g_p$ . Furthermore, as pointed out by Christillin (1981), the closure sum includes many excited states which are not allowed in the radiative process due to energy conservation.

There have been several approaches to attempt to bypass this problem. One approach involves obtaining the spectrum of excited states from some other source. Foldy and Walecka (1964) did this for OMC, by recognizing that much of the strength went to the giant dipole resonance state and that one could get this strength from empirical photoabsorption cross sections.<sup>25</sup> This idea was generalized to RMC by Fearing (1966) and further generalized by Christillin (1981) who added additional phenomenological components to account for transitions to quadrupole states. This approach lessened the dependence on  $k_{max}$  but did not totally eliminate it, as there were still matrix elements, *e.g.* the leading  $p/m$  corrections which could not be obtained this way.

Another approach involved sum rules, in which various matrix elements were evaluated using energy weighted

sum rules. This approach was considered for example by Sloboda and Fearing (1978) and more recently applied to OMC by Navarro and Krivine (1986). It was developed further and used more recently for RMC by Roig and Navarro (1990). While still somewhat phenomenological, and still depending to some extent on the closure approximation, this approach is much less sensitive to average excitation energies than the closure approximation.

In principle the best method is to calculate explicitly transitions to all possible excited states and sum the results. This takes the energy dependence into account properly, which can be important (Fearing and Welsh, 1992). One must always truncate the sum somewhere however, which in principle introduces errors. Modern shell model codes are good enough however to produce enough of the excited states so that for at least some nuclei the important transitions can be calculated and summed. Most recent calculations (Eramzhyan *et al.*, 1998; Gmitro *et al.*, 1990, 1986, 1991) have used this approach.

One can also attempt to modify or improve the basic Hamiltonian. Recall that the standard Hamiltonian (Rood and Tolhoek, 1965) is a single particle operator coming from the same basic five diagrams, Fig. 3(a)-(e), used for RMC on the proton. In principle one should include various meson exchange corrections, which lead to two body operators, in the same fashion as has been done for OMC in light nuclei (See Sec. IX.F.3). To our knowledge this has not been done, at least recently, for heavy nuclei.

An alternative approach is to look at these meson exchange corrections as effects of the intermediate pion rescattering in the nuclear medium. This leads to a renormalization of the effective couplings in the nuclear medium. This approach has a long and involved history, and applies to a number of processes involving axial current matrix elements. It is a bit outside the scope of this review however. The reader interested in pursuing this further can consider the recent papers of Kirchbach and Riska (1994) or Kolbe *et al.* (2000) or older studies such as that of Akhmedov *et al.* (1985).

Still another attempt to modify the basic Hamiltonian has been proposed by Gmitro *et al.* (1986). The idea here is to use current conservation to evaluate parts of the matrix element. This is analogous to the Siegert theorem approach which has been used for other processes, and originates in the observation that the nuclear matrix element of the impulse approximation Hamiltonian, unlike the nucleon matrix element, does not correspond to a conserved current. An attempt is made to fix this by expanding the photon field and using the continuity equation to eliminate parts of the three-vector current in favor of the charge distribution. This leads to some different terms and to what the authors call a modified impulse approximation (MIA).

Calculations using this MIA suggest that it is extremely important (Eramzhyan *et al.*, 1998; Gmitro *et*

<sup>25</sup> Later calculations extended this to consider  $SU_4$  breaking and the excitation of the spin dipole state by the axial current. For example see Cannata *et al.* (1970).

*al.*, 1990, 1986, 1991). It reduces the RMC rate by a factor of two or more and thus increases the value of  $g_p$  needed to fit a given experimental result rather dramatically. The approach also seems to produce rates which are much less sensitive to  $g_p$  than the IA. It does however suppress usual impulse approximation results so that they are in better agreement with phenomenological approaches. However there are some caveats. The very fact that what is effectively enforcing gauge invariance makes such a huge difference is worrisome. The results also depend, though not strongly, on an arbitrary choice among various ways to make the original expansion of the photon field. It also appears that one is using the continuity equation on only part of the current, still leaving some reference to the three vector current in the problem. Clearly this needs to be looked at more carefully to determine if it is indeed correct since it makes such a large difference in the final results.

Finally we should mention one other modern calculation (Fearing and Welsh, 1992) which uses a relativistic Fermi gas model together with relativistic mean field theory to examine the  $A$  and  $Z$  dependence of the RMC and OMC rates. The Fermi gas model was used in very early calculations, but is clearly too crude a model to give good results for specific details for individual nuclei. It does however allow one to elucidate general trends and select out features which are important. This will be discussed further in the next section.

## B. Measurement of nuclear RMC

The first observation of radiative capture was made at CERN by Conforto *et al.* (1962). Muons were stopped in Fe and photons were detected by gamma-ray conversion in a iron sheet/spark chamber sandwich and energy deposition in a large volume NaI crystal. After subtraction of backgrounds a total of five photons from RMC on Fe were identified and yielded a Fe RMC branching ratio of roughly  $10^{-4}$ . During the following ten years a few more studies of nuclear RMC were conducted by Conversi *et al.* (1964), Chu *et al.* (1965) and Rosenstein and Hammerman (1973). However the measurements remained extremely difficult because of the low signal rate and the high background rates. In particular under-counted neutron backgrounds most likely corrupted these early experiments.

More recently the availability of higher quality muon beams and higher performance pair spectrometers has dramatically improved the experimental situation. The new era for nuclear RMC was pioneered by Hart *et al.* (1977) for RMC on Ca. Later experimental programs at PSI in the late 1980's and TRIUMF in the early 1990's have produced an extensive body of nuclear RMC data. Today's beams and detection systems allow data collection on  $Z > 12$  targets at count rates of  $\sim 1000$  RMC photons/day with nearly background-free conditions.

In principle the method for determining the branch-

ing ratio for nuclear RMC is straightforward. It simply requires counting the incoming muons and outgoing photons and determining their detection efficiencies. However as discussed in detail in Sec. V.C.4 the small branching ratio means troublesome  $\gamma$ -ray backgrounds arise from  $\mu$  decay in the target material, radiative  $\mu$  capture in the neighboring materials, and the pion contamination in the muon beam. Additionally neutron backgrounds from ordinary capture in the target material and other sources on the accelerator site are dangerous if the  $n/\gamma$  discrimination is not highly effective.

Two basic types of pair spectrometers have been widely employed in the RMC studies of recent years. In one approach, as used by Frischknecht *et al.* (1988), the photons are converted in a relatively thin passive converter and the  $e^+e^-$  pair is tracked in a multiwire chamber arrangement. In another approach, as used by Döbeli *et al.* (1988), the photons are converted in a relatively thick active converter and the  $e^+e^-$  pair is measured by combinations of Cerenkov detectors and NaI crystals. The former approach offers good resolution, typically 1–2%, but at the expense of a low efficiency, typically  $10^{-5}$ . The latter approach offers high efficiency, typically 0.5%, but at the expense of a poor resolution, typically 20%. Such experimental set-ups have yielded excellent  $n/\gamma$  discrimination and provided nearly background-free RMC spectra.

Most recently a novel large solid-angle pair spectrometer was developed at TRIUMF by Wright *et al.* (1992) for RMC on  $^1\text{H}$ . The spectrometer offers both a relatively high detection efficiency and a relatively good energy resolution. It has permitted quick and straightforward measurements of nuclear RMC for numerous targets, and significantly extended the RMC data-set (Armstrong *et al.*, 1992; Bergbusch *et al.*, 1999; Gorringer *et al.*, 1998).

## C. Interpretation of nuclear RMC

The world data-set<sup>26</sup> for nuclear RMC, consisting of targets from carbon to bismuth, is summarized in Table XIII in which we tabulate the ratio  $R_\gamma$  of the  $E_\gamma > 57$  MeV partial radiative rate to the total ordinary rate. In addition we plot the data versus atomic number  $Z$  in Fig. 8 and versus neutron excess  $\alpha = (A - 2Z)/Z$  in Fig. 9. The figures illustrate some intriguing trends, *i.e.* that  $R_\gamma$  is observed to decrease from  $\sim 2$  to  $\sim 0.6$  with increasing  $Z$  and increasing  $\alpha$ .<sup>27</sup> Note the overall trend is somewhat smoother with neutron excess than atomic number. Specifically, the isotope effect in the mass <sup>58,60,62</sup>Ni isotopes and the odd/even- $A$  effect in the

<sup>26</sup> We omit the results from the early experiments of Conversi *et al.* (1964), Chu *et al.* (1965), and Rosenstein and Hammerman (1973) due to large neutron backgrounds.

<sup>27</sup> Note that in this section we will quote all values of  $R_\gamma$  in units of  $10^{-5}$ .

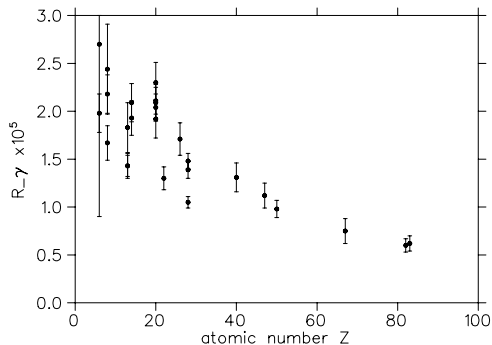


FIG. 8 The world data for  $R_\gamma$  versus  $Z$  on  $A > 3$  nuclei.

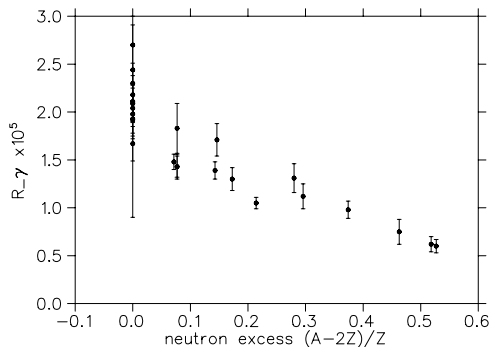


FIG. 9 The world data for  $R_\gamma$  versus  $\alpha = (A - 2Z)/Z$  on  $A > 3$  nuclei.

Al-Si, Ca-Ti pairs fit the  $\alpha$ -dependence but not the  $Z$ -dependence. Below we discuss the  $R_\gamma$ -data in the context of the determination of the coupling  $g_p$ .

For  $^{40}\text{Ca}$  the value of  $R_\gamma$  is well-established by numerous experiments. The average of those included in Table XIII is  $R_\gamma = 2.08 \pm 0.11$ . A number of calculations are available including the phenomenological models of Fearing (1966) and Christillin (1981), the microscopic shell model calculations of Gmitro *et al.* (1986) and the sum rule calculations of Roig and Navarro (1990). Unfortunately as discussed earlier the calculation of inclusive RMC on complex nuclei is notoriously difficult. It

is often difficult to quantify the effect of the various approximations and assumptions and so to set limits on the uncertainty in the theoretical predictions.

The phenomenological calculations of Christillin (1981), based on the Giant Dipole Resonance model (Fearing, 1966; Foldy and Walecka, 1964) with parameters determined from electromagnetic data but including effects of a quadrupole resonance with parameters fit to the OMC rate, gave  $R_\gamma = 2.4$  using the canonical value  $g_p/g_a \simeq 6.7$ . The calculation of Roig and Navarro (1990) used fairly realistic RPA wave functions but with the phenomenological aspects of a sum rule calculation to obtain  $R_\gamma = 1.87$ . The microscopic shell model calculation of Gmitro *et al.* (1986) used simple 1p-1h wave functions, with some corrections to obtain  $R_\gamma = 4.25$  in the standard IA and  $R_\gamma = 2.28$  in the MIA. Thus the MIA makes a large difference, and brings the results in closer agreement with the more phenomenological approaches. Note that all of these calculations, except the standard IA approach, apparently neglected the velocity or  $p/m$  terms which could be up to 10-20%.

On a superficial level all of these results, except perhaps for the standard IA result, are reasonably consistent with the experimental result. However if one turns the question around and asks what limits are set on  $g_p/g_a$  things become much less clear. A theoretical value of  $R_\gamma$  less than the experiment implies a larger value of  $g_p/g_a$  is needed to fit the data. Thus the sum rule calculation of Roig and Navarro (1990) requires  $g_p/g_a \sim 8$ . On the other hand the phenomenological calculations of Christillin (1981) and the MIA results of Gmitro *et al.* (1986) require  $g_p/g_a \sim 4-5$  and the IA result implies that  $g_p/g_a$  is much smaller. Thus one has to conclude that it is unreasonable to claim that  $g_p/g_a \sim 6.7$  is well-established by RMC on  $^{40}\text{Ca}$ .

For  $^{16}\text{O}$  a number of measurements and calculations are also available. Unfortunately measurement of RMC on  $^{16}\text{O}$  is more difficult, since the  $\gamma$ -ray yield per  $\mu^-$  stop is  $\sim 2 \times 10^{-5}$  for  $^{40}\text{Ca}$  and  $\sim 0.4 \times 10^{-5}$  for  $^{16}\text{O}$ , and most probably the earlier experiments have under-subtracted contamination from  $\gamma$ -ray backgrounds. Therefore we employ the recent result from Bergbusch *et al.* (1999) of  $R_\gamma = 1.67 \pm 0.18$ . Like  $^{40}\text{Ca}$ , both phenomenological calculations and microscopic calculations are available, but similarly the sensitivities of results to approximations are difficult to estimate. Taking  $g_p/g_a \simeq 6.7$  the phenomenological calculation of Christillin and Gmitro (1985) gave  $R_\gamma = 2.08$ , the shell model calculation of Gmitro *et al.* (1986) gave  $R_\gamma = 1.61$  in MIA and  $R_\gamma = 3.10$  in IA and sum rule calculation of Roig and Navarro (1990) gave  $R_\gamma = 1.73$ . Again, with the exception of the IA result, these are reasonably consistent with the experimental result (Bergbusch *et al.*, 1999)  $R_\gamma = 1.67 \pm 0.18$  with the sum rule and MIA approaches implying roughly the canonical value of  $g_p/g_a$  and the approach of Christillin and Gmitro (1985) requiring a somewhat smaller value. The IA result would require a significantly smaller value to fit the data. However, like RMC on  $^{40}\text{Ca}$ , due

TABLE XIII Summary of the world data on the quantity  $R_\gamma$  on  $A > 3$  targets, where  $R_\gamma$  is the ratio of the RMC rate with  $E_\gamma > 57$  MeV to the OMC rate in units of  $10^{-5}$ . In order to assist comparisons in most cases the quoted results are for the closure approximation spectra shape where the corresponding value of the parameter  $k_{max}$  is given in column four. The quantity  $\alpha$  is the neutron excess  $(A - 2Z)/Z$ .

Target	$\alpha$	$R_\gamma (\times 10^{-5})$	$k_{max} (\text{MeV})$
Bergbusch <i>et al.</i> (1999)			
$^{16}_8\text{O}$	0.000	$1.67 \pm 0.18$	$88.4 \pm 2.3$
$^{27}_{13}\text{Al}$	0.077	$1.43 \pm 0.11$	$90.1 \pm 1.8$
$^{28}_{14}\text{Si}$	0.000	$2.09 \pm 0.20$	$89.4 \pm 1.8$
$^{nat}_{22}\text{Ti}$	0.173	$1.30 \pm 0.12$	$89.2 \pm 2.0$
$^{nat}_{40}\text{Zr}$	0.280	$1.31 \pm 0.15$	$89.2 \pm 3.4$
$^{nat}_{47}\text{Ag}$	0.296	$1.12 \pm 0.13$	$89.0 \pm 3.2$
Gorringe <i>et al.</i> (1998)			
$^{58}_{28}\text{Ni}$	0.071	$1.48 \pm 0.08$	$92.0 \pm 2.0$
$^{60}_{28}\text{Ni}$	0.143	$1.39 \pm 0.09$	$90.0 \pm 2.0$
$^{62}_{28}\text{Ni}$	0.214	$1.05 \pm 0.06$	$89.0 \pm 2.0$
Armstrong <i>et al.</i> (1992)			
$^{27}_{13}\text{Al}$	0.077	$1.43 \pm 0.13$	$90.0 \pm 2.0$
$^{28}_{14}\text{Si}$	0.000	$1.93 \pm 0.18$	$92.0 \pm 2.0$
$^{40}_{20}\text{Ca}$	0.000	$2.09 \pm 0.19$	$93.0 \pm 2.0$
$^{nat}_{42}\text{Mo}$	0.283	$1.11 \pm 0.11$	$90.0 \pm 2.0$
$^{nat}_{50}\text{Sn}$	0.374	$0.98 \pm 0.09$	$87.0 \pm 2.0$
$^{nat}_{82}\text{Pb}$	0.527	$0.60 \pm 0.07$	$84.0 \pm 3.0$
Armstrong <i>et al.</i> (1991)			
$^{12}_6\text{C}$	0.000	$1.98 \pm 0.20$	
$^{16}_8\text{O}$	0.000	$2.18 \pm 0.20$	
$^{40}_{20}\text{Ca}$	0.000	$2.04 \pm 0.14$	
Frischknecht <i>et al.</i> (1988)			
$^{16}_8\text{O}$	0.000	$3.80 \pm 0.40$	
Döbeli <i>et al.</i> (1986)			
$^{12}_6\text{C}$	0.000	$2.70 \pm 1.80$	
$^{16}_8\text{O}$	0.000	$2.44 \pm 0.47$	$89.9 \pm 5.0$
$^{27}_{13}\text{Al}$	0.077	$1.83 \pm 0.26$	$88.8 \pm 1.8$
$^{40}_{20}\text{Ca}$	0.000	$2.30 \pm 0.21$	$92.5 \pm 0.7$
$^{nat}_{26}\text{Fe}$	0.146	$1.71 \pm 0.17$	$90.2 \pm 1.1$
$^{165}_{67}\text{Ho}$	0.463	$0.75 \pm 0.13$	$84.1 \pm 5.1$
$^{209}_{83}\text{Bi}$	0.518	$0.62 \pm 0.08$	$88.2 \pm 0.6$
Frischknecht <i>et al.</i> (1985)			
$^{40}_{20}\text{Ca}$	0.000	$1.92 \pm 0.20$	$90.8 \pm 0.9$
Hart <i>et al.</i> (1977)			
$^{40}_{20}\text{Ca}$	0.000	$2.11 \pm 0.14$	$86.5 \pm 1.9$

to the approximations in the calculations and the differences among the results of different calculations the case for  $g_p/g_a \sim 6.7$  in RMC on  $^{16}\text{O}$  is not firmly established.

There are also both theoretical and experimental results for  $^{12}\text{C}$ . The most recent result, and the one with by far the smallest uncertainty is that of Armstrong *et al.* (1991),  $R_\gamma = 1.98 \pm 0.20$ . This is to be compared with the sum rule result (Roig and Navarro, 1990) of  $R_\gamma = 1.42$ , and the IA result,  $R_\gamma = 3.60$ , and the MIA result,  $R_\gamma = 1.48$  (Gmitro *et al.*, 1990). In this case both MIA and sum rule results are too low, implying  $g_p/g_a \sim 10 - 13$ , to fit the data whereas the IA is too high, implying a very low value of  $g_p/g_a$ .

Finally we should mention the calculations for  $^{58,60,62}\text{Ni}$  of Eramzhyan *et al.* (1998) carried out in a microscopic model using the quasiparticle RPA. Again the IA results for  $R_\gamma$  are much higher than those in MIA, but even the MIA results are significantly higher than the experiment (Gorringe *et al.*, 1998).

Thus by now there have been a number of experiments and enough calculations that we can make comparisons of  $R_\gamma$  for several different nuclei. The situation can only be described as confused. The standard impulse approximation calculations are consistently too high, implying a value of  $g_p/g_a$  much smaller than the canonical value. The MIA start out too low for  $^{12}\text{C}$ , implying a large value of  $g_p/g_a$ , and rise with increasing  $A$  to become significantly too high for the Ni isotopes, implying there a small value of  $g_p/g_a$ . The phenomenological calculations of Christillin (1981) and Christillin and Gmitro (1985) for  $^{16}\text{O}$  and  $^{40}\text{Ca}$  are both too high and the sum rule calculations show no consistent pattern. It appears clear that we are not yet at a stage where theoretical uncertainties are sufficiently under control to consistently reproduce experimental results.

In addition to discussing the detailed calculations for specific nuclei it is worthwhile to consider the systematics of RMC data versus atomic number and neutron excess. Such systematics were examined in the non-relativistic Fermi-gas calculation of Christillin *et al.* (1980) and the relativistic Fermi-gas calculation of Fearing and Welsh (1992). These models clearly oversimplify the nuclear structure, for example omitting the important effects of giant resonances in muon capture, or the effects of shell closures. However they demonstrate a number of interesting dependences of muon capture on  $Z$  and  $\alpha$ .

For concreteness we consider the calculation of Fearing and Welsh (1992). These authors have carefully studied the dependence of inclusive OMC and inclusive RMC on the input parameters and the model assumptions. They stress that the OMC rate, the RMC rate, and their ratio, are highly sensitive to phase-space effects, *i.e.* things that alter the available energy for the neutrino and the photon. For example including the  $\mu^-$  atomic binding energy, which increases from  $\sim 0.1$  MeV in light nuclei to  $\sim 10$  MeV in heavy nuclei, decreases the OMC rate by a factor of two and the RMC rate by a factor of eight for the heaviest nuclei. Other parameters, *e.g.* for Fermi-gas

models the Coulomb energy, symmetry energy, etc., also have large effects on the available energy and therefore the rates. Consequently the authors caution that reliably extracting the coupling  $g_p$  from inclusive RMC on complex nuclei is difficult.

Despite such concerns the calculation of Fearing and Welsh (1992) does reproduce the overall dependence of  $R_\gamma$  data with  $Z$  and  $\alpha$ . This model–data agreement however suggests no reason to invoke a large–scale medium–modification of  $g_p/g_a$  to explain the  $Z$ –dependence of  $R_\gamma$  data.

Earlier suggestions for an  $A$ –dependence of the coupling  $g_p$ , as discussed by Gmitro and Truöl (1987) and Döbeli *et al.* (1988), were largely grounded in large values of  $g_p/g_a$  obtained from shell model calculations on light nuclei and small values of  $g_p/g_a$  obtained from Fermi–gas calculations on heavy nuclei. Given the different systematics of the various models and the difficulty of all models in consistently fitting the data, such differences do not provide real evidence for an  $A$ –dependence of the coupling  $g_p$ .

In summary, although the RMC rate on complex nuclei is undoubtedly  $g_p$ –dependent, the problem of separating the coupling constant and nuclear structure is extraordinarily tricky. While the overall features of nuclear RMC are generally accommodated by  $g_p/g_a = 6.7$  there is a model uncertainty of at least 50%. Thus RMC in heavy nuclei is not yet competitive with RMC or OMC in hydrogen or light nuclei as a source of information on  $g_p/g_a$ .

For inclusive RMC on complex nuclei we find the progress on model calculations is lagging the progress on experimental data, and a breakthrough on the theoretical side is needed before this particular tool for studying the coupling is competitive. However, exclusive RMC on complex nuclei, which is so far unmeasured, might offer interesting possibilities.

#### D. Comments on photon asymmetries in nuclear RMC

In RMC the gamma–ray direction and muon polarization are correlated according to

$$N(\theta) = N(1 + \alpha P_\mu \cos \theta) \quad (50)$$

where  $P_\mu$  is the muon polarization,  $\alpha$  is the asymmetry coefficient, and  $\theta$  is the angle between the  $\mu$ –spin axis and the  $\gamma$ –ray momentum axis. The left handedness of the neutrino leads to  $\alpha \simeq +1$ , and  $g_p$  is manifest as departures of  $\alpha$  from unity (Fearing, 1975). The specific dependence of  $\alpha$  on  $g_p/g_a$  for RMC on  $^{40}\text{Ca}$  was computed by Rood and Tolhoek (1965), Gmitro *et al.* (1981), Christillin (1981) and Gmitro *et al.* (1987).

To measure the asymmetry one stops the incoming muons in a suitable target, precesses the muon spin in a magnetic field, and measures the time spectrum of the outgoing photons. The resulting time spectrum consists of an exponential decay with a sinusoidal modulation, where the amplitude of the sine–wave is governed by the

TABLE XIV Summary of the world data on the photon asymmetry in radiative capture on calcium.

Ref.	asymmetry $\alpha$
Hart <i>et al.</i> (1977)	$0.90 \pm 0.50$
Döbeli <i>et al.</i> (1986)	$0.90 \pm 0.43$
Virtue <i>et al.</i> (1990)	$1.32^{+0.54}_{-0.47}$
world average	$1.02 \pm 0.25$

product  $P_\mu \alpha$ . Note that the time spectrum of the Michel electrons is employed to measure  $P_\mu$  and isolate  $\alpha$ . In the first measurement by di Lella *et al.* (1971) the authors used a single NaI crystal for  $\gamma$ –ray detection. In the later measurements by Hart *et al.* (1977), Döbeli *et al.* (1986) and Virtue *et al.* (1990) the authors used a separate  $\gamma$ –ray converter and NaI calorimeter. A  $^{40}\text{Ca}$  target was used in each experiment.

The experimental difficulties originate from the tiny RMC branching ratio and the small  $\mu$  residual polarization. Consequently the backgrounds are severe. They include  $\gamma$ –rays from pion capture in the target,  $\gamma$ –rays from Michel bremsstrahlung in the target, neutrons from muon capture in the target, and  $n/\gamma$  backgrounds from cosmic–ray and accelerator sources. Note that a prompt cut reduces the  $\gamma$ –rays following  $\pi$ –capture and a  $E > 57$  MeV cut reduces the bremsstrahlung following  $\mu$ –decay. The neutron background is reduced via the converter–calorimeter set–up and cosmic–ray background is reduced via combined passive and active shielding.

In Table XIV we summarize the results of Hart *et al.* (1977), Döbeli *et al.* (1986) and Virtue *et al.* (1990). We omit the earliest results of di Lella *et al.* (1971), which suffered severe neutron backgrounds. The various experiments are mutually consistent and yield a world average value  $\alpha = 1.02 \pm 0.25$ .

Unfortunately the effect of  $g_p$  on  $\alpha$  is (i) not large and (ii) model dependent. For example with  $g_p/g_a \simeq 6.7$  the phenomenological model of Christillin (1981) gives  $\alpha \simeq 0.80$  and the shell model of Gmitro *et al.* (1987) gives  $\alpha \simeq 0.90$ . Conservatively the measurements yield  $g_p/g_a < 20$ .

## XI. SUMMARY

The determination of  $g_p$  is important for several reasons. First, whereas the values of the proton’s other



weak couplings are nowadays well determined, the induced pseudoscalar coupling is still poorly determined. Second, based on chiral symmetry arguments a solid theoretical prediction for  $g_p$  with 2–3% accuracy is available. Third, the prediction is founded on some elementary properties of the strong interaction, and determining the coupling is therefore an important test of quantum chromodynamics at low energies.

Since the classic review of Mukhopadhyay (1977) an extensive body of experimental data on the coupling  $g_p$  has been accumulated. This work spans the elementary processes of ordinary muon capture and radiative muon capture on hydrogen, muon capture on few-body systems, and exclusive OMC and inclusive RMC on complex nuclei. The experimental approaches have ranged from ultra-high precision measurements to ultra-rare process measurements, and include some novel studies of spin phenomena in complex nuclei. The disentangling of the coupling constant from the physical observables has involved diverse fields from  $\mu$ -molecular chemistry to traditional nuclear structure and exchange current effects.

One would expect muon capture on hydrogen to be the most straightforward and most easily interpreted of the muon capture reactions. This is the situation from the nuclear perspective, but unfortunately there exist atomic and molecular complications which also must be thoroughly understood. For OMC there are a several older experiments together with the most recent and precise measurement of Bardin *et al.* (1981a) whereas for RMC there is only the TRIUMF experiment (Wright *et al.*, 1998). To extract  $g_p$  from these results we updated the theoretical calculations to include the current best values of the other weak couplings and their  $q^2$  dependences. Additionally we updated the capture rate of Bardin *et al.* (1981a) for the present world-average value of the positive muon lifetime. We found, for the standard values of the  $\mu$  chemistry parameters and specifically with  $\Lambda_{op} = 4.1 \times 10^4 \text{ s}^{-1}$ , values of  $g_p = 12.2 \pm 1.1$  from the TRIUMF RMC experiment (Wright *et al.*, 1998),  $g_p = 10.6 \pm 2.7$  from the Saclay OMC experiment (Bardin *et al.*, 1981a), and  $g_p = 10.5 \pm 1.8$  for the world average of all OMC experiments. These updates increased the  $g_p$  extracted from OMC, as compared to the original analysis, so that now both OMC and RMC give results larger than predicted by PCAC and in fact agree better with each other than with PCAC. When uncertainties are taken into account however, only the TRIUMF result is clearly inconsistent with PCAC, while the OMC results are only marginally inconsistent with PCAC.

Our strong prejudice that PCAC is not violated at such a level, makes the situation for  $\mu$  capture in hydrogen very puzzling. We therefore have examined some suggestions for solving the puzzle, such as modifications to the  $\mu$  chemistry and the role of the  $\Delta$  resonance. By ‘tuning parameters’ the discrepancy between the hydrogen data and the PCAC prediction can be reduced somewhat, but no clear-cut solution, which makes OMC and RMC simultaneously agree with PCAC, has emerged.

New work on  $\mu$  capture in liquid  $\text{H}_2$  and gaseous  $\text{H}_2$  is in progress. At TRIUMF an investigation of the  $\mu$  chemistry in liquid hydrogen has taken data, and at PSI a measurement of  $\mu^-$  lifetime in gaseous hydrogen is now under way. Hopefully these experiments will help to clarify the situation on  $g_p$ . Looking further ahead, perhaps both new facilities, *e.g.* an intense muon source at a neutrino factory, and new techniques, *e.g.* neutron polarizations or hyperfine effects, will permit a determination of  $g_p$  to an accuracy of 2-3% or better.

The situation for muon capture on pure deuterium is inconclusive. Recall that in deuterium the  $g_p$  sensitivity is smaller than in hydrogen, the neutron experiments are harder, and nuclear models are needed. At present the world data for muon capture in pure deuterium comprises the experiment of Cargnelli *et al.* (1989), which appears consistent with PCAC, and the experiment of Bardin *et al.* (1986), which may be inconsistent with PCAC. Also the results on  $\mu d$  capture by Bertin *et al.* (1973) using a  $\text{H}_2/\text{D}_2$  target are even more puzzling.

Further studies of  $\mu d$  capture are clearly worthwhile. Obviously resolving the possible discrepancy between the doublet rates obtained by Cargnelli *et al.* (1989) and Bardin *et al.* (1986) is important. Additionally we note the chemistry of muons in pure  $\text{H}_2$  and pure  $\text{D}_2$  is quite different in several ways, including a slower rate for hyperfine depopulation and near absence of muonic molecules in pure  $\text{D}_2$ . Such features may permit the study of  $g_p$  via alternative approaches, such the hyperfine dependence of the capture reaction.

In  $\mu + {}^3\text{He} \rightarrow {}^3\text{H} + \nu$  capture, the recent precision measurement of the statistical capture rate by Ackerbauer *et al.* (1998) and ground-breaking measurement of the recoil angular correlation by Souder *et al.* (1998), were major achievements. Preliminary data on the radiative capture rate in the  ${}^3\text{He} \rightarrow {}^3\text{H}$  channel are also available (Wright *et al.*, 2000). Further modern treatments of  $A = 3$  wave functions and 2-body exchange currents have been applied to the process by Congleton and Truhlik (1996) and others. The OMC results for  $g_p$  are completely consistent with PCAC, and the value of  $g_p = 8.53 \pm 1.54$  from Ackerbauer *et al.* (1998) is probably the best individual determination of  $g_p$ .

The extraction of the coupling from the measurement of the  $\mu + {}^3\text{He} \rightarrow {}^3\text{H} + \nu$  statistical rate is unfortunately limited by theoretical uncertainties in calculating contributions from exchange currents. Further theoretical work is definitely worthwhile to quantify the contributions arising from radiative corrections and nail-down the uncertainties arising from exchange currents, etc, but improvements in extracting the coupling may be difficult. A precision measurement of the recoil correlation, which has enhanced sensitivity to  $g_p$  and reduced sensitivity to exchange currents, would be extremely interesting.

A significant body of new data on exclusive transitions in ordinary capture on complex nuclei has been collected recently. This includes the measurement of  $\gamma$ -ray correlations in  $\mu^{28}\text{Si}$  and hyperfine dependences in  $\mu^{11}\text{B}$  and

$\mu^{23}\text{Na}$ . These data complement earlier investigations of polarizations in  $\mu^{12}\text{C}$  and rates in  $\mu^{16}\text{O}$ . Furthermore, modern well-tested models of nuclear structure in  $0p$ ,  $1s$ – $0d$  nuclei offer improved multi-particle wave functions for interpreting these experiments. In most cases, with the exception of  $^{28}\text{Si}$ , the values of  $g_p$  that are extracted from the experiments with such wave functions are consistent with PCAC. Generally the major uncertainty in extracting  $g_p$  originates in the interplay of the contributions from the pseudoscalar coupling, arising from the space part of the axial current, and the axial charge, arising from the time part of the axial current. Unfortunately it is difficult to precisely quantify such theoretical uncertainties.

Additional experiments on exclusive OMC could be helpful to our understanding of the interplay of the induced pseudoscalar contribution and the axial charge contribution. Clearly if a wealth of data were available for nuclear OMC a better assessment of model uncertainties would be possible. However, the experiments generally involve the use of methods and observables that cannot be applied to large numbers of exclusive transitions. Alternatively a measurement of observables in a transition such as  $^6\text{Li}(1^+, 0) \rightarrow ^6\text{He}(0^+, 0)$ , where highly accurate wave functions and related nuclear data are now-days available, is definitely interesting.

In inclusive RMC on complex nuclei the application of pair spectrometers has yielded data with good statistics and little background, and enabled the systematics of the RMC rate across the periodic table to be mapped-out. Unfortunately the situation in regards to the model calculation of the inclusive rate is less satisfactory. In general the models employed for inclusive RMC have too many assumptions and too many parameters in order to reliably extract the coupling  $g_p$ . Furthermore questions remain regarding the effective Hamiltonian for radiative capture on complex nucleus. Therefore we believe that earlier claims for large renormalizations of  $g_p$  in inclusive RMC on complex nuclei were premature and that, at the level of the uncertainties, the data are consistent with PCAC.

In conclusion we hope we have convinced the reader of the importance of the coupling  $g_p$ , both as a fundamental parameter in nucleon weak interactions and as an important test of low energy quantum chromodynamics. In recent years an impressive body of experimental data has been accumulated and most data are consistent, within sometimes large experimental and theoretical uncertainties, with the PCAC prediction for the coupling  $g_p$ . Unfortunately the results from  $\mu$  capture in hydrogen, which should be the simplest and cleanest process, are very puzzling. We believe that the resolution of this puzzle should be a high priority, and that, until the situation is clarified, the accurate determination of  $g_p$ , and implied testing of low energy QCD, remains an important task but an elusive goal.

## Acknowledgments

The authors would like to thank David Armstrong, Jules Deutsch, Mike Hasinoff, and David Measday for valuable discussions and Jean-Michel Poutissou for encouraging us to prepare this review and for supporting the sabbatical at TRIUMF of one of us (T. G.). We would also like to thank David Measday for a careful reading of the manuscript. This work was supported in part by grants from the Natural Sciences and Engineering Research Council of Canada and the U. S. National Science Foundation.

## References

- Abbott, D. J., *et al.*, 1997, “Diffusion of muonic deuterium and hydrogen atoms,” *Phys. Rev. A* **55**, 214.
- Ackerbauer, P., *et al.*, 1998, “A precision measurement of nuclear muon capture on  $^3\text{He}$ ,” *Phys. Lett. B* **417**, 224.
- Adam, J., E. Truhlik, S. Ciechanowicz, and K. M. Schmitt, 1990, “Muon capture in deuterium and the meson exchange current effect,” *Nucl. Phys. A* **507**, 675.
- Adamczak, A., C. Chiccoli, V. I. Korobov, V. S. Melezhik, P. Pasini, L. I. Ponomarev and J. Wozniak, 1992, “Muon transfer rates in hydrogen isotope - mesic atom collisions,” preprint JINR-E4-92-140.
- Adler, S. L. and Y. Dothan, 1966, “Low-Energy Theorem for the Weak Axial Vertex,” *Phys. Rev.* **151**, 1267; **164**, 2062(E).
- Ahrens, L. A., *et al.*, 1988, “A study of the axial-vector form factor and second-class currents in antineutrino quasielastic scattering,” *Phys. Lett. B* **202**, 284.
- Akhmedov, E. Kh., T. V. Tetereva, and R. A. Eramzhyan, 1985, “Influence of renormalization of weak nucleon form factors on radiative muon capture by nuclei,” *Yad. Fiz.* **42**, 67 [*Sov. J. Nucl. Phys.* **42**, 40 (1985)].
- Alberigi-Quaranta, A., A. Bertin, G. Matone, F. Palmonari, G. Torelli, P. Dalpiaz, A. Placci, and E. Zavattini, 1969, “Muon capture in gaseous hydrogen,” *Phys. Rev.* **177**, 2118.
- Ami, H., M. Kobayashi, H. Ohtsubo, and M. Morita, 1981, “Longitudinal polarization of  $^{12}\text{B}$  in muon capture reaction,” *Prog. Theor. Phys. (Kyoto)* **65**, 632.
- Ando, S., H. W. Fearing, D.-P. Min, 2002, “Polarized photons in radiative muon capture,” *Phys. Rev. C* **65**, 015502.
- Ando, Shung-ichi and Dong-Pil Min, 1998, “Radiative muon capture in heavy baryon chiral perturbation theory,” *Phys. Lett. B* **417**, 177.
- Ando, Shung-ichi, Fred Myhrer, and Kuniharu Kubodera, 2000, “Capture rate and neutron helicity asymmetry for ordinary muon capture on hydrogen,” *Phys. Rev. C* **63**, 015203.
- Ando, Shung-ichi, Fred Myhrer, and Kuniharu Kubodera, 2001a, “Analysis of ordinary and radiative muon capture in liquid hydrogen,” *nucl-th/0109068 v2*.
- Ando, S., T.S. Park, K. Kubodera, and F. Myhrer, 2001b, “The  $\mu$ -D capture rate in effective field theory,” *nucl-th/0109053*.
- Armstrong, D. S., *et al.*, 1991, “Radiative muon capture on carbon, oxygen, and calcium,” *Phys. Rev. C* **43**, 1425.

- Armstrong, D. S., *et al.*, 1992, "Radiative muon capture on Al, Si, Ca, Mo, Sn, and Pb," *Phys. Rev. C* **46**, 1094.
- Armstrong, D. S., *et al.*, 1995, "The ortho-para transition rate in muonic molecular hydrogen," *TRIUMF Expt.* 766.
- Arndt, Richard A., Igor I. Strakovsky, and Ron L. Workman, 1995, "Extraction of the  $\pi NN$  coupling constant from  $NN$  scattering data," *Phys. Rev. C* **52**, 2246.
- Astbury, A., L. B. Auerbach, D. Cutts, R. J. Esterling, D. A. Jenkins, N. H. Lipman, and R. C. Shafer, 1964, "Muon capture in oxygen," *Nuovo Cimento* **33**, 1020.
- Auerbach, L. B., R. J. Esterling, R. E. Hill, D. A. Jenkins, J. T. Lach, and N. H. Lipman, 1967, "Measurements of the muon capture rate in  $^3\text{He}$  and  $^4\text{He}$ ," *Phys. Rev.* **138**, B127.
- Auerbach, N., and B. A. Brown, 2002, "Weak interaction rates involving  $^{12}\text{C}$ ,  $^{14}\text{N}$ , and  $^{16}\text{O}$ ," *Phys. Rev. C* **65**, 024322.
- Bailey, J., C. Oram, G. Azuelos, J. Brewer, K. Erdman, and K. Crowe, 1983 "Triplet  $\mu^- p$  absorption in  $\text{H}_2$  gas," *TRIUMF Expt. Proposal No.* 273.
- Bakalov, D. D., M. P. Faifman, L. I. Ponomarev and S. I. Vinitzky, 1982, " $\mu$  capture and ortho-para transitions in the muonic molecule  $pp\mu$ ," *Nucl. Phys. A* **384**, 302.
- Bardin, G., 1982, "Mesure du taux de transition ortho-para de la molecule p- $\mu$ -p: Interpretation des mesures du taux de capture de  $\mu^-$  sur le proton et deduction de la constante de couplage pseudoscalaire  $F_p^\mu$ ," Ph. D. Thesis, Univ. Paris Sud (Orsay), October 1982.
- Bardin, G., J. Duclos, A. Magnon, J. Martino, A. Richter, E. Zavattini, A. Bertin, M. Piccinini, A. Vitale, and D. Measday, 1981a, "A novel measurement of the muon capture rate in liquid hydrogen by the lifetime technique," *Nucl. Phys. A* **352**, 365.
- Bardin, G., J. Duclos, A. Magnon, J. Martino, A. Richter, E. Zavattini, A. Bertin, M. Piccinini, and A. Vitale, 1981b, "Measurement of the ortho-para transition rate in the  $p\mu p$  molecule and deduction of the pseudoscalar coupling constant  $g_p^\mu$ ," *Phys. Lett. B* **104**, 320.
- Bardin, G., J. Duclos, J. Martino, A. Bertin, M. Capponi, M. Piccinini and A. Vitale, 1986, "A measurement of the muon capture rate in liquid deuterium by the lifetime technique," *Nucl. Phys. A* **453**, 591.
- Barton, A. S., P. Bogorad, G. D. Cates, H. Mabuchi, H. Middleton, N. R. Newbury, R. Holmes, J. McCracken, P. A. Souder, J. Xu, and D. Tupa, 1993, "Highly polarized muonic He produced by collisions with laser optically pumped Rb," *Phys. Rev. Lett.* **70**, 758.
- Beder, D., 1976, "Radiative  $\mu$  capture on protons and  $^3\text{He}$ ," *Nucl. Phys. A* **258**, 447.
- Beder, Douglas S. and Harold W. Fearing, 1987, "Contribution of the  $\Delta(1232)$  to  $\mu^- p \rightarrow n\nu\gamma$ ," *Phys. Rev. D* **35**, 2130.
- Beder, Douglas S. and Harold W. Fearing, 1989, "Radiative muon capture in hydrogen and nucleon excitation," *Phys. Rev. D* **39**, 3493.
- Bergbusch, P. C., *et al.*, 1999, "Radiative muon capture on O, Al, Si, Ti, Zr, and Ag," *Phys. Rev. C* **59**, 2853.
- Bernabeu, J., 1971, "Muon capture in  $^{11}\text{B}$ ," *Nuovo Cimento A* **4**, 715.
- Bernabeu J., 1975, "Restrictions for asymmetry and polarizations of recoil in muon capture," *Phys. Lett. B* **55**, 313.
- Bernard, V., N. Kaiser and U.-G. Meissner, 1992, "Determining the axial radius of the nucleon from data on pion electroproduction," *Phys. Rev. Lett.* **69**, 1877.
- Bernard, V., N. Kaiser and U.-G. Meissner, 1994, "QCD accurately predicts the induced pseudoscalar coupling constant," *Phys. Rev. D* **50**, 6899.
- Bernard, V., H. W. Fearing, T. R. Hemmert, and Ulf-G. Meissner, 1998, "The form factors of the nucleon at small momentum transfer," *Nucl. Phys. A* **635**, 121.
- Bernard, V., L. Elouadrhiri, and U.-G. Meissner, 2001a, "Axial structure of the nucleon," hep-ph/0107088.
- Bernard, V., T. R. Hemmert, and Ulf-G. Meissner, 2001b, "Ordinary and radiative muon capture on the proton and the pseudoscalar form factor of the nucleon," *Nucl. Phys. A* **686**, 290.
- Bernard, V., N. Kaiser, and Ulf-G. Meissner, 2001c, "Further comment on pion electroproduction and the axial form factor," hep-ph/0101062.
- Bertin, A., A. Vitale, A. Placci and E. Zavattini, 1973, "Muon capture in gaseous deuterium," *Phys. Rev. D* **8**, 3774.
- Bertolini *et al.*, 1962, Proc. inter. conf. on high energy physics, CERN, ed. by J. Prentki, p. 421.
- Bjorken, J. D. and S. D. Drell, 1964, *Relativistic Quantum Mechanics* (McGraw-Hill, New York).
- Bleser, E., L. Lederman, J. Rosen, J. Rothberg, and E. Zavattini, 1962, "Muon capture in liquid hydrogen," *Phys. Rev. Lett.* **8**, 288.
- Bogorad, P., *et al.*, 1997, "A combined polarized target/ionization chamber for measuring the spin dependence of nuclear muon capture in laser polarized muonic  $^3\text{He}$ ," *Nucl. Instrum. Methods Phys. Res. A* **398**, 211.
- Bracci, L., and G. Fiorentini, 1982, "Mesic molecules and muon catalyzed fusion," *Phys. Rep.* **86**, 169.
- Breunlich, W. H., 1981, "Muon capture in hydrogen isotopes," *Nucl. Phys. A* **353**, 201c.
- Breunlich, W. H., P. Kammel, J. S. Cohen, and M. Leon, 1989, "Muon catalyzed fusion," *Ann. Rev. Nucl. Sci.* **39**, 311.
- Briançon, Ch., *et al.*, 2000, "The spin-neutrino correlation revisited in  $^{28}\text{Si}$  muon capture: A new determination of the induced pseudoscalar coupling  $g_p/g_a$ ," *Nucl. Phys. A* **671**, 647.
- Brown, B. A., W. A. Richter, R. E. Julies and B. H. Wildenthal, 1988, "Semi-empirical effective interactions for the 1s-0d shell," *Ann. Phys. (N.Y.)* **182**, 191.
- Brown, G. E., and A. M. Green, 1966, "Even parity states of  $^{16}\text{O}$  and  $^{17}\text{O}$ ," *Nucl. Phys.* **75**, 401.
- Brudanin, V., *et al.*, 1995, "Measurement of the induced pseudoscalar form factor in the capture of polarized muons by Si nuclei," *Nucl. Phys. A* **587**, 577.
- Budyashov, Yu. G., V. G. Zinov, A. D. Konin, S. V. Medved, A. I. Mukhin, E. B. Ozerov, A. M. Chatrchyn, and R. A. Er-amzhyan, 1970, "Excited nuclear states during capture of negative muons by carbon and oxygen," *Zh. Eksp. Teor. Fiz.* **58**, 1211 [*Sov. Phys. JETP* **31**, 651 (1970)].
- Bukat, G. M., and N. P. Popov, 1964, "Capture of  $\mu$ -mesons by the  $^{10}\text{B}$  nucleus," *J. Exptl. Theoret. Phys. (USSR)* **46**, 1782 [*Sov. Phys. JETP* **19** 1200 (1964)].
- Bukhvostov, A. P., and N. P. Popov, 1967a, " $\gamma$ -neutrino correlations in allowed nuclear  $\mu$ -meson capture," *Phys. Lett. B* **24**, 497.
- Bukhvostov, A. P., and N. P. Popov, 1967b, "Correlation of neutrino and  $\gamma$ -quantum in allowed capture of a polarized muon," *Yad. Fiz.* **6**, 1241 [*Sov. Jour. Nucl. Phys.* **6**, 903 (1968)].
- Bukhvostov, A. P., and N. P. Popov, 1967c, "Correlations of neutrino and gamma quanta in nuclear muon capture," *Yad. Fiz.* **6**, 809 [*Sov. Jour. Nucl. Phys.* **6**, 589 (1968)].

- Bukhvostov, A. P., and N. P. Popov, 1970, "Time dependence of particle correlations in muon capture," Nucl. Phys. A **147**, 385.
- Bystritski, V. M., *et al.*, 1974, "Measurement of muon capture rate in gaseous hydrogen," Zh. Eksp. Teor. Fiz. **66**, 43 [Sov. Phys. JETP, **39**, 19 (1974)].
- Cannata, F., R. Leonardi, and M. Rosa Clot, 1970, "Breakdown of SU<sub>4</sub> invariance and total muon capture rates: <sup>4</sup>He, <sup>12</sup>C, <sup>16</sup>O, <sup>40</sup>Ca," Phys. Lett. B **32**, 6.
- Cargnelli, M., W. Breunlich, H. Fuhrmann, P. Kammel, J. Marton, P. Pawlek, J. Werner, J. Zmeskal, W. Bertl, and C. Petitjean, 1989, "Measurement of the muon capture rate in gaseous deuterium," Nuclear Weak Process and Nuclear Structure, Yamada Conference XXIII, ed. by M. Morita, H. Ejiri, H. Ohtsubo, and T. Sato, (World Scientific), p. 115.
- Cheon, I.-T. and M. K. Cheoun, 1998, "Induced pseudoscalar coupling constant," nucl-th/9811009 v2.
- Cheon, I.-T. and M. K. Cheoun, 1999, "Axial vector current and induced pseudoscalar coupling constant on  $\mu^- p \rightarrow n\nu_\mu\gamma$  reaction," nucl-th/9906035.
- Choi, S., *et al.*, 1993, "Axial and pseudoscalar nucleon form factors from low energy pion electroproduction," Phys. Rev. Lett. **71**, 3927.
- Christillin, P., 1981, "Radiative muon capture for N=Z nuclei," Nucl. Phys. A **362**, 391.
- Christillin, P. and M. Gmitro, 1985, "Radiative muon capture on <sup>16</sup>O," Phys. Lett. B **150**, 50.
- Christillin, P., M. Rosa-Clot, and S. Servadio, 1980, "Radiative muon capture in medium-heavy nuclei," Nucl. Phys. A **345**, 331.
- Christillin, P. and S. Servadio, 1977, "About low energy expansion of two current amplitudes," Nuovo Cimento **42A**, 165.
- Chu, W. T., I. Nadelhaft, and J. Ashkin, 1965, "Radiative  $\mu^-$  capture in copper," Phys. Rev. **137**, B352.
- Ciechanowicz, S., 1976, "Allowed partial transitions in muon capture by <sup>28</sup>Si," Nucl. Phys. A **267**, 472.
- Ciechanowicz, S., 1981, "Recoil nuclei polarization in the partial  $\mu^- + ^{12}\text{C} \rightarrow \nu + ^{12}\text{B}$  transitions," Nucl. Phys. A **372**, 445.
- Ciechanowicz, S., F. C. Khanna, and E. Truhlik, 1998, "On the muon capture in <sup>28</sup>Si and extraction of  $g_p$ ," Proceedings of the 7th International Conference on Mesons and Light Nuclei 98, Pruhonice, Prague, Czech Republic, 478.
- Ciechanowicz S., and Z. Oziewicz, 1984, "Angular correlation for nuclear muon capture," Fortsch. Phys. **32**, 61.
- Clay, D. R., J. W. Keuffel, R. L. Wagner, and R. M. Edelstein, 1965, "Muon capture in <sup>3</sup>He," Phys. Rev. **140**, B586.
- Cohen, R. C., S. Devons, and A. D. Kanaris, 1963, " $\mu$  capture in oxygen," Phys. Rev. Lett. **11**, 134.
- Cohen, R. C., S. Devons, and A. D. Kanaris, 1964, "Muon capture in oxygen," Nucl. Phys. **57**, 255.
- Cohen, S., and D. Kurath, 1967, "Spectroscopic factors for the 1p shell," Nucl. Phys. A **101**, 1.
- Congleton, J. G., 1994, "Muon capture by <sup>3</sup>He: the hyperfine effect," Nucl. Phys. A **570**, 511.
- Congleton, J. G. and H. W. Fearing, 1993, "Determination of the nucleon pseudoscalar coupling using muon capture by <sup>3</sup>He," Nucl. Phys. A **552**, 534.
- Congleton, J. G., and E. Truhlik, 1996, "Nuclear muon capture by <sup>3</sup>He: meson exchange currents for the triton channel," Phys. Rev. C **53**, 956.
- Conforto, G., M. Conversi, and L. di Lella, 1962, "Observation of radiative capture of negative muons in iron," Phys. Rev. Lett. **9**, 22.
- Conversi, M., R. Diebold, and L. di Lella, 1964, "Radiative muon capture in <sup>40</sup>Ca and the induced pseudoscalar coupling constant," Phys. Rev. **136**, B1077.
- Coon, Sidney A. and M. D. Scadron, 1981, "Goldberger-Treiman discrepancy and the momentum variation of the pion-nucleon form factor and pion decay constant," Phys. Rev. C **23**, 1150.
- Coon, Sidney A. and M. D. Scadron, 1990, " $\pi NN$  couplings, the  $\pi NN$  form factor, and the Goldberger-Treiman discrepancy," Phys. Rev. C **42**, 2256.
- Culligan, G., J. F. Lathrop, V. L. Telegdi, R. Winston, and R. A. Lundy, 1961, "Experimental proof of the spin dependence of the muon capture interaction, and evidence for its (F - GT) character," Phys. Rev. Lett. **7**, 458.
- Cummings, W. J., *et al.*, 1992, "Energetic protons and deuterons emitted following  $\mu^-$  capture by <sup>3</sup>He nuclei," Phys. Rev. Lett. **68**, 293.
- Del Guerra, A., A. Giazotto, M. A. Giorgi, A. Stefanini, D. R. Botterill, H. E. Montgomery, P. R. Norton, and G. Matone, 1976, "Threshold  $\pi^+$  electroproduction at high momentum transfer: A determination of the nucleon axial vector form factor," Nucl. Phys. B **107**, 65.
- de Swart, J. J., M. C. M. Rentmeester, and R. G. E. Timmermans, 1997, "The status of the pion-nucleon coupling constant," Proceedings of MENU97, ed. by D. Drechsel, G. Hohler, W. Kluge, H. Leutwyler, B. M. K. Nefkens, and H.-M. Staudenmaier, TRUIMF Report TRI-97-1.
- Deutsch, J., 1983, "Time dependence of neutron polarization in hydrogen muon capture: A possible experiment for LAMPF II," *Proceedings of the Third LAMPF II Workshop*, LA-9933-C, Vol II, 628.
- Deutsch, J. P., L. Grenacs, J. Lehmann, P. Lipnik, and P. C. Macq, 1968, "Hyperfine effect in the mu-mesonic <sup>11</sup>B atom and information on <sup>11</sup>Be from muon capture measurements," Phys. Lett. B **28**, 178.
- Deutsch, J. P., L. Grenacs, J. Lehmann, P. Lipnik, and P. C. Macq, 1969, "Measurement of muon partial capture rates in <sup>16</sup>O and the induced pseudoscalar coupling constant in muon capture," Phys. Lett. B **29**, 66.
- Devanathan, V., R. Parthasarathy, and P. R. Subramanian, 1972, "Recoil nuclear polarization in muon capture," Ann. Phys. (N.Y.) **73**, 291.
- di Lella, L., I. Hammerman and L. M. Rosenstein, 1971, "Photon asymmetry for radiative  $\mu$  capture in calcium," Phys. Rev. Lett. **27**, 830.
- Döbeli, M., M. Doser, L. van Elmbt, M. Schaad, P. Truöl, A. Bay, J.-P. Perroud, J. Imazato, 1986, "Experimental results on radiative muon capture in complex nuclei," Czech. J. Phys. B **36**, 386.
- Döbeli, M., M. Doser, L. van Elmbt, M. W. Schaad, P. Truöl, A. Bay, J.-P. Perroud, J. Imazato, and T. Ishikawa, 1988, "Radiative muon capture in nuclei," Phys. Rev. C **37**, 1633.
- Dogotar, G. E., R. A. Eramzhyan, and E. Truhlik, 1979, "Exchange currents and extraction of  $a_{nn}$  and  $g_p$  from negative muon capture in deuterium," Nucl. Phys. A **326**, 225.
- Doi, M., T. Sato, H. Ohtsubo, and M. Morita, 1990, "Effect of meson exchange current on deuteron muon capture," Nucl. Phys. A **511**, 507.
- Doi, M., T. Sato, H. Ohtsubo, and M. Morita, 1991, "Muon capture in hyperfine states of muonic deuterium," Prog. Theor. Phys. **86**, 13.
- Donnelly, T. W., and W. C. Haxton, 1979, "Multipole opera-

- tors in semileptonic weak and electromagnetic interactions with nuclei: Harmonic oscillator single-particle matrix elements,” *At. Data Nucl. Data Tables* **23**, 103.
- Donnelly, T. W., and W. C. Haxton, 1980, “Multipole operators in semileptonic weak and electromagnetic interactions with nuclei: General single-particle matrix elements,” *At. Data Nucl. Data Tables* **25**, 1.
- Donnelly, T. W., and G. E. Walker, 1970, “Inelastic electron scattering and supermultiplets in the particle-hole model for  $^{12}\text{C}$ ,  $^{16}\text{O}$ ,  $^{28}\text{Si}$ ,  $^{32}\text{S}$ , and  $^{40}\text{Ca}$ ,” *Ann. Phys. (N.Y.)* **60**, 209.
- Doyle, B. C., and N. C. Mukhopadhyay, 1995, “Phenomenological transition amplitudes in selected 1p-shell nuclei,” *Phys. Rev. C* **52**, 1947.
- Drechsel, D. and L. Tiator, 1992, “Threshold pion photoproduction on nucleons,” *J. Phys. G: Nucl. Part. Phys.* **18**, 449.
- Eramzhyan, R. A., M. Gmitro, R. A. Sakaev, and L. A. Tosunjan, 1977, “Towards a better understanding of  $^{16}\text{O}$  nuclear structure: Muon capture and radiative pion capture reactions,” *Nucl. Phys. A* **290**, 294.
- Eramzhyan, R. A., V. A. Kuz'min, and T. V. Tetereva, 1998, “Calculations of ordinary and radiative muon capture on  $^{58,60,62}\text{Ni}$ ,” *Nucl. Phys. A* **642**, 428.
- Esaulov, A. S., A. M. Pilipenko and Yu. I. Titov, 1978, “Longitudinal and transverse contributions to the threshold cross section slope of single pion electroproduction by a proton,” *Nucl. Phys. B* **136**, 511.
- Faifman M. P., 1989, “Nonresonant formation of hydrogen isotope mesic molecules,” *Muon Catal. Fusion* **4**, 341.
- Faifman, M. P., and L. I. Men'shikov, 1999, “Influence of ion-molecular reactions on  $\mu$ -capture in hydrogen and on fusion in  $^3\text{He-d-}\mu$  muonic molecules,” *Hyperfine Interactions* **118**, 187.
- Falomkon, I. V., A. L. Filippov, M. M. Kulyukin, B. Pontecorvo, Yu. A. Scherbakov, R. M. Sulyaev, V. M. Tsupko-Sitnikov, and O. A. Zamidoroga, 1963, “Measurement of the  $\mu + ^3\text{He} \rightarrow ^3\text{H} + \nu$  reaction rate: final results,” *Phys. Lett.* **3**, 229.
- Favart, D., F. Brouillard, L. Grenacs, P. Igo-Kemenes, P. Lipnik, and P. C. Macq, 1970, “Depolarization of negative muons in low-Z muonic atoms with nonzero nuclear spin,” *Phys. Rev. Lett.* **25**, 1348.
- Fearing, H. W., 1966, “Radiative muon capture and the giant dipole resonance in  $^{40}\text{Ca}$ ,” *Phys. Rev.* **146**, 723.
- Fearing, H. W., 1975, “Theorem for the photon asymmetry in radiative muon capture,” *Phys. Rev. Lett.* **35**, 79.
- Fearing, H. W., 1980, “Relativistic calculation of radiative muon capture in hydrogen and  $^3\text{He}$ ,” *Phys. Rev. C* **21**, 1951.
- Fearing, H. W., 1998a, “Comment on ‘Induced pseudoscalar coupling constant’ by Il-Tong Cheon and Myung Ki Cheon (nucl-th/9811009),” nucl-th/9811027 v2.
- Fearing, H. W., 1998b, “Nucleon-nucleon bremsstrahlung: An example of the impossibility of measuring off-shell amplitudes,” *Phys. Rev. Lett.* **81**, 758.
- Fearing, H. W., 2000, “The off-shell nucleon-nucleon amplitude: Why it is unmeasurable in nucleon-nucleon bremsstrahlung,” *Few Body Systems Suppl.* **12**, 263.
- Fearing, Harold W., Randy Lewis, Nader Mobed, and Stefan Scherer, 1997, “Muon capture by a proton in heavy baryon chiral perturbation theory,” *Phys. Rev. D* **56**, 1783.
- Fearing, H. W., and S. Scherer, 2000, “Field transformations and simple models illustrating the impossibility of measuring off-shell effects,” *Phys. Rev. C* **62**, 034003.
- Fearing, H. W., and M. S. Welsh, 1992, “Radiative muon capture in medium heavy nuclei in a relativistic mean field theory model,” *Phys. Rev. C* **46**, 2077.
- Flamand, G., and K. W. Ford, 1959, “Muon capture by  $^{12}\text{B}$  and beta decay of  $^{12}\text{B}$ ,” *Phys. Rev.* **116**, 1591.
- Foldy, L. L. and J. D. Walecka, 1964 “Muon capture in nuclei,” *Nuovo Cimento* **34**, 1026.
- Frischknecht, A., *et al.*, 1985, “Radiative muon absorption in calcium,” *Phys. Rev. C* **32**, 1506.
- Frischknecht, A., *et al.*, 1988, “Radiative muon absorption in oxygen,” *Phys. Rev. C* **38**, 1996.
- Froelich, P., 1992, “Muon catalysed fusion: Chemical confinement of nuclei within the muonic molecule  $d\mu$ ,” *Adv. Phys.* **41**, 405.
- Fujii, A., and H. Primakoff, 1959, “Muon capture on certain light nuclei,” *Nuovo Cimento* **12**, 327.
- Fukui, M., K. Koshigiri, T. Sato, H. Ohtsubo, M. Morita, 1983a, “The average polarization of  $^{12}\text{B}$  in the muon capture reaction,” *Phys. Lett. B* **132**, 255.
- Fukui, M., K. Koshigiri, T. Sato, H. Ohtsubo, and M. Morita, 1983b, “Nuclear polarization of  $^{12}\text{B}$  in muon capture reaction,” *Prog. Theor. Phys. (Kyoto)* **70**, 827.
- Fukui, M., K. Koshigiri, T. Sato, H. Ohtsubo, and M. Morita, 1987, “Polarizations of  $^{12}\text{B}$  in muon capture reaction with higher order configuration mixing,” *Prog. Theor. Phys. (Kyoto)* **78**, 343.
- Galindo, A., and P. Pascual, 1968, “Asymmetry of recoil nuclei in capture of polarized muons,” *Nucl. Phys. B* **4**, 295.
- Giffon, M., A. Goncalvès, P. A. Guichon, J. Julien, L. Roussel, and C. Samour, 1981, “ $\mu^-$  partial capture rates in  $^{10}\text{B}$ ,  $^{12}\text{C}$  and  $^{14}\text{N}$ ,” *Phys. Rev. C* **24**, 241.
- Gmitro, M., S. S. Kamalov, T. V. Moskalenko and R. A. Eramzhyan, 1981, “Radiative muon capture on nuclei: Microscopic calculation for  $^{16}\text{O}$  and  $^{40}\text{Ca}$ ,” *Czech. J. Phys. B* **31**, 499.
- Gmitro, M., S. S. Kamalov and A. A. Ovchinnikova, 1987, “Radiative capture of polarized muons on  $^{16}\text{O}$  and  $^{40}\text{Ca}$ ,” *Nucl. Phys. A* **468**, 404.
- Gmitro, M., S. S. Kamalov, F. Šimkovic, and A. A. Ovchinnikova, 1990, “Ordinary and radiative muon capture on  $^{12}\text{C}$ ,” *Nucl. Phys. A* **507**, 707.
- Gmitro, M. and A. A. Ovchinnikova, 1981, “Current divergences, pion photoproduction and radiative muon capture,” *Nucl. Phys. A* **356**, 323.
- Gmitro, M., A. A. Ovchinnikova, and T. V. Tetereva, 1986, “Continuity-equation constraint in the two-vertex nuclear processes: Radiative muon capture on  $^{16}\text{O}$  and  $^{40}\text{Ca}$ ,” *Nucl. Phys. A* **453**, 685.
- Gmitro, M., O. Richter, H. R. Kissener, and A. A. Ovchinnikova, 1991, “Ordinary and radiative muon capture on  $^{14}\text{N}$ ,” *Phys. Rev. C* **43**, 1448.
- Gmitro, M. and P. Truöl, 1987, “Radiative muon capture and the weak pseudoscalar coupling in nuclei,” in *Advances in Nuclear Physics*, edited by J. W. Negele and E. Vogt, (Plenum, New York) **18**, 241.
- Godfrey, T. N. K., 1953, “Negative  $\mu$ -meson capture in carbon,” *Phys. Rev.* **92**, 512.
- Goity, Jose L., Randy Lewis, Martin Schvellinger, and Longzhe Zhang, 1999, “The Goldberger-Treiman discrepancy in  $\text{SU}(3)$ ,” *Phys. Lett.* **B454**, 115.
- Goldberger, M. L. and S. B. Treiman, 1958, “Form factors in  $\beta$  decay and  $\mu$  capture,” *Phys. Rev.* **111**, 354.
- Goldman, M. R., 1972, “Order  $\alpha$  corrections to muon capture

- in hydrogen," Nucl. Phys. B **49**, 621.
- Gorringe, T. P., D. S. Armstrong, S. Arole, M. Boleman, E. Gete, V. Kuz'min, B. A. Mofteh, R. Sedlar, T. J. Stocki, and T. Tetereva, 1999, "Measurement of partial muon capture rates in 1s-0d shell nuclei," Phys. Rev. C **60**, 055501.
- Gorringe, T. P., D. S. Armstrong, C. Q. Chen, E. Christy, B. C. Doyle, P. Gumplinger, H. W. Fearing, M. D. Hasinoff, M. A. Kovash and D. H. Wright, 1998, "Isotope dependence of radiative muon capture on the  $^{58,60,62}\text{Ni}$  isotopes," Phys. Rev. C **58**, 1767.
- Gorringe, T. P., B. L. Johnson, D. S. Armstrong, J. Bauer, M. D. Hasinoff, M. A. Kovash, D. F. Measday, B. A. Mofteh, R. Porter, and D. H. Wright, 1994, "Hyperfine effect in  $\mu^-$  capture on  $^{23}\text{Na}$  and  $g_p/g_a$ ," Phys. Rev. Lett. **72**, 3472.
- Gorringe, T. P., B. L. Johnson, J. Bauer, M. A. Kovash, R. Porter, P. Gumplinger, M. D. Hasinoff, D. F. Measday, B. A. Mofteh, D. S. Armstrong, and D. H. Wright, 1993, "Measurement of hyperfine transition rates in muonic  $^{19}\text{F}$ ,  $^{23}\text{Na}$ ,  $^{31}\text{P}$ , and  $^{nat}\text{Cl}$ ," Phys. Lett. B **309**, 241.
- Goulard, B., B. Lorazo, and H. Primakoff, 1982, "Muon capture by the deuteron with outgoing neutrinos of very small momentum," Phys. Rev. C **26**, 1237.
- Govaerts, Jan and Jose-Luis Lucio-Martinez, 2000, "Nuclear muon capture on the proton and  $^3\text{He}$  within the standard model and beyond," Nucl. Phys. A **678**, 110.
- Grenacs, L., 1985, "Induced weak currents in nuclei," Ann. Rev. Nucl. Part. Sci. **35**, 455.
- Grenacs, L., J. P. Deutsch, P. Lipnik, and P. C. Macq, 1968, "A method to measure neutrino-gamma angular correlation in muon capture," Nucl. Instrum. Methods **58**, 164.
- Guichon, P. A. M., 2001, "Comment about pion electroproduction and the axial form factors," Phys. Rev. Lett. **87**, 019101.
- Guichon, P. A. M., B. Bihoreau, M. Giffon, A. Gonçalves, J. Julien, L. Roussel, and C. Samour, 1979, " $\mu^-$  partial capture rates in  $^{16}\text{O}$ ," Phys. Rev. C **19**, 987.
- Guichon, P. A. M., M. Giffon, and C. Samour, 1978, "Possible evidence for mesonic exchange correction in  $^{16}\text{N}(0^-) \leftrightarrow ^{16}\text{O}(0^+) \beta$  decay and  $\mu$  capture reactions," Phys. Lett. B **74**, 15.
- Guichon, P. A. M., and C. Samour, 1979, "Nuclear wave functions and mesonic exchange currents in the weak transition  $^{16}\text{O}(0^+) \leftrightarrow ^{16}\text{N}(0^-)$ ," Phys. Lett. B **82**, 28.
- Haberzettl, H., 2000, "Pion photo- and electroproduction and the partially-conserved axial current," Phys. Rev. Lett. **85**, 3576.
- Haberzettl, H., 2001, "Reply to 'Comment about pion electroproduction and the axial form-factors'," Phys. Rev. Lett. **87**, 019102.
- Halpern, Alvin, 1964a, "Muon capture rate in  $(p\mu p)$ ," Phys. Rev. A **135**, 34.
- Halpern, Alvin, 1964b, " $(p\mu p)^+$  molecule: muon capture in hydrogen," Phys. Rev. Lett. **13**, 660.
- Hambro, L., and N. C. Mukhopadhyay, 1975 "Effects of non-statistical hyperfine populations in muon capture by polarized nuclei," Lett. Nuovo Cim. **14**, 53.
- Hambro, L., and N. C. Mukhopadhyay, 1977, "Repolarization of muons in muonic atoms with polarized nuclei," Phys. Lett. B **68**, 143.
- Hart, R. D., C. R. Cox, G. W. Dodson, M. Eckhause, J. R. Kane, M. S. Pandey, A. M. Rushton, R. T. Siegel, and R. E. Welsh, 1977, "Radiative muon capture in calcium," Phys. Rev. Lett. **39**, 399.
- Hauge, P. S., and S. Maripuu, 1973, "Shell-model calculations for  $A = 6-14$  nuclei with a realistic interaction," Phys. Rev. C **8**, 1609.
- Haxton, W. C., 1978, "Threshold pion photoproduction in  $^{12}\text{C}$  and the 15.11 MeV M1 form factor," Phys. Lett. B **76**, 165.
- Haxton, W. C., and C. Johnson, 1990, "Weak-interaction rates in  $^{16}\text{O}$ ," Phys. Rev. Lett. **65**, 1325.
- Hayes, A. C., and I. S. Towner, 2000, "Shell-model calculations of neutrino scattering from C-12," Phys. Rev. C **61**, 044603.
- Hildebrand, Roger H., 1962, "Observation of  $\mu^-$  capture in liquid hydrogen," Phys. Rev. Lett. **8**, 34.
- Hildebrand, R., and J. H. Doede, 1962, in *Proc. Inter. Conf. on High Energy Physics, Geneva, 1962*, ed. by J. Prentki, p. 418.
- Hirshfelder, J. O., H. Eyring, B. Topley, 1936, "Reactions involving hydrogen molecules and atoms," J. Chem. Phys. **4**, 170.
- Ho, E. C. Y., H. W. Fearing, and W. Schadow, 2002, "Radiative muon capture by  $^3\text{He}$ ," Phys. Rev. C (in press).
- Ho-Kim, Q., J. P. Lavine, and H. S. Picker, 1976, "Final state interactions in muon capture by deuterons," Phys. Rev. C **13**, 1966.
- Hwang, W.-Y. P. and B.-J. Lin, 1999, "Muon capture in deuterium," Int. Jour. Mod. Phys. E **8**, 101.
- Hwang, W.-Y. P. and H. Primakoff, 1978, "Theory of radiative muon capture with applications to nuclear spin and isospin doublets," Phys. Rev. C **18** 414.
- Immele, J. D., and N. C. Mukhopadhyay, 1975, "An open-shell finite Fermi systems approach to the structure of  $A = 12$  nuclei," Phys. Lett. B **56**, 13.
- Ivanov, E., and E. Truhlik, 1979a, "Hard pions and axial meson exchange currents in nuclear physics," Nucl. Phys. A **316**, 437.
- Ivanov, E. and E. Truhlik, 1979b, "Hard pions and axial meson exchange current effects in negative muon capture in deuterium," Nucl. Phys. A **316**, 451.
- Johnson, B. L., T. P. Gorringe, D. S. Armstrong, J. Bauer, M. D. Hasinoff, M. A. Kovash, D. F. Measday, B. A. Mofteh, R. Porter, and D. H. Wright, 1996, "Observables in muon capture on  $^{23}\text{Na}$  and the effective weak couplings  $\tilde{g}_a$  and  $\tilde{g}_p$ ," Phys. Rev. C **54**, 2714.
- Jones, H. F. and M. D. Scadron, 1975, "Goldberger-Treiman relation and chiral-symmetry breaking," Phys. Rev. D **11**, 174.
- Jonkmans, G., *et al.*, 1996, "Radiative muon capture on hydrogen and the induced pseudoscalar coupling," Phys. Rev. Lett. **77**, 4512.
- Junker, K., V. A. Kuz'min, A. A. Ovchinnikova, and T. V. Tetereva, 2000, "Sensitivity of muon capture to the ratios of nuclear matrix elements," Phys. Rev. C **61**, 044602.
- Kameyama, H., M. Kamimura and Y. Fukushima, 1989, "Coupled-rearrangement-channel gaussian-basis variational method for trinucleon bound states," Phys. Rev. C **40**, 974.
- Kammel, P., W. H. Breunlich, M. Cargnelli, H. G. Mahler, J. Zmeskal, W. H. Bertl, C. Petitjean, and W. J. Kossler, 1982, "First observation of hyperfine transitions in muonic deuterium atoms via resonant  $d\mu d$  formation at 34K," Phys. Lett. B **112**, 319.
- Kammel, P., W. H. Breunlich, M. Cargnelli, H. G. Mahler, J. Zmeskal, W. H. Bertl and C. Petitjean, 1983, "First ob-

- servation of muonic hyperfine effects in pure deuterium,” *Phys. Rev. A* **28**, 2611.
- Kammel, P., *et al.*, (2000), “Precision Measurement of  $\mu$ p capture in a hydrogen TPC,” *Nucl. Phys. A* **663**, 911c.
- Kane, F. R., M. Eckhause, G. H. Miller, B. L. Roberts, M. E. Vislay, and R. E. Welsh, 1973, “Muon capture rates on  $^{16}\text{O}$  leading to bound states of  $^{16}\text{N}$ ,” *Phys. Lett. B* **45**, 292.
- Kim, C. W. and H. Primakoff, 1965, “Theory of muon capture with initial and final nuclei treated as ‘elementary’ particles,” *Phys. Rev.* **140**, B566.
- Kirchbach, M., and D. O. Riska, 1994, “The effective induced pseudoscalar coupling constant,” *Nucl. Phys. A* **578**, 511.
- Kleib, L., 1982, “Impulse approximation versus elementary particle method: Radiative muon capture in  $^3\text{He}$  and the pion- $^3\text{He}$ - $^3\text{H}$  coupling,” Ph. D. dissertation, University of Groningen, the Netherlands.
- Klieb, L., 1985, “Hard meson corrections to the amplitude for radiative muon capture and the elementary particle method,” *Nucl. Phys. A* **442**, 721.
- Klieb, L. and H. P. C. Rood, 1981, “Radiative muon capture in  $^3\text{He}$ : A comparison of the impulse approximation with elementary particle calculations,” *Nucl. Phys. A* **356**, 483.
- Klieb, L. and H. P. C. Rood, 1984a, “Impulse approximation versus elementary particle method:  $\pi$ - $^3\text{He}$ - $^3\text{H}$  coupling constant,” *Phys. Rev. C* **29**, 215.
- Klieb, L. and H. P. C. Rood, 1984b, “Impulse approximation versus elementary particle method: Pion photoproduction and radiative muon capture,” *Phys. Rev. C* **29**, 223.
- Kobayashi, M., N. Ohtsuka, H. Ohtsubo, and M. Morita, 1978, “Average polarization of  $^{12}\text{B}$  in polarized muon capture,” *Nucl. Phys. A* **312**, 377.
- Kolbe, E., K. Langanke and P. Vogel, 2000, “Muon capture on nuclei with  $N > Z$ , random phase approximation, and in-medium value of the axial-vector coupling constant,” *Phys. Rev. C* **62**, 055502.
- Kortelainen, M., M. Aunola, T. Siiskonen, and J. Suhonen, 2000, “Mean-field effects on muon-capture observables,” *J. Phys. G* **26**, L33.
- Koshigiri, K., Y. Kakudo, H. Ohtsubo, and M. Morita, 1985, “Muon capture in complex nuclei of nonzero spin,” *Prog. Theor. Phys. (Kyoto)* **74**, 736.
- Koshigiri, K., R. Morita and M. Morita, 1997, “Induced pseudoscalar weak interaction and muon capture reaction,” in *Non-Nucleonic Degrees of Freedom Detected in Nucleus (NNDF '96), Proc. of the Intern. Symp.*, eds. T. Minamisono, Y. Nojiri, T. Sato and K. Matsuta, (World Scientific, Singapore, 1997), p. 238.
- Koshigiri, K., H. Ohtsubo, and M. Morita, 1982, “Muon capture in hyperfine states of  $^{11}\text{B}$  muonic atom,” *Prog. Theor. Phys. (Kyoto)* **68**, 687.
- Koshigiri, K., H. Ohtsubo, and M. Morita, 1984, “Muon capture in  $^{11}\text{B}$  muonic atom and hyperfine spin dependence,” *Prog. Theor. Phys. (Kyoto)* **71**, 1293.
- Kubodera, K., J. Delorme, and M. Rho, 1978, “Axial currents in nuclei,” *Phys. Rev. Lett.* **40**, 755.
- Kudoyarov, M. F., *et al.*, 1998, in *Heavy Ion Physics, Proceedings of the VI International School-Seminar, Dubna, Russia, 1997*, eds. Yu. Ts. Oganessian and R. Kalpakchieva, (World Scientific, Singapore, 1998), p. 742.
- Kuhn, S. E., *et al.*, 1994, “Multinucleon effects in muon capture on  $^3\text{He}$  at high energy transfer,” *Phys. Rev. C* **50**, 1771.
- Kuno, Y., J. Imazato, K. Nishiyama, K. Nagamine, T. Yamazaki, and T. Minamisono, 1984, “New pulsed-beam measurement of the average polarization of  $^{12}\text{B}(\text{g.s.})$  produced in the polarized-muon capture reaction  $^{12}\text{C}(\mu^-, \nu_\mu)^{12}\text{B}$ ,” *Phys. Lett. B* **148**, 270.
- Kuno, Y., J. Imazato, K. Nishiyama, K. Nagamine, T. Yamazaki and T. Minamisono, 1986, “Measurement of the average polarization of  $^{12}\text{B}$  in the polarized-muon capture by  $^{12}\text{C}$ : Magnitude of the induced pseudoscalar form factor,” *Z. Phys. A* **323**, 69.
- Kuno, Y., K. Nagamine, and T. Yamazaki, 1987, “Polarization transfer from polarized nuclear spin to  $\mu^-$  spin in muonic atom,” *Nucl. Phys. A* **475**, 615.
- Kuo, T. T. S., and G. E. Brown, 1966, “Structure of finite nuclei and the free nucleon-nucleon interaction: An application to  $^{18}\text{O}$  and  $^{18}\text{F}$ ,” *Nucl. Phys.* **85**, 40.
- Kuz'min, V. A., A. A. Ovchinnikova, and T. V. Tetereva, 1994, “Muon capture by  $^{10,11}\text{B}$  nuclei: Sensitivity to the choice of nuclear model,” *Yad. Fiz.* **57**, 1954 [*Phys. Atom. Nucl.* **57**, 1881 (1994)].
- Kuz'min, V. A., and T. V. Tetereva, 2000, “Properties of isovector  $1+$  states in  $A = 28$  nuclei and nuclear muon capture,” *Yad. Fiz.* **63**, 1966 [*Phys. Atom. Nucl.* **63**, 1874 (2000)].
- Kuz'min, V. A., T. V. Tetereva, and K. Junker, 2001, “On the strength of spin-isospin transitions in  $A=28$  nuclei,” *Yad. Fiz.* **64**, 1246 [*Phys. Atom. Nucl.* **64**, 1169 (2001)].
- Lee, Y. K., T. J. Hallman, L. Madansky, S. Trentalange, G. R. Mason, A. J. Caffrey, E. K. McIntyre, and T. R. King, 1987, “Energetic neutron emission from  $\mu^-$  capture in deuterium,” *Phys. Lett. B* **188**, 33.
- Love, W. A., S. Marder, I. Nadelhaft, R. T. Siegel, and A. E. Taylor, 1959, “Helicity of negative muons from pion decay,” *Phys. Rev. Lett.* **2**, 107.
- Luyten, J. R., H. P. C. Rood, and H. A. Tolhoek, 1963, “On the theory of muon capture by complex nuclei (I),” *Nucl. Phys.* **41**, 236.
- Maier, E. J., R. M. Edelman, and R. T. Siegel, 1964, “Measurement of the reaction  $\mu^- + ^{12}\text{C} \rightarrow ^{12}\text{B} + \nu$ ,” *Phys. Rev.* **133**, B663.
- Marcucci, L. E., R. Schiavilla, S. Rosati, A. Kievsky, and M. Viviani, 2001, “Theoretical study of the  $^3\text{He}(\mu^-, \nu_\mu)^3\text{H}$  capture,” nucl-th/0112008.
- Martínez-Pinedo G., and P. Vogel, 1998, “Shell model calculation of the  $\beta^-$  and  $\beta^+$  partial half-lives of  $^{54}\text{Mn}$  and other unique second forbidden  $\beta$  decays,” *Phys. Rev. Lett.* **81**, 281.
- Martino, J., 1982, “Measurement of the capture ratio in liquid hydrogen by the lifetime method,” Ph. D. Thesis, Univ. Paris Sud (Orsay), April 1982.
- Martino, J., 1984, “Muon capture in hydrogen,” in *Erice 1984: Fundamental Interactions in Low-energy Systems*, edited by P. Dalpiaz, G. Fiorentini, G. Torelli, Ettore Majorana International Science Series, **23**, 43 (Plenum Press, N. Y., 1985).
- McGrory, J. B., and B. H. Wildenthal, 1971, “A truncated shell model calculation of  $^{23}\text{Na}$ ,  $^{24}\text{Mg}$  and  $^{28}\text{Si}$ ,” *Phys. Lett. B* **34**, 373.
- Measday, D. F., 2001, “The nuclear physics of muon capture,” *Phys. Rep.* **354**, 243.
- Meissner, T., F. Myhrer, and K. Kubodera, 1998, “Radiative muon capture by a proton in chiral perturbation theory,” *Phys. Lett. B* **416**, 36.
- Mergell, P., Ulf-G. Meissner, and D. Drechsel, 1996,

- “Dispersion-theoretical analysis of the nucleon electromagnetic form factors,” Nucl. Phys. A **596**, 367.
- Miller, G. H., M. Eckhause, F. R. Kane, P. Martin, and R. E. Welsh, 1972a, “Negative muon capture in carbon leading to specific final states,” Phys. Lett. B **41**, 50.
- Miller, G. H., M. Eckhause, F. R. Kane, P. Martin, and R. E. Welsh, 1972b, “Gamma-neutrino angular correlations in muon capture,” Phys. Rev. Lett. **29**, 1194.
- Miller, G. H., M. Eckhause, P. Martin, and R. E. Welsh, 1972c, “Yields of gamma rays emitted following capture of negative muons by  $^{28}\text{Si}$  and  $^{24}\text{Mg}$ ,” Phys. Rev. C **6**, 487.
- Minamisono, K., *et al.*, 2001, “New limit of the G-parity irregular weak nucleon current detected in  $\beta$  decays of spin aligned  $^{12}\text{B}$  and  $^{12}\text{N}$ ,” Phys. Rev. C **65**, 015501.
- Mintz, S. L., 1973, “Muon capture rate in deuterium and the weak form factors in the timelike region,” Phys. Rev. D **8**, 2946.
- Mintz, S. L., 1983, “Differential muon capture rate and the deuterium form factors in the timelike region,” Phys. Rev. C **28**, 556.
- Moftah, B. A., E. Gete, D. F. Measday, D. S. Armstrong, J. Bauer, T. P. Gorringer, B. L. Johnson, B. Siebels, and S. Stanislaus, 1997, “Muon capture in  $^{28}\text{Si}$  and  $g_p/g_a$ ,” Phys. Lett. B **395**, 157.
- Morita, M., and A. Fujii, 1960, “Theory of allowed and forbidden transitions in muon capture reactions,” Phys. Rev. **118**, 606.
- Morita, M. and R. Morita, 1992, “Muon capture in hyperfine states of muonic deuterium and induced pseudoscalar form factor,” Z. Phys. C **56**, S156.
- Morita, M., R. Morita, M. Doi, T. Sato, H. Ohtsubo, and K. Koshigiri, 1993, “Induced pseudoscalar interaction in weak nucleon current and muon capture in hyperfine states of muonic deuterium,” Hyperfine Interactions **78**, 85.
- Morita, M., R. Morita, and K. Koshigiri, 1994, “Induced terms of weak nucleon currents in light nuclei,” Nucl. Phys. A **577**, 387.
- Mukhopadhyay N. C., 1977, “Nuclear muon capture,” Phys. Rept. **30**, 1.
- Mukhopadhyay, N. C., and M. H. Macfarlane, 1971, “Transition rate for ground state to ground state in the capture of negative muons by  $^{12}\text{C}$ ,” Phys. Rev. Lett. **27**, 1823; **28**, 1545(E).
- Mukhopadhyay, N. C., and J. Martorell, 1978, “An improved impulse approximation treatment of the “allowed” weak and analogue electromagnetic transitions in  $^{12}\text{C}$ ,” Nucl. Phys. A **296**, 461.
- Mulhauser, F., *et al.*, 1996, “Measurement of muon transfer from proton to triton and  $pp\mu$  molecular formation in solid hydrogen,” Phys. Rev. A **53**, 3069.
- Myhrer, F., 1999, private communication.
- Nasrallah, N. F., 2000, “Goldberger-Treiman discrepancy,” Phys. Rev. **D62** 036006.
- Navarro, J. and H. Krivine, 1986, “A sum rule approach to total muon capture rates,” Nucl. Phys. A **457**, 731.
- Newbury, N. R., A. S. Barton, P. Bogorad, G. D. Cates, M. Gatzke, B. Saam, L. Han, R. Holmes, P. A. Souder, J. Xu, and D. Benton, 1991, “Laser polarized muonic helium,” Phys. Rev. Lett. **67**, 3219; **69**, 391(E).
- Nguyen, Nguyen Tien, 1975, “Neutrino disintegration and muon capture in the deuteron,” Nucl. Phys. A **254**, 485.
- O’Connell, J. S., T. W. Donnelly, and J. D. Walecka, 1972, “Semileptonic weak interactions with  $^{12}\text{C}$ ,” Phys. Rev. C **6**, 719.
- Opat, G. I., 1964, “Radiative muon capture in hydrogen,” Phys. Rev. **134**, B428.
- Oziewicz, Z., and N. P. Popov, 1965, “ $\gamma$ -neutrino correlations in first forbidden nuclear  $\mu$ -meson capture,” Phys. Lett. **15**, 273.
- Parthasarathy, R., and V. N. Sridhar, 1978, “Gamma-neutrino angular correlation in muon capture by  $^{28}\text{Si}$ ,” Phys. Rev. C **18**, 1796.
- Parthasarathy, R., and V. N. Sridhar, 1981, “Gamma-neutrino angular correlations in muon capture by  $^{28}\text{Si}$ . II,” Phys. Rev. C **23**, 861.
- Particle Data Group, 2000, “Review of particle physics,” Eur. Phys. J. C **15**, 1.
- Pascual, P., R. Tarrach and F. Vidal, 1972, “Muon capture in deuterium,” Nuovo Cimento **12A**, 241.
- Peterson, E. A., 1968, “Muon capture in  $^3\text{He}$ ,” Phys. Rev. **167**, 971.
- Petitjean, C., *et al.*, 1990/91, “The  $ppd$  fusion cycle,” Muon Catal. Fusion **5/6**, 199.
- Phillips, A. C., F. Roig, and J. Ros, 1975, “Muon capture in  $^3\text{He}$ ,” Nucl. Phys. A **237** 493.
- Ponomarev, L. I., 1973, “Molecular structure effects on atomic and nuclear capture of mesons,” Annu. Rev. Nucl. Sci. **23**, 395.
- Ponomarev L. I., and M. P. Faifman, 1976, “Calculation of the hydrogen  $\mu$ -mesic molecule deexcitation rates,” Sov. Phys. JETP **44**, 886.
- Popov, N. P., 1963, “ $\gamma$ -neutrino correlation in nuclear muon capture,” J. Exptl. Theoret. Phys. (USSR) **44**, 1679 [Sov. Phys. JETP **17**, 1130 (1963)].
- Possoz, A., Ph. Deschepper, L. Grenacs, P. Lebrun, J. Lehmann, L. Palfy, A. de Moura Gonclaves, C. Samour and V. I. Telegdi, 1977, “Average polarization of  $^{12}\text{B}$  in  $^{12}\text{C}(\mu, \nu)^{12}\text{B}(\text{g.s.})$  reaction: Helicity of the  $\pi$ -decay muon and nature of the weak coupling,” Phys. Lett. B **70**, 265.
- Possoz, A., D. Favart, L. Grenacs, J. Lehmann, P. Macq, D. Meda, L. Palfy, J. Julien, and C. Samour, 1974, “Measurement of the average polarization of  $^{12}\text{B}$  produced by polarized muons in the  $\mu^- + ^{12}\text{C} \rightarrow \nu_\mu + ^{12}\text{B}$  reaction,” Phys. Lett. B **50**, 438.
- Primakoff, H., 1959, “Theory of muon capture,” Rev. Mod. Phys. **31**, 802.
- Reifenröther, G., E. Klempt, and R. Landua, 1987, “Cascade of muonic helium atoms,” Phys. Lett. B **191**, 15.
- Reynolds, G. T., D. B. Scarl, A. Swanson, J. R. Waters, and R. A. Zdanis, 1963, “Muon capture on carbon,” Phys. Rev. **129**, 1790.
- Roesch, L. Ph., N. Schlumpf, D. Taquq, V. L. Telegdi, P. Truttmann, and A. Zehnder, 1981a, “Measurement of the capture rates to the excited states in  $^{12}\text{C}(\mu^-, \nu)^{12}\text{B}^*$  and a novel technique to deduce the alignment of  $^{12}\text{B}^*(1^-)$ ,” Phys. Lett. B **107**, 31.
- Roesch, L. Ph., V. L. Telegdi, P. Truttmann, A. Zehnder, L. Grenacs, and L. Palfy, 1981b, “Measurement of the average and longitudinal recoil polarizations in the reaction  $^{12}\text{C}(\mu^-, \nu)^{12}\text{B}(\text{g.s.})$ : Magnitude of the induced pseudoscalar coupling,” Phys. Rev. Lett. **46**, 1507.
- Roig, F., and J. Navarro, 1990, “Radiative muon capture and the value of  $g_p$  in nuclei,” Phys. Lett. B **236**, 393.
- Rood, H. P. C., and H. A. Tolhoek, 1965, “The theory of muon capture by complex nuclei (III). Radiative muon capture,” Nucl. Phys. **70**, 658.
- Rosenfelder, R., 1979, “Semileptonic weak and electromagnetic interactions in nuclei: Recoil polarization in muon



- capture," Nucl. Phys. A **322**, 471.
- Rosenstein, L. M., and I. S. Hammerman, 1973, "Photon spectrum from radiative  $\mu$  capture in calcium," Phys. Rev. C **8**, 603.
- Rothberg, J. E., E. W. Anderson, E. J. Bleser, L. M. Lederman, S. L. Meyer, J. L. Rosen, and I-T. Wang, 1963, "Muon capture in hydrogen," Phys. Rev. **132**, 2664.
- Scherer, S., and H. W. Fearing, 2001, "A simple model illustrating the impossibility of measuring off-shell effects," Nucl. Phys. A **684**, 499.
- Schottmueller, J., A. Badertscher, M. Daum, P. F. A. Goudsmit, M. Janousch, P.-R. Kettle, J. Koglin, V. E. Markushin, and Z. G. Zhao, 1999, "Kinetic energy of  $\pi^-p$  atoms in liquid and gaseous hydrogen," Hyperfine Interactions **119**, 95.
- Shiomi, H., 1996, "Second class current in QCD sum rules," Nucl. Phys. A **603**, 281.
- Siebels, B., T. P. Gorringer, W. P. Alford, J. Bauer, J. Evans, S. El-Kateb, K. P. Jackson, A. Trudel, and S. Yen, 1995, "Gamow-Teller strength in  $^{23}\text{Na}(n,p)$  and a comparison to  $^{23}\text{Na}(\mu^-, \nu)$ ," Phys. Rev. C **52**, 1488.
- Sigg, D., *et al.*, 1996, "The strong interaction shift and width of the ground state of pionic hydrogen," Nucl. Phys. A **609**, 269; **617**, 526(E).
- Siiskonen, T., J. Suhonen, and M. Hjorth-Jensen, 1999, "Towards the solution of the  $C_P/C_A$  anomaly in shell-model calculations of muon capture," Phys. Rev. C **59**, 1839.
- Siiskonen, T., J. Suhonen, V. A. Kuz'min and T. V. Tetereva, 1998, "Shell-model study of partial muon-capture rates in light nuclei," Nucl. Phys. A **635**, 446; **651**, 437(E).
- Skibinski, R., J. Golak, H. Witala, and W. Glöckle, 1999, "Final state interaction effects in  $\mu$ -capture induced two-body decay of  $^3\text{He}$ ," Phys. Rev. C **59**, 2384.
- Sloboda, R. S. and H. W. Fearing, 1978, "Radiative muon capture rates and the maximum photon energy," Phys. Rev. C **18**, 2265.
- Sloboda, R. S. and H. W. Fearing, 1980, " $O(1/m^2)$  and nuclear effects in radiative muon capture in  $^{40}\text{Ca}$ ," Nucl. Phys. A **340**, 342.
- Smejkal, J. and E. Truhlik, 1998, "Comments on the last development in constructing the amplitude for the radiative muon capture," nucl-th/9811080.
- Smejkal, J., E. Truhlik and F. C. Khanna, 1999, "Chiral Lagrangians and the transition amplitude for radiative muon capture," Few Body Syst. **26**, 175.
- Sotona, M. and E. Truhlik, 1974, "Muon capture in deuterium with realistic potentials," Nucl. Phys. A **229**, 471.
- Souder, P. A., D. E. Casperson, T. W. Crane, V. W. Hughes, D. C. Lu, H. Orth, H. W. Reist, M. H. Yam, and G. zu Putlitz, 1975, "Formation of the muonic helium atom,  $\alpha\mu^-e^-$  and observation of its Larmor precession," Phys. Rev. Lett. **34**, 1417.
- Souder, P. A., *et al.*, 1998, "Laser polarized muonic  $^3\text{He}$  and spin dependent  $\mu^-$  capture," Nucl. Instrum. Methods Phys. Res. A **402**, 311.
- Stoks, V., R. Timmermans and J. J. de Swart, 1993, "Pion-nucleon coupling constant," Phys. Rev. C **47**, 512.
- Subramanian, P. R., and V. Devanathan, 1979, "Orientations of the recoil nucleus in muon capture," Phys. Rev. C **20**, 1615.
- Subramanian, P. R., R. Parthasarathy and, V. Devanathan, 1976, "Nuclear orientation following muon capture by spin zero nuclei," Nucl. Phys. A **262**, 433.
- Suzuki, T., 1997, "Effects of neutron halo on  $\mu$  capture by  $^{11}\text{B}$ ," in *Non-Nucleonic Degrees of Freedom Detected in Nucleus (NNDF '96)*, Proc. of the Intern. Symp., eds. T. Minamisono, Y. Nojiri, T. Sato and K. Matsuta, (World Scientific, Singapore, 1997), p. 349.
- Suzuki, T., D. F. Measday, and J. P. Roalsvig, 1987, "Total nuclear capture rates for negative muons," Phys. Rev. C **35**, 2212.
- Švarc, A. and Ž. Bajzer, 1980, "The extraction of the neutron-neutron scattering length from muon capture by a deuteron," J. Phys. G: Nucl. Phys. **6**, 1397.
- Švarc, A., Ž. Bajzer and M. Furic, 1978, "Kinematical and dynamical considerations of muon capture by deuteron," Z. Phys. A **285**, 133.
- Švarc, A., Z. Bajzer, and M. Furic, 1979, "The influence of the neutron-neutron off-energy-shell interaction on the differential  $\mu$ -d capture rates," Z. Phys. A **291** 271.
- Tatara, Naoko, Y. Kohyama and K. Kubodera, 1990, "Weak interaction processes on deuterium: Muon capture and neutrino reactions," Phys. Rev. C **42**, 1694.
- Telegdi, V. L., 1959, "Consequences of atomic conversion for the interpretation of experiments on the spin dependence of muon absorption," Phys. Rev. Lett. **3**, 59.
- Towner, I. S., 1986, "Meson exchange currents in time-like axial charge transitions," Ann. Rev. Nucl. Part. Sci. **36**, 115.
- Towner, I. S., and F. C. Khanna, 1981, "Role of 2p-2h states in weak  $0^+ \rightarrow 0^-$  transitions in  $A = 16$  nuclei," Nucl. Phys. A **372**, 331.
- Truhlik, E., 1972, "Neutron-neutron interaction and muon capture by deuteron," Nucl. Phys. B **45**, 303.
- Truhlik, E., 2001, "Pion electroproduction amplitude," Phys. Rev. C **64**, 055501.
- Truhlik, E. and F. Khanna, 2001, "On radiative muon capture in hydrogen," nucl-th/0102006 v2.
- Truttmann, P., H. Brändle, L. Ph. Roesch, V. L. Telegdi, A. Zehnder, and L. Grenacs, 1979, "Qualitative measurement of the longitudinal recoil polarization in the reaction  $^{12}\text{C}(\mu^-, \nu)^{12}\text{B}$  (g.s.)," Phys. Lett. B **83**, 48.
- Vainshtein, A. I. and V. I. Zakharov, 1972, "Low energy theorems for photo- and electropion production at threshold," Nucl. Phys. B **36**, 589.
- Virtue, C. J., K. A. Aniol, F. E. Entezami, M. D. Hasinoff, D. Horvath, H. W. Roser, and B. C. Robertson, 1990, "Photon asymmetry in radiative muon capture on calcium," Nucl. Phys. A **517**, 509.
- Walecka, J. D., 1975, "Semi-leptonic weak interactions in nuclei," in *Muon Physics*, V. Hughes and C.S. Wu, eds., Vol. II, p. 114 (Academic Press, N. Y. 1975).
- Wang, I-T., 1965a, "Study of the "breakup" channels of muon capture by  $\text{He}^3$ ," Phys. Rev. **139**, B1544.
- Wang, I-T., 1965b, "Muon capture by deuterons," Phys. Rev. **139**, B1539.
- Wang, I-T., E. W. Anderson, E. J. Bleser, L. M. Lederman, S.L. Meyer, J. L. Rosen, and J. E. Rothberg, 1965, "Muon capture in  $(p\mu d)^+$  molecules," Phys. Rev. **139**, B1528.
- Warburton, E. K., 1992, "Second-forbidden unique  $\beta$  decays of  $^{10}\text{Be}$ ,  $^{22}\text{Na}$ , and  $^{26}\text{Al}$ ," Phys. Rev. C **45**, 463.
- Warburton, E. K., I. S. Towner, and B. A. Brown, 1994, "First-forbidden  $\beta$  decay: Meson-exchange enhancement of the axial charge at  $A \sim 16$ ," Phys. Rev. C **49**, 824.
- Weinberg, Steven, 1960, "Muon absorption in liquid hydrogen," Phys. Rev. Lett. **4**, 575.
- Wessel, W. Roy and Paul Phillipson, 1964, "Quantum mechanics of the  $(p - \mu - p)^+$  molecular ion," Phys. Rev. Lett.

- 13**, 23.
- Wiaux, V., R. Prieels, J. Deutsch, J. Govaerts, V. Brudanin, V. Egorov, C. Petitjean, and P. Truöl, 2002, "Muon capture by  $^{11}\text{B}$  and the hyperfine effect," *Phys. Rev. C* **65**, 025503.
- Wildenthal, B. H., and J. B. McGrory, 1973, "Shell model calculations for masses 27, 28 and 29: General methods and specific applications to  $^{27}\text{Al}$ ,  $^{28}\text{Si}$  and  $^{29}\text{Si}$ ," *Phys. Rev. C* **7** 714.
- Wildenthal, B. H., 1984, "Empirical strengths of spin operators in nuclei," *Progress in Particle and Nuclear Physics*, D. H. Wilkinson, ed., Vol. 11, p. 5 (Pergamon Press, Oxford, 1984).
- Wilkinson, D. H., 2000a, "Limits to second-class nucleonic and mesonic currents," *Eur. Phys. J. A* **7**, 307.
- Wilkinson, D. H., 2000b, "Limits to second-class nucleonic currents," *Nucl. Instrum. Meth. Phys. Res. A* **455**, 656.
- Winston, R., 1963, "Observable hyperfine effects in muon capture by complex nuclei," *Phys. Rev.* **129**, 2766.
- Wolfenstein, L., 1970, in *High Energy Physics and Nuclear Structure*, edited by S. Devons (Plenum, New York, 1970), p. 661.
- Wright, D. H., *et al.*, 1992, "The TRIUMF Radiative Muon Capture Facility," *Nuclear Instruments and Methods* **A320**, 249.
- Wright, D. H., *et al.*, 1998, "Measurement of the induced pseudoscalar coupling using radiative muon capture on hydrogen," *Phys. Rev. C* **57**, 373.
- Wright, D. H., *et al.*, 2000, "Radiative muon capture on  $^3\text{He}$ ," *Few Body Systems Suppl.* **12**, 275.
- Wulschleger, A. and F. Scheck, 1979, "Radiative muon capture on  $^{12}\text{C}$  and  $^{16}\text{O}$ ," *Nucl. Phys. A* **326** 325.
- Zaimidoroga, O. A., M. M. Kulyukin, B. Pontecorvo, R. M. Sulyaev, I. V. Falomkin, A. I. Filippov, V. M. Tsupko-Sitnikov, and Yu. A. Scherbakov, 1963, "Measurement of the total muon capture rate in  $^3\text{He}$ ," *Phys. Lett.* **6**, 100.
- Zel'dovich, Ia. B., S. S. Gershtein, 1959, "Formation of hydrogen mesic molecules," *J. Exptl. Theoret. Phys. (USSR)* **35** 833 [*Sov. Phys. JETP* **8**, 451 (1959)].